Thesis

A Novel Green Hybrid Hypergolic Bi-propellant with Viscoelastic Nature of the Fuel

by I.A. Molenberg

Student number	4494776
Date of Delivery	June 14, 2021
Supervisor	Jyoti Botchu Vara Siva

Delft University of Technology

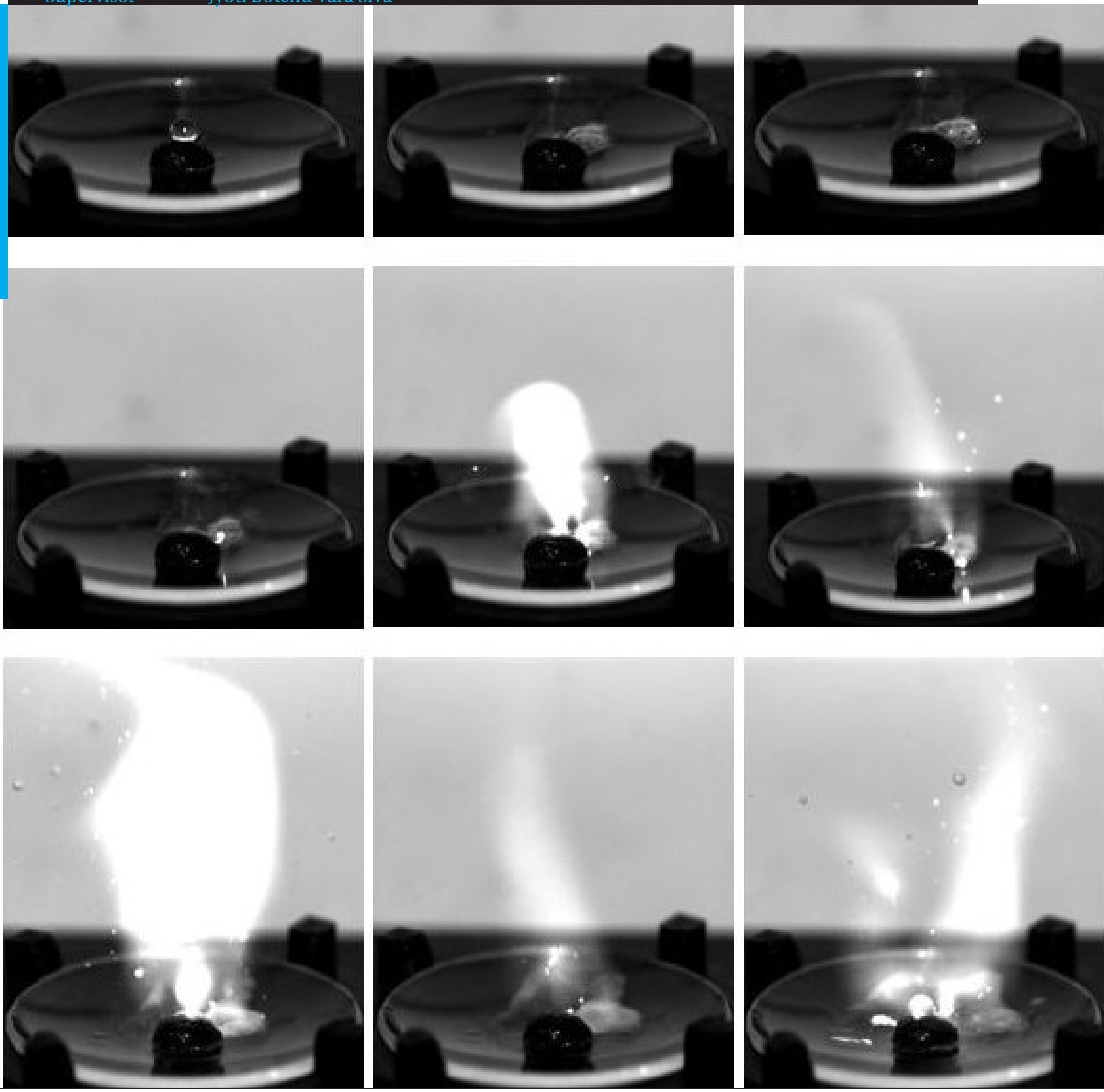

Challenge the future

The Investigation and Development of a Novel Green Hybrid Hypergolic Bi-propellant with Viscoelastic Nature of the Fuel

I.A. Molenberg

This thesis report is written as part of the Master Aerospace Engineering - Space Flight of the Delft University of Technology. The thesis was started in November 2020 and completed by June 30, 2021. The objective is to investigate and develop a novel green hybrid hypergolic bi-propellant system with a viscoelastic nature of the fuel. This propellant should provide an alternative for the traditional highly toxic propellants and fulfill society's need for green propellants for space applications to comply with the trend in environmental sustainability. The formulation of this novel bi-propellant consists of highly concentrated hydrogen peroxide and a gelled alcohol in which a catalyst is suspended. The fuel's viscoelastic nature is analysed based on a rheology study and the performance of this catalytically induced hypergolic propellant is evaluated by means of a multi-drop test.

Per ardua ad astra

Student number:	4494776
Thesis committee:	Dr. B. V. S. Jyoti, TU Delft, supervisor
	Prof. dr. E.K.A. Gill, TU Delft, chair
	Ir. R. Noomen, TU Delft, external examiner

PREFACE

This thesis report is written as part of the Master Aerospace Engineering - Space Flight of Delft University of Technology. I did my thesis on the topic of green propulsion during a 30 week period from week 48, 2020 to week 26, 2021. I was very happy that I could do my thesis on this interesting topic and that I was, despite the current COVID-19 pandemic, still allowed to conduct an experimental research thesis. It has been an instructive process in which I was able to apply knowledge and skills that I acquired during my studies. Also, I have developed new valuable skills.

I would like to express my gratitude to my thesis supervisor Botchu Vara Siva Jyoti for her effort, time, and coaching. The numerous meetings in which she provided me with feedback and helping to improve my research were really appreciated. Without her support the thesis would not have been at the level it is now. Furthermore, I would like to express my gratitude to the employees of the Faculty of Civil Engineering, in special Armand Middeldrop, Jane Erkemij, and Patricia van der Bos for their contribution. Additionally, I would like to thank Marlies Nijemeisland and Durga Mainali for their help in the physics lab and chemical lab of the Faculty of Aerospace Engineering. Last but not least, I would like to acknowledge the great support I had from friends and family during my thesis.

Delft, June 14, 2021

CONTENTS

ABSTRACT

Purpose

Currently, the space industry is dominated by traditional highly toxic propellants which typically consist of hydrazine. Since the REACH makes provisions for a ban on hydrazine and due to the awareness about environmental sustainability, there is an urgent need for a feasible alternative propellant. A green hybrid bi-propellant would offer a reliable, safe, cost-efficient alternative that has the capability of numerous firings and throttling. By making use of hypergolic ignition, the complexity and mass of the ignition system can be reduced. Catalytically induced hypergolic ignition can be achieved by suspending a suitable catalyst to the fuel in combination with the right oxidizer.

Development of the Viscoelastic Fuel for the Hybrid Bi-propellant System

The viscoelastic nature of the fuel is achieved by making use of gelling technology whereby the viscosity of fuel is altered due to the formation of a weak cohesive internal structure. Alcohol will form the basis of this green fuel, as alcohols are green, non-toxic, and economically beneficial. Low carbon chain alcohol such as ethanol (EtOH) will form the basis of the fuel. To investigate the influence of the fuel's carbon length on the viscoelastic behaviour, butanol (BuOH) fuel too was investigated. As a gelling agent, an organic gelling agent is favoured due to the additional positive heat of formation to the fuel, improving its performance. The literature revealed that propyl cellulose showed promising results and that the presence of an -OH group has a synergistic effect with the catalyst. Therefore, the gelling agents hydroxypropyl cellulose (HPC) and hydroxypropyl methylcellulose (HPMC) are selected. The critical concentration is found based on an observational study. It resulted in a formulation of four samples with critical gelling concentrations. For ethanol fuel solidification, 3.5% HPC is the required critical concentration. As for the butanol fuel, it was around 3.0 wt% HPC. With the gelling agent HPMC, ethanol and butanol solidification was unsuccessful as the methyl-groups prevent the connection between the OH-group of the alcohol to the propyl cellulose of the gelling agent. Water needs to be introduced to obtain a solidified fuel as water acts as a bridge. The ethanol fuel showed solidified behaviour at compositions of 15 wt% water and between 4.5 wt% and 5.0 wt% of HPMC. The butanol fuel showed solidification at a lower concentration of the gelling agent, namely at compositions of 15 wt% water and between 4.0 wt% and 4.5 wt% of HPMC. This difference could be due to the length of the carbon chain. Butanol has a carbon chain that is twice as long as the carbon chain of ethanol. This longer chain results in the packing of molecules that is more viscous.

The rheology study was performed to analyse and characterize the viscoelastic nature of the gelled fuel. The main characteristics to evaluate the fuel's viscoelastic nature are its Linear Viscoelastic Range, yield point, and loss factor, which expresses the ratio between the viscous modulus (G") over the elastic modules (G’). The Linear Viscoelastic Range (LVR) indicates the range at which the internal structure remains intact and can be investigated via an amplitude stress sweep study with a frequency of 5 Hz. When G" > G’, the fuel shows a gel-like or solid structure and can be termed a viscoelastic solid material. The butanol fuel gelled with HPMC has a longer linear viscoelastic range than ethanol fuel (see Figure 1). The yield point indicates the transition from a gel-like (elastic dominant) to a liquid-like state (viscous dominant) induced by shearing. A stress ramp study with a time duration of 30 s revealed that fuels gelled with HPMC have a higher yield point than fuels gelled with HPC, this is independent of alcohol basis (Figure 2). The loss factor and time-dependent behaviour can be investigated via a frequency sweep study with frequencies between 0.1 Hz and 10 Hz. It revealed that fuels gelled with HPC show less dependency on frequency than fuels gelled with HPMC. Additionally, fuels gelled with HPC show behaviour that is more closely resembling that of an ideal elastic material than with HPMC.

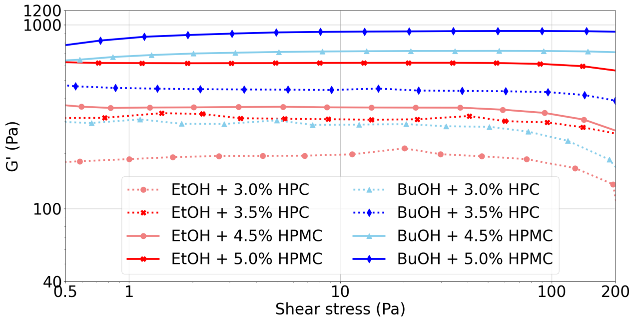

Figure 1: Amplitude stress sweep study to obtain the Linear Viscoelastic Range

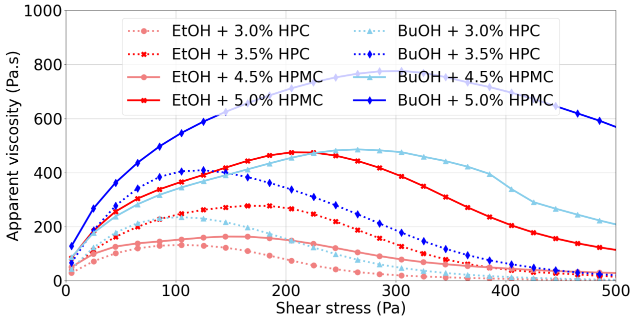

Figure 2: Shear stress ramp study to obtain the yield point

Table 1: Overview of the results of the rheology study of the fuel including its Linear Viscoelastic Range, yield point, and time-dependent behaviour

Composition of the Fuel	LVR (Pa)		Yield Point (Pa)		Time-dependent behaviour	
	t = 4 / t=5 $days$	t = 35 $days$	t = 4 / t=5 $days$	t = 35 $days$	t = 4 / t=5 $days$	t = 35 $days$
EtOH + 3.0% HPC	62	104	110	90	G' >G"	G' = G" at 8.3 Hz
EtOH + 3.5% HPC	95	92	175	120	G' = G" at 9.3 Hz	G' = G" at 8.9 Hz
BuOH + 3.0% HPC	51	112	105	90	G' >G"	G' = G" at 8.8 Hz
BuOH + 3.5% HPC	117	172	120	130	G' >G"	G' >G"
EtOH + 4.5% HPMC + 15% DI water	47	88	135	130	G' = G" at 8.5 Hz	G' = G" at 9.1 Hz
EtOH + 5.0% HPMC + 15% DI water	88	144	220	190	G' >G"	G' >G"
BuOH + 4.5% HPMC + 15% DI water	239	239	275	210	G' = G" at 0.2 Hz	G' >G"
BuOH + 5.0% HPMC + 15% DI water	237	224	310	280	G' >G"	G' >G"

The stability study for one month was performed to observe the gelled fuel's viscoelastic behaviour during storage. During this study, it was found that most fuel samples showed a large increase in LVR (>50%), and only some showed a slight change or remained constant. Additionally, the yield point decreased over time for all fuel samples except for the butanol fuel gelled with 5.0 wt% HPC. See Table 1 for an overview of all the results. A temperature study ranging from 0 ^oC to 45 ^oC was attempted as well. Due to the dysfunctioning of the temperature control of the rheometer, several issues were encountered. The temperature study showed that the apparent viscosity of the fuel has a strong dependency on especially the higher temperatures.

Achieving a Hybrid Bi-propellant Hypergolic System

A suitable oxidizer for the gelled fuel is highly concentrated hydrogen peroxide. This oxidizer decomposes into environmentally friendly products such as oxygen, water, and heat. Additionally, hydrogen peroxide is not a carcinogen and does not cause systemic toxicity. However, the oxidizer hydrogen peroxide had additional stabilizing elements. These elements could affect the catalyst performance to achieve hypergolicity for a wide range of applications. So, pure hydrogen peroxide is desired for propulsion application. Based on ion chromatography and inductively coupled plasma mass spectrometry analysis of different hydrogen peroxide samples, it was discovered that 90% H2O2 made from a 30% H2O2 1 L bottle results in the purest oxidizer.

A hypergolic system is achieved by suspending a suitable catalyst to the fuel by lowering the fuel's activation energy. The investigated catalysts are; iron(II, III)oxide, manganese(III)oxide, copper(II)oxide, and manganese(II)acetylacetonate. These are selected based on their environmental impact or already proven capabilities. The concentration added to the system is 2.5 wt%. The hypergolicity was examined with a multi-drop test executed at atmospheric conditions. The results of these experiments showed that catalysts iron(II, III)oxide, manganese(III)oxide, and copper(II)oxide are unable to lower the activation energy of the fuel sufficiently to achieve ignition. Also, no signs of potential, such as fizzing of the hydrogen peroxide or sparkling, were visible. On the other hand, 2.5% manganese(II)acetylacetonate did achieve ignition in both the ethanol fuel gelled with HPC and the ethanol fuel gelled with HPMC.

As the propellant consisting of ethanol gelled fuel with 2.5 wt% manganese(II)acetylacetonate and highly concentrated hydrogen peroxide did achieve ignition, its performance is further analysed. The critical catalyst concentration for testing under atmospheric conditions is equal to 2.5wt%. However, in a pressurized propulsion system, this critical concentration will likely be around 2.0wt% or below. The main parameters to characterize the propellant performances are the Ignition Delay Time (IDT), the regression rate, and the energy content. Since a calorimeter is unavailable, the energy content is examined based on the temperature profile. The results are presented in Table 2. For all compositions, the average IDT is above the desired <100 ms for all the experiments performed at atmospheric conditions. The temperature profile showed around 20% to 30% of the temperature was lost over an area of only 1 cm. It confirms that the IDT of the fuels will decrease when tested in a propulsion system.

Table 2: Overview of the results of the analysis of the performance of the propellant including its Ignition Delay Time, regression rate, and energy content

Composition of the Fuel	Ignition Delay Time		Regression rate		Energy content	
	Droplets (-)	IDT (ms)	Burn time (s)	Regression rate (mm/s)	Temp. at grain	Temp. in flame
EtOH + 3.5% HPC + 2.0 % Mn(acac)2	2.3	1003	-	-	-	-
EtOH + 3.5% HPC + 2.5 % Mn(acac)2	1.5	538	44	0.10	>1260 ^{o}C	± 1260 ^{o}C
EtOH + 3.5% HPC + 3.0 % Mn(acac)2	1.3	342	38	0.12	-	-
EtOH + 5.0% HPMC + 15% DI water + 2.0% Mn(acac)2	2.0	894	-	-	-	-
EtOH + 5.0% HPMC + 15% DI water + 2.5% Mn(acac)2	2.6	1320	43	0.11	>1260 ^{o}C	± 1260 ^{o}C
EtOH + 5.0% HPMC + 15% DI water + 3.0% Mn(acac)2	2.4	1207	>46	<0.10	-	-

The ignition process of ethanol fuel gelled with HPC can be seen in Figure 3. The clear white dot of light indicates the fuel's potential to ignite, but the fuel's auto-ignition temperature has not yet been achieved. Due to the addition of water and methyl group presence in the HPMC, foam formed during the ignition process of the gelled ethanol fuel (see Figure 4). This foam formation is an unfavourable feature and leads to a longer IDT. The water and foam act as heat sink, absorbing the heat formed during the ignition process, delaying the ignition. Furthermore, ethanol fuel gelled with HPC performance is predictable, while the performance of the ethanol fuel gelled with HPMC lacks this consistency.

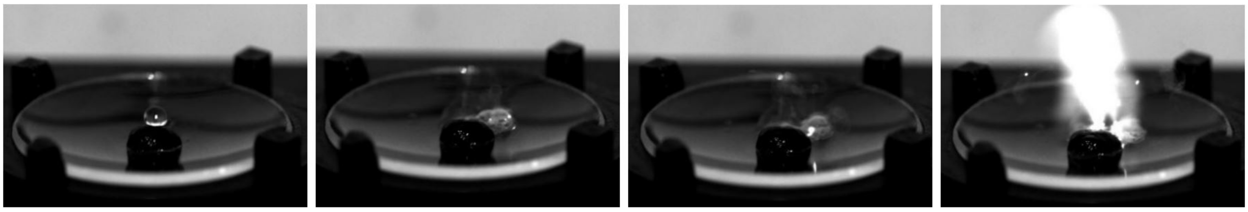
Moment of first contact | Fizzing of H2O2 and sparkling | Clear white dot of light | Ignition

Figure 3: Ignition process of ethanol fuel gelled with HPC and Mn(acac)2

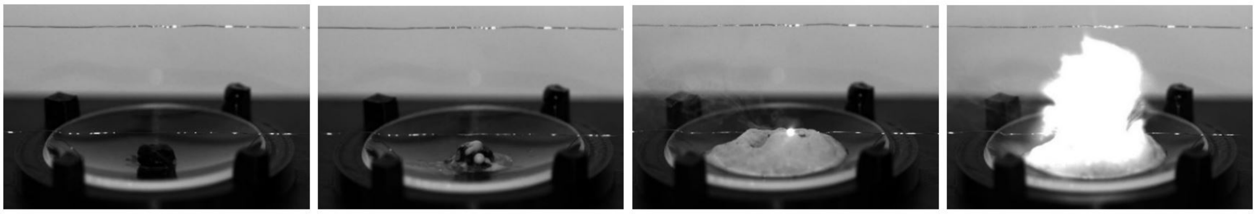
Before impact of droplet | Formation of foam | Foam covering entire fuel and clear white dot of light | Ignition

Figure 4: Ignition process of ethanol fuel gelled with HPMC and Mn(acac)2

In conclusion, the formulation of the ethanol fuel gelled with HPC is less complex, and the critical concentration of gelling agent is lower. Furthermore, the ignition process is without foam formation and the IDT is shorter. Additionally, the performance is of ethanol fuel gelled with HPC is more consistent. Hence, ethanol fuels gelled with HPC and catalysed with manganese(II)acetylacetonate show the most promise as a green alternative hypergolic propellant with highly concentrated hydrogen peroxide as oxidizer.

LIST OF FIGURES

LIST OF TABLES

Nomenclature

List of Abbreviations

b	Below detection limit
CD	Controlled strain mode
CS	Controlled stress mode
DASML	Delft Aerospace Structures and Materials Laboratory
DI water	Deionized water
ESA	European Space Agency
g	Gas formation influenced detection
h	Above detection limit
HCS	Hazard Communication Standard
IC	Ion Chromatography
IC PMS	Inductively coupled plasma mass spectrometry
IDT	Ignition Delay Time
LVR	Linear Viscoelastic Range
ppb	Parts per billion
ppm	Parts per million
REACH	Registration, Evaluation, Authorization and restriction of CHemicals
SVHC	Substance of very high concern
TFK	Fine gauge K-type Thermocouple
wt%	Weight percentage

List of Chemicals

BuOH	Butanol
CCAT	Copper(II)chloride
EtOH	Ethanol
H2O	Water
H2O2	Hydrogen peroxide
HPC	Hydroxypropyl cellulose
HPMC	Hydroxypropyl methylcellulose
IRFNA	Inhibited red fuming nitric acid
LAH	Lithium aluminium hydrid
LOX	Liquid oxygen
MC	Methylcellulose
MCAT	Manganese(III)acetylacetonate
MMH	Monomethylhydrazine
Mn(acac)2	Manganese(II)acetylacetonate

MON	Mixed oxides of nitrogen
N2O	Nitrous oxide
NTO	Nitrogen tetroxide
PDCPD	Polydicyclopentadiene
PVP	Polyvinylpyrroliadine
UDMH	Unsymmetrical dimethylhydrazine
WFNA	White fuming nitric acid

List of Symbols

δ	Damping factor in $[-]$
$\dot{r}$	Regression rate in mm/s
τ	Shear stress in Pa
A	Area in m^2
C	Specific heat of water in $J/^oC$
E_a	Activation energy in J/mol
f	Frequency in Hz
$G"$	Viscous modules in Pa
G'	Elastic modules in Pa
H	Heat released by combustion in J
h	Height of the grain in mm
k	Reaction rate constant in $[-]$
m	Mass of the water in g
R	Universal gas constant in $J/K\ mol$
r	Radius in m
T	Temperature in K
t	Time after production in $days$
t_{burn}	Burn time in s

1

INTRODUCTION

The space industry is dominated by traditional highly toxic propellants, namely hydrazine. Hydrazine is an inorganic compound with the chemical formula N_2H_4 and is highly toxic. Due to its carcinogenic nature, it is a substance of very high concern (SVHC). Provided the propellant hydrazine is identified as SVHC, its use within the European Union is subjected to authorization under the REACH Regulation. The REACH makes provisions for a ban on hydrazine [4], increasing the pressure on finding a feasible alternative propellant. Additionally, in society, there is more awareness about environmental sustainability, so is the space industry. It results in a need for so-called "green propellants" for space applications. An overview of the requirements for such an alternative propellant can be seen in Table 1.1.

Unlike the car industry, green propellants for space applications are still in their infancy. Therefore, also no universally accepted definition of a green propellant exists. It is more or less standard to define it as a propellant with low toxicity. However, no standards are available that define "low" toxicity. The low toxicity is mainly of importance during the handling of the propellant. Chemical characteristics such as low vapour pressure will decrease the likelihood of imposing dangerous levels of gas due to accumulation [5]. ESA even takes it a step further, as they aim to reduce air pollution during rocket launches. Green propellant's additional benefit is; the reduced toxicity and ease of handling make it feasible to decrease the transport and storage cost [6].

Table 1.1: Top level requirements

Label	Requirement description
PROP – TOP – 1	The propellant shall be eco-friendly
PROP – TOP – 2	The propellant shall be non-hazardous.
PROP – TOP – 3	The ignition delay time of the propellant shall be below 100 ms
PROP – TOP – 4	The propellant shall ignite by a simplified ignition system
PROP – TOP – 5	The performance of the propellant shall be comparable to existing propellants

The focus of this research is on a green hybrid bi-propellant. Bi-propellant consists of two components, an oxidizer, and a fuel, kept in separate compartments before combustion. See Figure 1.1[1] for a basic system illustration. For a green propellant, both the oxidizer and fuel are green. A hybrid system defines that the propellant consists of two phases. In the classical configuration, the oxidizer is in a liquid state and the fuel in a solid. A hybrid bi-propellant is chosen due to its many advantages, as can be seen in Table 1.2. In general, they are safer and more robust than conventional chemical propulsion systems. This is due to the phase difference between the oxidizer and fuel. The phase difference prevents rapid mixing in the event of failure [7]. And the system is relatively simple, which typically reduces the cost and increases reliability. Regarding performance, hybrid rocket motors have a higher specific impulse than solid rocket motors and a higher density specific impulse than liquid bi-propellant rocket engines. Additionally, hybrid systems can have numerous firings, which is beneficial for orbital control. Lastly, hybrid rocket engines are capable of throttling by changing the oxidizer flow rate (usually by a throttling valve in the oxidizer feed line) [8]. Hence, hybrid systems have benefits related to safety, cost, and performance.

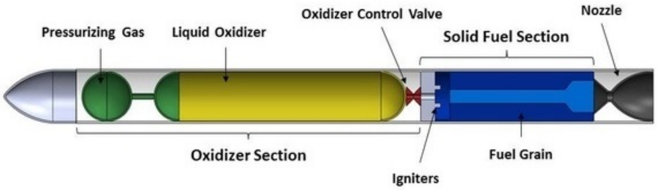

Figure 1.1: Basic system illustration of a hybrid bi-propellant rocket engine [1]

---

[1] https://www.machinedesign.com/3d-printing-cad/article/21835784/will-3dprinting-prepare-hybrid-rocket\-for-takeoff [visited:13-11-2020]

Table 1.2: Advantage and disadvantage of different propulsion systems (based on [2])

Propulsion system	Disadvantage	Advantage
Liquid rocket engine	- Complex due to pumping system of the fuel and oxidizer - High mass of propulsion system	- High specific impulse - Throttleable - Can be shut down
Solid rocket engine	- It can never be switched off by command - Cannot be throttled	- It can provide huge amounts of thrust, and therefore it is often used as a booster - Very simple and therefore reliable
Hybrid rocket engine	- Low burn rate as the mixing between the oxidizer and fuel is more difficult	- Quite simple in construction - Throttleable and can be shut down - Very safe since the fuel and oxidizer can be stored and shipped individually, and each component by itself is completely safe - Higher density specific impulse than liquid bi-propellant rocket engines

As a source of ignition, ignition by hypergolicity is desired due to its advantage of high reliability, reduce mass, reduced complexity of the fuel ignition system, and its capabilities for controlled use of the propulsion system. In Table 1.3 the advantage and disadvantage of different ignition methods can be seen. Hypergolic ignition means that the fuel and oxidizer ignite spontaneously upon contact. It should happen in a few milliseconds. There are combinations of oxidizers and fuels known that are hypergolic. The most widely used hypergolic propellants are hydrazine derivates with nitrogen tetroxide as the oxidizer [9]. These propellants are hypergolic by nature. The currently used nitrogen tetroxide (NTO) and monomethylhydrazine (MMH) or unsymmetrical dimethylhydrazine (UDMH) are all highly toxic. Hence, unsuited as a green bi-propellant. Based on the literate study [3], green bi-propellants are not hypergolic by nature. With a suitable catalyst, hypergolicity can be achieved by lowering the activation energy. Although adding more catalysts to a fuel reduces the ignition delay time, it adversely affects the combustion and decreases the energy efficiency of the propellant [10]. By suspending the catalyst to the fuel [11], the decomposition of hydrogen peroxide (the oxidizer) followed by auto-ignition of the fuel without an external ignition source is achieved in bi-propellant mode. Hence, the topic of this research.

Table 1.3: Advantage and disadvantage of different ignition methods (based on [3])

Ignition method	Disadvantage	Advantage
Spark ignition	- Requires hardware which increases the mass of the propulsion system - Mostly effective to ignite a liquid rocket engine	- Repeated starts - Most suitable for smaller rocket engines
Hypergolic ignition	- Current hypergolic bi-propellants are highly toxic - May ignite spontaneously on contact with air [2]	- No ignition system required - Simple design and therefore reliable - Numerous firerings possible
Catalytic ignition	- Short life cycle due to catalyst - High temperatures are not possible - Catalyst bed increase mass and size of the propulsion system - Pressure drop issues	- Lowers the activation energy of the fuel

A promising candidate is a gelled alcohol with a short carbon chain as fuel and hydrogen peroxide as an oxidizer. These components are found based on a trade-off. For operational purposes, there are several oxidizers commonly used in the space industry, these are shown in Table 1.4. Of these, only three liquid oxidizers are green [2], namely liquid oxygen (LOX), hydrogen peroxide (H2O2), and nitrous oxide (N2O). Because liquid oxygen is stored at cryogenic temperatures, this option is ruled out. For hydrogen peroxide, a high concentration is desired to generate sufficient heat during decomposition at standard pressure. Therefore, High Test Hydrogen Peroxide is often used as a propellant. These solutions contain at least 85% to 98% of hydrogen peroxide. An additional benefit of a high concentration of hydrogen peroxide is that the solution becomes more stable with a higher peroxide content. Both hydrogen peroxide and nitrous oxide decompose in only environmentally friendly products. However, the density of hydrogen peroxide (1.45 g/cm^3) is higher than that of nitrous oxide ($1.53 \cdot 10^{-3}$ g/cm^3). The molar mass of nitrous oxide is 44.013 g/mol, while the molar mass of hydrogen peroxide is only 34.0147 g/mol. Lower molar mass will ultimately result in a higher specific impulse, and therefore hydrogen peroxide is selected as oxidizer [12], [13]. Additionally, due to the foundation of SolvGE, hydrogen peroxide in any desired concentration becomes easily available, overcoming logistic issues.

Table 1.4: Advantage and disadvantage of common oxidizers

Oxidizer	Disadvantage	Advantage
Nitric acid	- Toxic	- Hypergolic properties
Nitrogen tetroxide	- Toxic	- Hypergolic properties
Liquid Oxygen	- Stored at cryogenic temperatures	- Green
Hydrogen Peroxide	- High freezing point	- Green - Molar mass of 34.0147 g/mol - Became easily available via SolvGE
Nitrous oxide	- Molar mass of 44.013 g/mol - Gas state at room temperature	- Green

As a fuel, lower carbon chain gelled alcohols are promising. The gelling of the liquid fuel provides a solution for the difficult mixing of the oxidizer and fuel typically associated with hybrid rocket engines. While introducing a catalyst to fuel, its solubility is important. Gelled alcohols seem a promising fuel with ease of ignition and acceptable delay time with the suspension of catalyst in gel medium. Also, the literature study revealed promising temperature profiles [14], rheology characteristics [15], and ignition delay times [16], [17].

The purpose of this thesis is grasped into the following objective: *To investigate and develop a novel green hybrid bi-propellant hypergolic system with a viscoelastic nature of the fuel.* To answer this, the following two main questions with sub-questions are formulated;

1. **How to develop a viscoelastic fuel for a hybrid bi-propellant system?**
    (a) What kind of fuel can be used that is greener in nature and can be used in hybrid systems?
    (b) How can the liquid fuel be transformed into a solid phase through viscoelasticity?
        - What approach should be used to achieve viscoelastic behaviour?
        - Which thickening agent can be used to achieve a viscoelastic nature?
        - How can the weight percentage of the thickening agent be minimized such that it does not compromise the performance and the viscoelastic nature of the fuel?
    (c) What are the characteristics of the solid fuel?
        - How does the solid fuel behaviour in terms of viscoelastic nature?
        - How does the solid fuel behaviour change over time?

2. **How to achieve a hybrid bi-propellant hypergolic system?**
    (a) What kind of oxidizer can be used to achieve a green hypergolic bi-propellant system?
    (b) How can the green propellant be made hypergolic?
        - What type of catalyst can be used to achieve hypergolic ignition?
        - How can the weight percentage of the catalyst be minimized such that it does not compromise the performance and still a hypergolic system is achieved?
    (c) What are the characteristics of the hypergolic system in terms of its performance?
    (d) Which type of fuel is most promising to further develop a novel green hybrid propellant system?

To answer these research questions it is deemed most fitted to perform experimental research rather than using models to simulate the transformation from liquid to solid or define the performance characteristics of the propellant. This research will focus on using already existing technology and chemicals, but bringing this technology to the next level and improve the system. The literature describes general techniques to solidify a substance, however, these papers discuss processes involving high concentrations of gelling agent to achieve a gelled system. This is unsuited for propellant applications as it decreases the energy content of the system. This thesis research will focus on optimizing the existing technology to further improve the formulation of the fuel such that it is suitable for propulsion applications. The same holds for the techniques to achieve hypergolicity in substances that are not hypergolic by nature. The literature describes catalysts that are capable of lowering the activation energy sufficiently. But again, large concentrations were used, which is not promising for a propellant. By lowering these concentrations, the performance of the propellant can be improved. Because of this lack of knowledge, a model or simulation could not be used. A model or simulation is only as good as the rules used to create it. It is very difficult to create an entirely realistic model or simulation because assumptions are based on research and past events. As no research has been done on this topic, it is considered appropriate to first do proper experimental research to confirm whether it is possible to decrease the concentrations of components that have a negative effect on the energy content of the system. Hence, the reason for performing intensive research based on experiments to achieve the objective of this research.

To realize this objective, the rest of this report is structured as follows: Chapter 2 describes the oxidizer most suited for this hybrid bi-propellant system (answering question 2a). Then the formulation of the green fuel is described in Chapter 3 and answers question 1a and 1b. Chapter 4 provides the methods and results to evaluate the viscoelastic behaviour of the fuel (answering question 1c). After this, the investigation into a suitable catalyst to achieve ignition, question 2b, is explained in Chapter 5. Followed by Chapter 6 which describes the analysis of the novel propellant in terms of its performance, answering question 2c. Lastly, the conclusion is made in Chapter 7 to reveal the answer to question 2d. Additionally, recommendations to further develop this novel green hybrid bi-propellant system are provided.

2

COMPOSITION OF THE OXIDIZER

The oxidizer of the novel bi-propellant will be highly concentrated hydrogen peroxide. Typically, stabilizers are added to prevent the decomposition of hydrogen peroxide. Therefore, the oxidizer will not only consist of an aqueous solution of hydrogen peroxide, but additional elements will be present. These elements affect the performance of the propellant as the catalyst can be sensitive to these elements. Therefore, it is of interest to know what elements are present and in what concentration. When this is known, the behaviour of the propellant can be better understood. Additionally, to use hydrogen peroxide for a wide range of applications, there are restrictions to certain elements. For example, chloride ion causes corrosion and should not be present in the oxidizer. To comply with most regulations, if present, the foreign elements should not exceed a concentration of 20-25 ppm. The hydrogen peroxide available to use as oxidizer is given in Section 2.1. Elements that can be expected to be present in the oxidizer are shown in Section 2.2. By performing an ion chromatography analysis (Section 2.3) and inductive coupled plasma mass spectrometry analysis (Section 2.4) the present elements are investigated. An overview of the results and a conclusion about which oxidizer is best to use is given in Section 2.5.

2.1. HYDROGEN PEROXIDE

Hydrogen peroxide is considered a green option as oxidizer. The decomposition of hydrogen peroxide results in solely environmentally friendly products as only oxygen and water are formed along with heat. Furthermore, hydrogen peroxide is not considered to be carcinogenic. The main health effects are irritation at the site of contact, but it does not cause systemic toxicity [18]. Other benefits of hydrogen peroxide as oxidizer are that it is easily accessible via SolvGE, storable at room temperature, non-sensitive to impact, and has a low vapour pressure. The only direct downside is its high freezing point, which forces strict temperature restrictions for use in space. Hydrogen peroxide is a chemical that consists of three covalent bonds. The most important parameter is its concentrations. Although pure hydrogen peroxide exists, it is more common as a percentage of concentration in aqueous solutions, whereby the solvent is water (H_2O). To use hydrogen peroxide as oxidizer for propellant, high concentrations of at least 85% are required.

During this research, samples with different concentrations of hydrogen peroxide will be analyst. One can order a bottle of 30% hydrogen peroxide or a bottle of 50% hydrogen peroxide. Those two will be analyst to investigate what type of elements are used to stabilize the hydrogen peroxide, in what concentration those elements are present, and if there is a difference in stabilizers based on the concentration of hydrogen peroxide. By analysing both the 30% hydrogen peroxide sample and the 50% hydrogen peroxide sample, it can be observed if there is a difference in type and/or concentration of elements. Additionally, SolvGE has developed a technique to increase the hydrogen peroxide concentration. However, it is unknown what kind of effect this has on the stabilizers. Therefore, also two highly concentrated hydrogen peroxide samples will be analysed. One sample will be based on the 30% hydrogen peroxide, and one sample will be based on the 50% hydrogen peroxide. Hence, in total four different samples will be analyst;

- 30% hydrogen peroxide (from production bottle)
- 50% hydrogen peroxide (from production bottle)
- 90+% hydrogen peroxide made from 30% hydrogen peroxide
- 90+% hydrogen peroxide made from 50% hydrogen peroxide

2.2. EXISTING STABILIZERS

To stabilize hydrogen peroxide, organic or inorganic compounds can be used. The effectiveness of inorganic stabilizers is low as the solubility of inorganic compounds in strong acid peroxide solutions is small. As a result, either a cloudy solution is obtained or not enough stabilizer can be introduced [19]. However, hydrogen peroxide is a weak acid, so it might be the case that hydrogen peroxide is stabilized with organic compounds. A few patent-pending and existing stabilizers are listed below:

- Pyroprosphoric acid: Hydrogen peroxide solutions can be stabilized with pyrophosphoric acid due to the stabilizing effect of the hydrogen ion and pyrophosphate ion. This stabilizer only shows small losses when hydrogen peroxide is stored for long periods at temperatures observe above that of normal storage temperature. Additionally, to stabilize the hydrogen peroxide only small amounts (0.025 g to 1.5 g) of pyrophosphoric acid are dissolved per liter of hydrogen solution [19].

- Carboxylate stabilizer: A carboxylate is the conjugate base of a carboxylic acid and can be added to the hydrogen peroxide as sodium citrate, sodium malonate, or sodium phytate. The stabilizer slows down the normal rapid decomposition of peroxide.
- Poly vinyl alcohol: It is found that Poly vinyl alcohol stabilizes hydrogen peroxide placed on a paper substrate following exposure to air. The addition of poly vinyl alcohol to hydrogen peroxide significantly suppressed its degradation [20].
- Ascorbic acid: This stabilizer is non-toxic, water-soluble and stable in air. Due to its non-toxic nature, it is also used for food products. It can be used to stabilize hydrogen peroxide on its own, but recently it is also tested using a mixture composed of sulfuric acid and hydrofluoric acid [21].
- Akali metal meta- and pyrophosphates: To stabilize aqueous hydrogen peroxide solutions catalysed by a combination of iron and copper, alkali metal meta- and pyrophosphates can be added to the solution. This results in an effective solution to prevent decomposition.

These stabilizers give a direction about the elements that can be expected to stabilize the hydrogen peroxide. Elements that can be expected are phosphorus (P), sulfur (S), fluor (F), sodium (Na), phosphate (PO4), and sulfuric acid (SO4) but to be sure, a detailed analysis will be performed to detect as many elements as possible.

2.3. ION CHROMATOGRAPHY ANALYSIS

Chromatography is used to determine the content of a chemical when the content is unknown. In ion chromatography (or ion-exchange chromatography) ions and polar molecules are separated based on their affinity to the ion exchanger. It can be used to detect almost any charged molecule, including proteins, nucleotides, and amino acids. The Civil Engineering WaterLab has a Metrohm IC that can measure inorganic and short-chain organic anions and cations. A picture of the IC can be seen in Figure 2.1[1]. The device is capable of detecting the ions of; fluor (F), natrium (Na), magnesium (Mg), calcium (Ca), chlorine (Cl), bromine (Br), and potassium (K). Furthermore, the following polyatomic ions could be measured; nitrate (NO3), nitrite (NO2), sulfate (SO4), phosphate (PO4), and ammonium (NH4). It is unknown which elements to expect in the hydrogen peroxide samples, however, based on the existing stabilizers fluor (F), sodium (Na), phosphate (PO4), and sulphuric acid (SO4) could be present. However, the analysis will be including all elements measurable by the Metrohm IC. A typical test will take around 30 minutes. The concentrations measured using IC are in the range of parts per million (ppm). This is very suited as it is in line with the range of interest, as one of the goals is to determine if the concentrations are below 20-25 ppm.

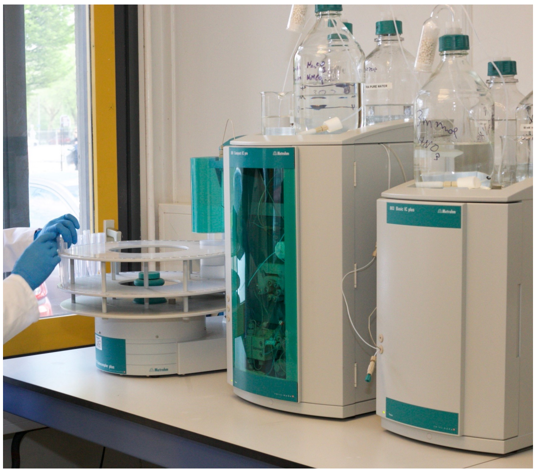

Figure 2.1: Metrohm IC present at the WaterLab of Civil Engineering [1]

2.3.1. PREPARING THE SAMPLES

Four different samples had to be analysed as explained in Section 2.1. The minimum sample size the IC machine can handle is 3 mL, however, it is more common to use 10 mL for a sample. To prepare the samples, they had to be filtered using a 0.45 micrometer filter. The syringe can be screwed on top of the filter. Then the piston can be removed from the syringe to pour the sample into the syringe. The piston can then be placed back into the syringe to press the liquid

---

[1] `https://www.tudelft.nl/citg/over-faculteit/afdelingen/watermanagement/research/waterlab/equipment/ion-chromatography-ic` [visited: 04-06-2020]

through the filter. A new syringe and a new filter should be used for every sample. Filtering the samples with 30% H2O2 (sample A2) and 50% H2O2 (sample B2) was very easy. For the sample containing 90% H2O2 made from 30% H2O2 (sample C2), already a bit more pressure was needed to force the fluid through the filter. For the sample containing 90% H2O2 made from 50% H2O2 (sample D2), a lot of pressure was required to filter the samples. This caused gas formation in the sample. The samples are then stored in a refrigerator at 3 ^oC for a longer shelf life until the IC analysis is performed. In Table 2.1 and Table 2.2 the details of the samples can be seen.

Table 2.1: Composition of the samples used for IC analysis (samples A2, B2, C2 and D2)

Sample number	Content according to bottle	Measured Brix%	Concentration H2O2	Notes
A2	30% H2O2 diluted	- - -	- - -	Came from a leftover sample of last week (1L)
B2	50% H2O2	23.5	53.5 %	Came right from the production bottle
C2	30% H2O2 made to 90% H2O2	41	92.8 %	Produced by SolvGE
D2	50% H2O2 made to 90% H2O2	42.5	96 %	Produced by SolvGE

As the concentrations are expected to be within the measuring range of the IC device, dilution was not required. However, sample A2 was diluted due to insufficient quantity. The 30% hydrogen peroxide bottle was of insufficient volume to make a 10 mL sample and therefore this sample was diluted with DI water. This sample consists of 4.5 mL of 30% hydrogen peroxide and 5.5 mL of diluted water.

Table 2.2: Composition of the samples used for IC analysis (samples A4, B4, C4 and D4)

Sample number	Content according to bottle	Measured Brix%	Concentration H2O2	Notes
A4	30% H2O2	14.5 %	33 %	Came right from the production bottle (2.5L)
B4	50% H2O2	21 %	47.8 %	Came right from the production bottle
C4	30% H2O2 made to 90% H2O2	39.5 %	89.5 %	Produced by SolvGE
D4	50% H2O2 made to 90% H2O2	39.5 %	89.5 %	Produced by SolvGE

The sample of series 4 had a total volume of 5 mL per sample. This is in contrast to sample of series 2 which had a total volume of 10 mL per sample. Additionally, the 30% H2O2 from series 2 (sample A2) is from a 1L production bottle, while the 30% H2O2 from series 4 (sample A4) is from a 2.5 L production bottle. The samples from series 2 and 4 were in storage for respectively 13 and 15 days. The concentration of hydrogen peroxide was measured with an optical refractometer (ATC) on the day the samples were handed in (so not on the testing day), however, it is expected that the concentration of hydrogen peroxide will not decrease in such a short time frame.

2.3.2. RESULTS

The results of the first analysis can be seen in Table 2.3. The performance of the Metrohm IC is verified using a standard solution and a blank solution. The results from the verification can be seen in Table B.1. All elements are measured with an accuracy of <0.01%, only the elements F and NH4 are measured with an accuracy of <0.4%. Furthermore, in Table 2.3 a ratio of the 90% H2O2 over its "parent" is shown. It can be seen that there is not a constant factor of which the elements are increased with increasing concentration. Note that the $\frac{sample\ C}{sample\ A}$ is corrected for the dilution of the 30% H2O2 (sample A2). Thus sample A2 is corrected by $\frac{10}{4.5}$. Another interesting feature is that the ion Cl is only measured in sample A2. It is likely that this sample was contaminated, as one would otherwise expect sample C2 to also contain Cl. Furthermore, elements K and PO4 are measured in only sample C but not in sample A. This could be explained based on the detection limitations of the device. K could be present in sample A as well, but that the concentration is too low to detect. The only odd element is Mg, this is present in lower concentration in sample D compared to sample B. One would expect the concentration to increase and not decrease. It is unlikely that the technique used by SolvGE removes an element from the solution. This is furthermore supported by the fact that for samples A2 and C2 the concentrations do increase for the 90% H2O2. The only explanation for the odd Mg concentration is that contamination has occurred in sample B2, increasing its Mg concentration.

Table 2.3: Results of IC analysis series 2

Sample number		Sample A2 30% H2O2	Sample C2 90% H2O2	Sample B2 50% H2O2	Sample D2 90% H2O2	$\frac{Sample\ C}{Sample\ A}$	$\frac{Sample\ D}{Sample\ B}$
Element		Concentration (ppm)	Concentration (ppm)	Concentration (ppm)	Concentration (ppm)	Factor (-)	Factor (-)
Anion	F	5.43	25.08	19.64	44.90	2	2
	NO2	0.32	0.86	0.32	0.66	1	2
	NO3	0.54	2.65	40.94	209.29	2	5
	PO4	0.00	3.42	30.41	211.88	-	7
	SO4	0.78	4.23	0.60	18.43	2	31
	Cl	0.73	0.00	0.00	0.00	0	1
Cation	Na	2.64	5.65	18.51	105.55	1	6
	NH4	0.25	1.47	8.70	73.73	3	8
	Mg	0.06	0.24	0.97	0.28	2	0
	Ca	1.36	1.72	0.18	0.60	1	3
	K	0.00	2.57	0.00	0.00	-	1

The data of Table 2.3 is plotted and can be seen in Figure 2.2. To use the oxidizer for a wide range of applications, the concentrations of foreign elements should be below 20-25 ppm. The two horizontal lines represent that threshold. It can be clearly seen that 90% hydrogen peroxide made from 50% hydrogen peroxide (sample D2) contains concentrations above this threshold. This is undesirable as it limits the application purposes for the propellant. In Figure 2.3 a close up can be seen, the y-axis is shortened to 50 ppm. From this plot, it can be seen that the 30% H2O2 (blue bars) is quite pure when compared with the 50% H2O2 (red bar). These two samples came directly from the manufacture and hence it can be concluded that different stabilizers are used for different concentrations of hydrogen peroxide. For 30% H2O2 almost no stabilizers are used, while for 50% H2O2 the elements F, NO3, and PO4 are used in concentrations of 20 ppm or higher. When comparing the 90% hydrogen peroxide (green and yellow bars), the hydrogen peroxide made from 30% is therefore also purer than the one made from 50%. Therefore, the 90% H2O2 made from 30% is the most promising. For this sample, only the element F is higher than desired, as it is above the threshold of 20 ppm.

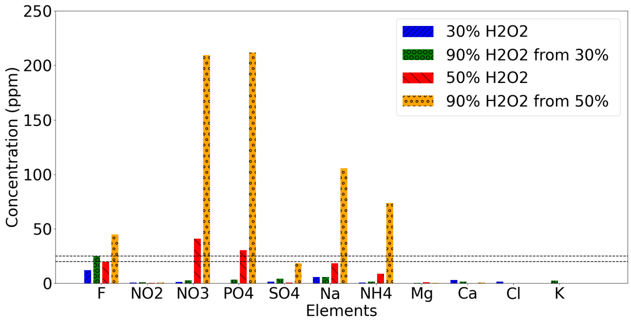

Figure 2.2: IC analysis of series 2

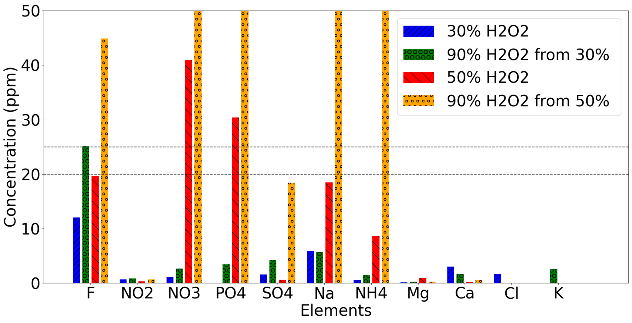

Figure 2.3: IC analysis of series 2 (close up)

A second analysis was performed on new samples. The fact that series 2 contained chloride was odd, and therefore new samples were made to redo the analysis to increase accuracy. Additionally, this time, the 30% H2O2 was not diluted and came straight from the production bottle. Also, a 2.5L bottle was used instead of a 1.0 L bottle. In Table 2.3 the concentrations measured for the 30% H2O2 sample were very low because the sample was diluted. IC analysis is not designed for such low concentrations and hence series 4 should have a more reliable result. The results can be found in Table 2.4. Firstly, it can be seen that the chloride concentration is now zero for all samples. Secondly, the factors between the 90% H2O2 over its "parent" are completely different this time. Before the $\frac{SampleC}{sampleA}$ was on average 2. This time the factor is 47 on average.

Table 2.4: Results of IC analysis series 4

Sample number		Sample A4 30% H2O2	Sample C4 90% H2O2	Sample B4 50% H2O2	Sample D4 90% H2O2	$\frac{Sample\ C}{Sample\ A}$	$\frac{Sample\ D}{Sample\ B}$
Element		Concentration (ppm)	Concentration (ppm)	Concentration (ppm)	Concentration (ppm)	Factor (-)	Factor (-)
Anion	F	33.29	97.49	46.45	77.18	3	2
	NO2	0.00	0.00	1.13	0.00	1	0
	NO3	2.62	258.27	44.25	193.80	99	4
	PO4	5.83	279.13	38.26	204.82	48	5
	SO4	0.94	18.74	5.41	20.97	20	4
	Cl	0.00	0.00	0.00	0.00	1	1
	Br	1.04	4.15	4.15	3.12	4	1
Cation	Na	1.38	112.22	18.31	78.00	81	4
	NH4	0.75	62.60	9.93	0.00	84	0
	Mg	0.00	0.53	0.00	0.23	-	-
	Ca	0.03	0.90	0.00	0.46	35	-
	K	0.00	1.60	0.00	0.00	-	1

The data of Table 2.4 is plotted and can be seen in Figure 2.4. It is immediately clear that this time the 90% H202 from 30% has concentrations much higher than was measured during the first test (Figure 2.2). Also, the element bromide is measured during this analysis. Its concentration is below the maximum limit of 20-25 ppb. When looking at the $\frac{sample\ D}{sample\ B}$ one can see that some elements decrease. This is the case for the elements NO2, Br, and NH4. These are different elements than the element Mg that showed this behaviour in the first test. A reason for this could be contamination of the samples. Since the concentrations are well below the maximum of 20-25 ppm, this does not affect the conclusions that can be drawn from this analysis.

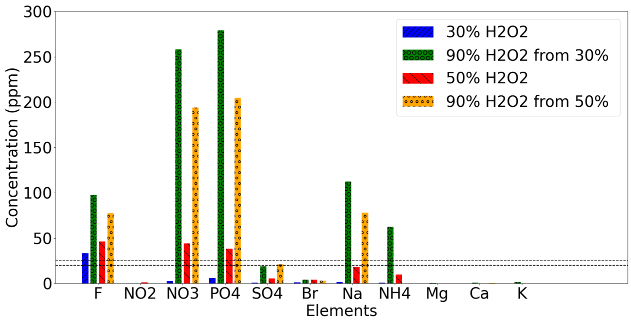

Figure 2.4: IC analysis of series 4

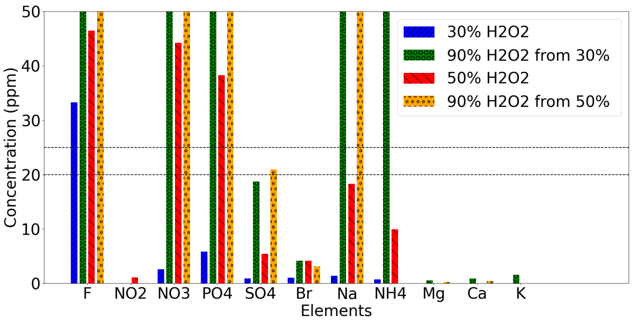

Figure 2.5: IC analysis of series 4 (close up)

The test results of both the first and second IC analysis are shown in Figure 2.6. In this plot, the elements of which all samples had a concentration below 2 ppm are not shown. Also, bromide is not shown as this was not tested during the first IC analysis. It can be observed that the concentrations of 50% H2O2 are very similar to each other. Also, the concentrations of the 90% H2O2 from 50% are similar to each other, only the HN4 is deviating as the second test did not contain any NH4. However, most noticeable is the extreme difference between the 90% H2O2 from 30%. This difference is so significant that something has to be happening. A meeting with solvGE revealed that a change in their technique had occurred between the first and second analysis. To increase their operation speed, two different samples were mixed. These mix samples had been increased to a high concentration of H2O2, decomposed, and were now increased in concentration again. This caused a tremendous increase in concentration in sample B4.

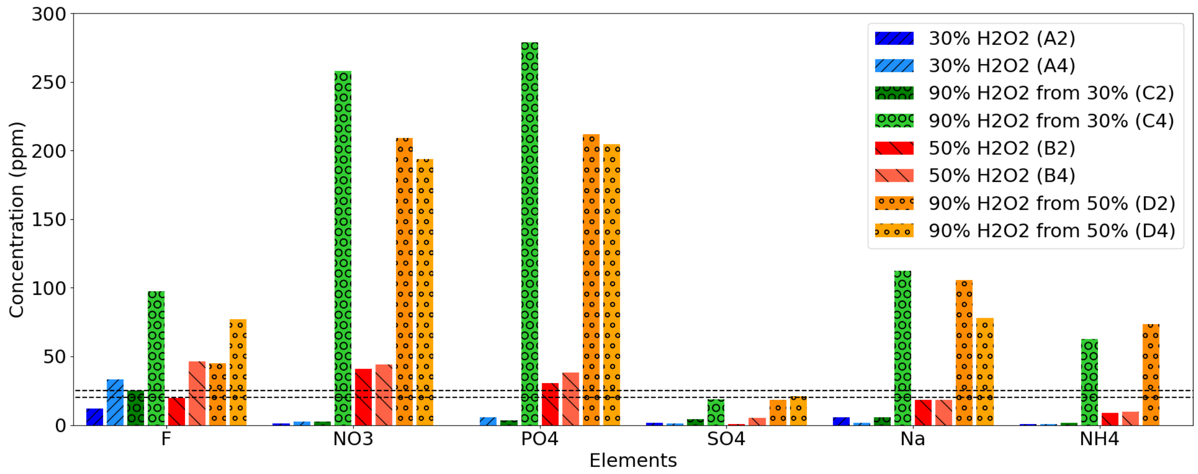

Figure 2.6: IC comparison between series 2 and series 4

The 30% H2O2 came from two different bottles, the first one (sample A2) came from a 1 L bottle while the second one (sample A4) came from a 2.5 L bottle. It can be seen that the concentrations vary between the two. Both samples do not contain the element K. Also the elements NO2, Mg, and Ca are not present in 1 L bottle, but they are present in 2.5 L bottle. On the other hand, PO4 is only present in 2.5 L bottle and not in 1 L bottle. Thus, although the manufacture sells these 30% H2O2 bottles as the same chemical, for different volumes of the bottle, different stabilizers are used.

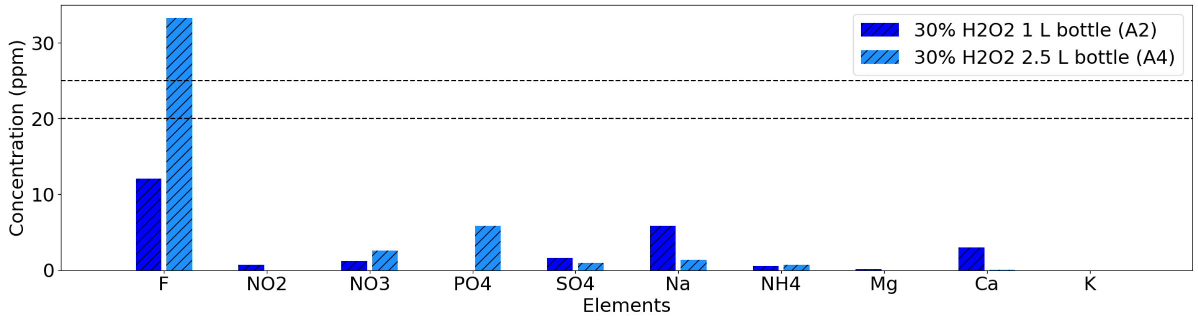

Figure 2.7: IC analysis of the 30% H2O2 for different volumes (1 L and 2.5 L)

2.4. INDUCTIVELY COUPLED PLASMA MASS SPECTROMETRY ANALYSIS

Inductively coupled plasma mass spectrometry (ICP-MS) is a type of mass spectrometry that uses an inductive coupled plasma to ionize the sample. It is capable of complex separations and has high sensitivity and selectivity. This allows for unambiguous peak identifications. The device is capable of detecting concentrations in the range of parts per billions. An ICP-MS is present at the faculty of Civil Engineering. Their device is from Analytik Jena model Plasma Quant MS. A picture of the device can be seen in Figure 2.8[2].

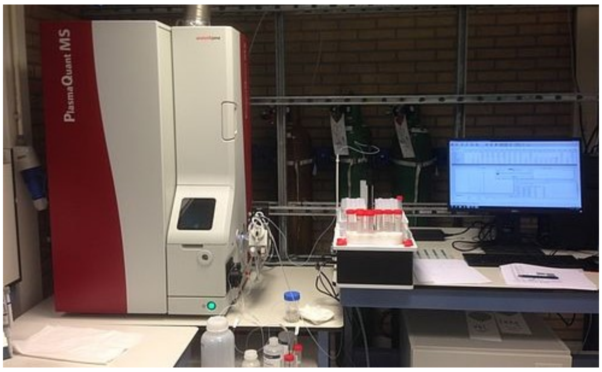

Figure 2.8: Metrohm IC present at the WaterLab of Civil Engineering [2]

---

[2] https://www.tudelft.nl/2017/citg/watermanagement/icp-ms-of-analytikal-jena-plasmaquant-ms [visited: 04-06-2020]

The advantage of ICP-MS over IC is that it is capable of measuring more elements. ICP-MS can detect 28 elements. However, the device can not handle chlorine (Cl) and therefore it has to be sure that the hydrogen peroxide samples do not contain chlorine. It is expected that the hydrogen peroxide samples will contain metal elements as these are typically used to stabilize H2O2. At least it is expected that the hydrogen peroxide samples contain the element phosphor (P).

2.4.1. PREPARING THE SAMPLES

The expected concentrations of metals are in the range of 20 ppm, and therefore it is not necessary to make a series of dilutions. To perform an ICP MS analysis, a sample size of 10 mL is required. Hence, the four combinations as described in Section 2.1 were made in a sample of 10 mL at the Lab of Civil Engineering. Before the hydrogen peroxide solution can be analyst by the ICP MS machine, they have to be acidified and filtered.

1. **Acidification**
   The total sample volume of 10 mL has to consist of 1 volume% nitric acid to acidify the sample. Therefore, the minimum volume is 9.9 mL of hydrogen peroxide solution with 0.1 mL of 69% HNO_3. One can use a pipet to exactly obtain the volume in the correct quantity. For every sample, a new pipet tip has to be used to not contaminate the sample. It is of importance to first add the hydrogen peroxide to the sample and secondly the nitric acid to avoid vigorous reactions. Also, adding the liquids should be under a 90-degree angle. Additionally, as safety precautions, one should wear gloves at all times. Furthermore, adding the nitric acid to the sample should take place in the foomhood while wearing extra thick gloves over the normal gloves.

2. **Mixing**
   After acidifying the sample, one can mix it by placing it on a vortex mixer (speed set at 7) for around 5 seconds.

3. **Filtering**
   Then the sample has to be filtered using 0.2 micrometer pores. The syringe can be screwed on top of the filter. Then the piston can be removed from the syringe to pour the sample into the syringe. The piston can then be placed back into the syringe to press the liquid through the filter. A new syringe and a new filter should be used for every sample.

The samples are kept in the refrigerator at $3^{o}C$ for longer shelf life. They will be analysed by a specialized employee who will provide the data with the results. For series 1, small amounts of samples were brought to the Civil Engineering lab. This made it more challenging to pipet the correct volumes of sample. Also, a lot of force was required to filter sample D. The details of all samples are shown in Table 2.5. According to the employee who executed the ICP SM analysis the samples showed gas formation, especially sample C. Due to this gas formation in the samples, these sample series could not be tested. The fact that only sample C has shown large quantities of gas formation, gave rise to the belief that sample C has a different element in it. An element that reacts with the nitric acid resulting in gas formation. The other samples do not have gas formation, or in sample A the concentration of the element might be too low to cause gas formation.

Table 2.5: Composition of the samples used for ICP MS analysis (samples A1, B1, C1 and D1)

Sample number	Content according to bottle	Measured Brix%	Concentration H2O2	Notes
A1	30% H2O2 (diluted)	- - -	- - -	Came from a leftover sample of last week (1L)
B1	50% H2O2	23.5	53.5 %	Came right from the production bottle
C1	30% H2O2 made to 90% H2O2	41	92.8 %	Produced by SolvGE
D1	50% H2O2 made to 90% H2O2	40.5 40.0	91.7 % 90.6 %	Produced by SolvGE

Therefore, a second series of samples was made. The details of these samples are shown in Table 2.6. For this series, the amount of sample that is acidified is higher. This is done as it was believed that the gas formation might arise due to a reaction between an element present in the sample and the NO3. To improve the quality of the samples and reduce the amount of gas in the samples, more volume per sample was made. This time 25 mL was prepared instead of exactly 10 mL. To still have 1.0% nitric acid, 24.75 mL of sample was mixed with 0.25 mL of 69% HNO3. The same steps as before were applied. However, more attention was paid to the formation of gas. After mixing the sample on the vortex mixer, a lot of gas is formed in all samples. This could be a sign of reaction between something in the sample and the nitric acid.

Table 2.6: Composition of the samples used for ICP MS analysis (samples A3, B3, C3 and D3)

Sample number	Content according to bottle	Measured Brix%	Concentration H2O2	Notes
A3	30% H2O2	14.5 %	33 %	Came right from the production bottle (2.5L)
B3	50% H2O2	21 %	47.8 %	Came right from the production bottle
C3	30% H2O2 made to 90% H2O2	39.5 %	89.5 %	Produced by SolvGE
D3	50% H2O2 made to 90% H2O2	39.5 %	89.5 %	Produced by SolvGE

To limit the amount of gas in the samples, they were put to rest for 60 minutes. During this resting time, the samples containing low concentrations of H2O2 (samples A and B) degassed, and almost no gas was visible. The samples containing high concentrations of H2O2 (samples C and D) still showed gas formation. This is also visible in Figure 2.9. To degas the samples completely, all samples were degassed using a vacuum/inert gas manifold system (Schlenk lines). In samples A and B nothing visible happened during the degassing procedure. In sample C first the amount of gas reduced, however, it did not completely disappear, and later more gas formed again. This sample was also put on a magnetic stirrer to help the gas to move upwards in the sample. However, this did not work. During the degassing of sample D, big gas bubbles were formed at first, but ultimately the amount of gas was reduced. Figure 2.10 shows the samples after degassing. This shows clearly that only the samples containing a high concentration of H2O2 made from 30% H2O2 still have gas. The reason that only this sample still shows gas has to do with the purity of the sample. In Subsection 2.3.2 it was already concluded that the 30% H2O2 was a very pure sample with very few stabilizers present. Therefore, the 90% H2O2 based on 30% (sample C) will decompose the quickest and will show the gas formation. Hence, it can be concluded, the gas formation is not due to a reaction with the NO3, but due to the decomposing H2O2 itself. This also is in line with the large gas bubbles seen during degassing using the Schlenk lines, this is simply the H2O2 decomposing.

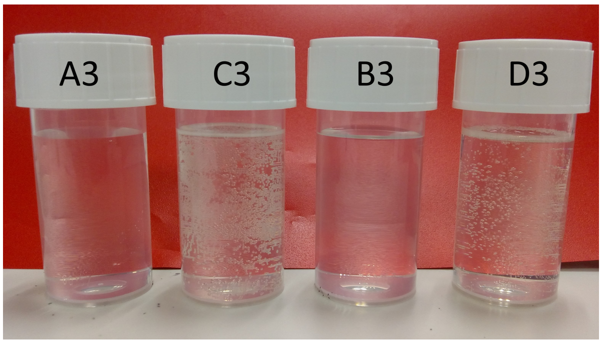

Figure 2.9: Gas formation in hydrogen peroxide samples

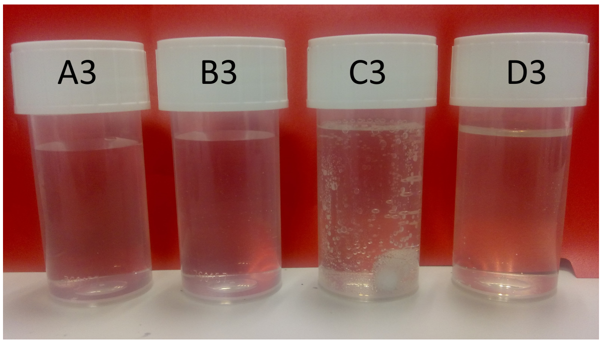

Figure 2.10: Hydrogen peroxide samples after degassing

After degassing, the samples were filtered and put into the tube suited for the ICP MS machine. This was still a 10 mL sample. The filtration of samples A and B went again very smoothly, however, samples C and especially sample D were harder to filter. A lot of force was required to force the liquid through the filter. After filtering samples A and B did not have gas in them, sample D has a very small amount of gas formation. Sample C has a lot of large gas bubbles in it. The results of these samples can be found in Subsection 2.4.2

A third series was made with samples that were not acidified but only filtered using a filter with 0.2 micrometer pores. In Table 2.7 the details of these samples can be found. The aim was that these samples would show less decomposition of hydrogen peroxide and therefore contain less gas. During the production of the sample, it could be visually determined that less gas was formed.

Table 2.7: Composition of the samples used for ICP MS analysis (samples A5 and C5)

Sample number	Content according to bottle	Measured Brix %	Concentration H2O2	Notes
A5	30% H2O2	14.0	31.8 %	Came right from the production bottle (2.5L)
C5	30% H2O2 made to 90% H2O2	40.5	91.7 %	Produced by SolvGE

2.4.2. Results

The first series of samples could not be tested due to the formation of gas in the samples. Therefore, no results are obtained. The second series was tested, but due to the formation of gas, the outcome of these results should be interpreted qualitatively instead of quantitatively. The ICP MS device is designed to suck up a fixed quantify of samples. The concentrations of elements measured are then based on that fixed quantify. However, due to the presence of gas, less quantity is sucked up by the ICP MS device. Consequently, the results are inaccurate. The results can be seen in Table 2.8. The b means that the concentration is below the detection limit, the h means that the concentration is above the detection limit, the g means that the gas has influenced the measurement, and $high$ means that the concentration was too high to be measured.

Table 2.8: Results of ICP MS analysis with acidification

Sample number	Sample A3 30% H2O2	Sample C3 90% H2O2 from 30%	Sample B3 50% H2O2	Sample D3 90% H2O2 from 50%
Element	Concentration (ppb)	Concentration (ppb)	Concentration (ppb)	Concentration (ppb)
Li7	0.2433b	6.35	0.6575b	4.70
Be9	0.0047b	0.0373b	0.0146b	0.0333b
B11	0.3116b	107.8674h	18.70	84.99
Na23	998.82	110132.3h	21339.11h	93879.55h
Mg24	32.31	96.69	96.69	401.56
Al27	7.11	high	2197.086h	high
Si28	11.45	1726.32	346.34	1402.63
P31	356.58	high	29897.9h	high
K39	75.21	869.06	79.74	520.15
Ca44	289.72	6520.71	189.21	1309.63
Ti49	0.3663b	6.25	2.07	5.35
V51	0.125b	0b	0b	0b
Cr52	1.06	58.69	17.36	57.24
Mn55	0.2837b	19.26	2.48	9.96
Fe56	6.00	121.65	71.76	57.76
Co59	0.0887b	0.503b	0.1112b	0.2719b
Ni60	1.92	36.21	4.10	18.96
Cu65	0.00	47.98	0.39	9.33
Zn66	109.5625h	high	177.2843h	high
As75	0.0943b	0.3488b	0.7829b	0.2127b
Se78	0.0329b	0.1599b	0.0024b	0.0704b
Sr88	1.01	10.79	0.54	2.90
Mo98	0.4069b	15.86	0g	3.5122g
Ag107	0.0864b	22.1468g	0g	38.9659g
Cd114	0b	0.00	high	high
Sb121	0.0167b	0.7298b	0.8102g	0.4558g
Ba137	3.22	39.87	5.95	15.88
Pb	1.23	22.19	0.7764b	3.31

In Table 2.8 a few aspects are visible. First of all, some elements are below the detection limit for all the samples and the concentrations are <1 ppb. This is the case for the elements Be, V, Co, As, Se and Sb. Therefore, it can be concluded that these elements are negligible. Secondly, the element Cu is not measured in the sample containing 30% H2O2 (sample A3) but is present in the 90% H2O2 from 30% (sample C3). This is odd as one would expect an element to be present in either both or in none. This could be caused by contamination of the sample.

Due to the high sensitivity of this analysis, only low concentrations are within the detection capabilities of the ICP MS device. To use the oxidizer for a wide range of applications, the concentration of foreign elements should be below 20-25 ppm. From Table 2.8 it can be seen that some elements are within or above the maximum range of <20-25 ppm (or 20 000 - 25 000 ppb). This is the case for the element Na for the 50% H2O2 and both 90% H2O2. This is in line with the finding in Subsection 2.3.2 which showed that the element Na is only barely within the range for the 50% H2O2. The deviation between the IC result and ICP MS results for the 50% sample is very low (IC:18.31 ppm Na vs ICP MS:21.34 ppm Na[3]). Furthermore, element P is also above the range for the 50% H2O2 and 90% H2O2. The elements Al and Zn indicated a "high" for both 90% H2O2 indicating that these are potential also above the 20-25 ppm range. However, as the 30% H2O2 contains less of these elements than the 50% H2O2 it is likely that the 90% H2O2 from 30% also contains less of the elements than the 90% H2O2 from 50%. This indicates that the 30% basis is more suitable to use for a wide range of applications. Additionally, for the element Cd, the 50% H2O2 and 90% H2O2 from 50% are both indicated high, indicating that these are potential also above the 20-25 ppm range. However, the 30% H2O2 and 90% H2O2 from 30% are zero. This all indicates that 90% H2O2 from 30% is much more suitable for a wide range of applications. This is in line with the conclusions drawn in Subsection 2.3.2.

The results are plotted in Figure 2.11. Based on the fact that ICP MS is used to measure small concentrations, the range is set from 0 to 1000 bbp. When the axis is set to 20-25 ppm, most elements will not be visible and consequently the increase in concentration (the factor between 90% H2O2 and its "parent") could not be seen. The elements that were labelled as 'high' are represented by the bars with stars. In this plot it can be seen that the 30% hydrogen peroxide is a very pure substance, as most concentrations are extremely low (<100 ppb), only four of the tested elements (28 elements are tested) have a value above that. For the 50% hydrogen peroxide there are eight elements that have a value above 100 ppb. Regarding the 90% H2O2 samples, many elements are represented with "high" and hence drawing a conclusion is difficult. Hence, a third series was tested, this time without acidification to reduce the amount of gas and achieve a more accurate result.

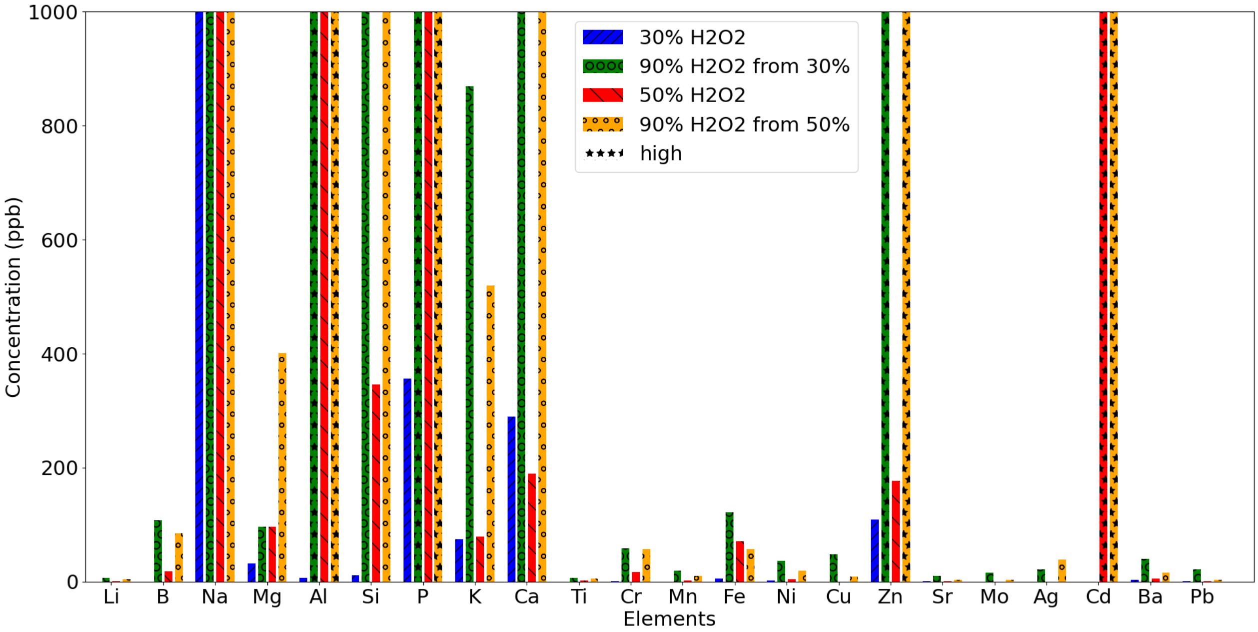

Figure 2.11: ICP MS analysis of series 3

As it is already clear that the 30% H2O2 and the 90% H2O2 from 30% show the most promises regarding the uses for a wide range of applications. Only those two samples were tested for the third time. By not acidifying the samples, less gas formation occurred, and the samples could be processed by the ICP MS device without further issues. The results can be found in Table 2.9. Here it can be seen that there are no longer elements present with a *b* or *g*. This shows that the ICP MS device could measure the samples better this time, compared to the samples from series 2. The results of the third series were thus found to be more reliable. Just as in series two, the elements Be, V, Co, As, Se, and Sb are detected in

---

[3] One should compare to IC-sample 4 as these come from the same production bottle

concentrations below or close to 1 ppb and can be neglected. Additionally, this series also had concentrations of below 1 ppb for the elements Pb and Cd. Therefore, these elements will not be shown in the plot. The plot of the data can be seen in Figure 2.12.

Table 2.9: Results of ICP MS analysis after only filtering

Sample number	Sample A5 30% H2O2	Sample C5 90% H2O2 from 30%
Element	Concentration (ppb)	Concentration (ppb)
Li7	2.19	2.24
Be9	0.00	0.01
B11	high	high
Na23	16000.19h	84133.55h
Mg24	20.56	370.41
Al27	162.3017h	425.7318h
Si28	1264.99	1308.37
P31	38527.65h	high
S34	632.10	693.14
K39	35.35	403.30
Ca44	44.63	2466.41
Ti49	2.54	5.72
V51	0.00	0.00
Cr52	18.69	97.55
Mn55	1.88	7.64
Fe56	77.69	213.98
Co59	0.29	1.03
Ni60	10.18	57.10
Cu65	1.62	128.2191h
Zn66	4.63	61.56
As75	0.05	0.33
Se78	0.00	0.02
Sr88	0.40	8.01
Mo98	2.19	36.26
Ag107	0.04	9.92
Cd144	0.00	0.00
Sb121	0.17	1.07
Ba137	1.60	3.30
Pb	0.30	0.85

It can be seen that the concentrations are different when comparing the first results (Table 2.8) with the second results (Table 2.9). Although both samples are made from the 2.5L bottle of H2O2 30%. Hence, no difference should occur. From all the elements shown in the plot only 5 elements match. Additionally, when only looking at the elements for which the device did not indicate a problem (so no l, h, or g in the table), the variations are between a factor 0.1 and 110.5. The results of Table 2.9 are considered more reliable than the results from Table 2.8.

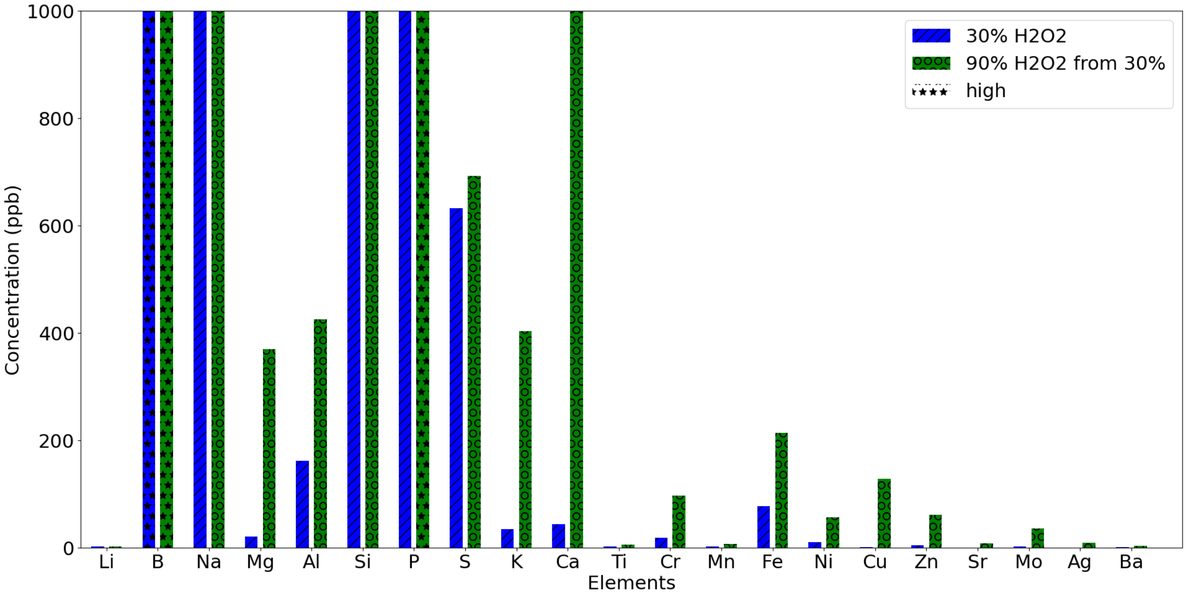

Figure 2.12: ICP MS analysis of series 5

Based on Figure 2.12 and Table 2.7, which are considered more reliable, only the elements B, Na, Si and P are present in concentrations above 1000 ppb. For the 90% H2O2 from 30% also Ca is present in a concentration above 1000 ppb. Regarding the maximum limit of 20-25 ppm (20 000 - 25 000 ppb), only the element P is above this limit for both concentrations. And the element Na is above this concentration for the 90% H2O2 sample. For element B it is unknown which concentration is present as concentrations above 107 ppb are already out of range.

2.5. CONCLUSION

An overview of the investigated hydrogen peroxide consisting of different concentrations is given in Table 2.10. The elements present in the concentration above 25 ppm are also shown in the table.

The 30% H2O2 is a relatively pure substance with almost no stabilizers present. The 50% H2O2 contains more stabilizers, and the IC analysis showed that the elements NO3, Na, PO4, and Na are present in concentrations around the maximum desired concentration of 20 - 25 ppm. Additionally, it was found that bottles containing different volumes of 30% H2O2 consisted of different concentrations of stabilizers. The concentrations of tested elements of the 1.0 L bottle are below the desired 20-25 ppm, in contrast to the 2.5 L bottle. Lastly, based on the IC analysis, it can be concluded that there is no constant factor between the 90% H2O2 and its "parent".

When looking at the highly concentrated hydrogen peroxide, the concentration of some elements was above the desired limit of 20-25 ppm. Based on the IC analysis, the 90% H2O2 from this 30% bottle only contained the element F in a concentration above 20 ppm. The 90% H2O2 from 50% had a concentration of the elements F, NO2, PO4, Na, and NH4 above the limit. Based on the IC PMS samples without acidification, the 90% H2O2 showed that the elements Na and P are above a concentration of 25 ppm. For element B the results were inconclusive. Keep in mind that this IC PMS is only conducted on the 2.5L bottle of 30% H2O2.

It can be concluded that the 30% H2O2 1.0 L volume bottle contained the least amount of stabilizers and is the purest. This purity is also showing in the highly concentrated hydrogen peroxide with concentrations above 90% that is made from 30% H2O2. Therefore, this sample is deemed most suitable to be used for a wide range of space applications. Also, the subsequent experiments (Chapter 5 and Chapter 6) will be performed using 90+ % H2O2 from 30% 1.0 L H2O2 as the catalyst performance will benefit from the purity of this oxidizer.

Table 2.10: Overview of the composition of different concentrations and volumes of hydrogen peroxide

Description	IC analysis		IC PMS analysis		
	Sample	Elements in concentrations above 25 ppm	Sample	Elements in concentrations above 25 ppm	Elements possible in concentrations above 25 ppm
30% H2O2 (1 L bottle)	A2	none	-	-	-
30 % H2O2 (2.5 L bottle)	A4	F (33 ppm)	A5	P (± 39 ppm)	B
50 % H2O2	B2, B4	F (33 ppm) PO3 (43 ppm) PO4 (34 ppm)	B3	P (30 ppm)	Zn
90 % H2O2 from 30%	C2	F (25 ppm)	C5	Na (84 ppm) P (>39 ppm)	Al, B, Zn
90 % H2O2 from 30% (mixed)	C4	F (97 ppm) NO2 (258 ppm) PO4 (279 ppm) Na (112 ppm) NH4 (63 ppm)	-	-	-
90 % H2O2 from 50%	D2, D4	F(59 ppm) NO2 (202 ppm) PO4 (209 ppm) Na (92 ppm) NH4 (37 ppm)	D3	Na (± 94 ppm) P (>30 ppm)	Al, Zn, Cd

3

FORMULATION OF THE FUEL

The first step in developing the fuel of the novel green bi-propellant is finding its chemical compounds. Hydrogen peroxide (H_2O_2) is the oxidizer and the literature study revealed that a gelled alcohol would be a good candidate as fuel. The process of formulating the fuel is shown in this chapter. Firstly, in Section 3.1 the principles behind gelling technology are explained. Then in Section 3.2 the alcohol that forms the basis of the fuel is selected. Lastly, in Section 3.3 the selection of the gelling agents and the process to achieve a solidified system are described.

3.1. GELLING TECHNOLOGY

Gelation is a general way to convert a fluid to a solid. Via gelling technology, the viscosity of a substance is altered due to the formation of a weak cohesive internal structure. Gelling technology is used to achieve solidification of the alcohol fuel by adding a thickening agent or gelling agent. Additionally, it is believed that viscoelastic nature can be achieved this way. The gelling process depends on parameters such as; mixing time, type of gelling agent, type of solvent, amount of gelling agent, and processing temperature. After mixing, the fuel should be left alone for at least a day to allow the gel internal structure to form [15].

Gelling technology changes the viscosity of the fuel. Viscosity can be defined as a quantity expressing the magnitude of internal friction in a fluid and is measured by the force per unit area resisting uniform flow. One of the most important characteristics the green fuel should possess is the ability of shear-thinning. This means that the gelled fuel's viscosity should decrease with the rate of shear strain. This is important because it improves the mixing process between the fuel and oxidizer. Currently, there exists no simple but correct expression for the viscosity of a fluid. Therefore, it is also unknown exactly what parameters and to what extent those parameters influence the viscosity of the fuel. Known parameters are;

- **Temperature**: The temperature has a strong influence on the viscosity. This has to do with two aspects: firstly, the temperature reduces molecular viscosity because it induces kinetic energy to the molecules that can counter the molecular attraction between them. Secondly, higher temperatures result in lower densities.
- **Density or molecular structure**: In general, viscous materials tend to have a higher density than less viscous materials. In liquids, the packing of the molecules (hence the density) can be viewed as a random packing of spheres whereby the radius of each sphere is equal to the atomic radius or the approximate length of a molecule. An exception to this are some oddly shaped molecules as they won't pack that well resulting in a lower density, however, this won't be the case for the fuel used during this research. Therefore, it is valid to assume that liquid density is simply a function of atomic weight.
- **Pressure**: Pressure results in an increase in viscosity. However, it has a much greater effect on gasses than on liquids as liquids are close to non-compressible.
- **Shear rate**: Newtonian liquids are independent of external force and hence, the shear rate would not be a parameter. However, for the fuel developed and investigated during this research non-Newtonian fluids are of interest. In these non-Newtonian fluids, the viscosity changes with the shear rate and the viscosity decreases when the shear rate is increased (hence shear thinning behaviour occurs).
- **Flow conditions**: The flow conditions are essential for obtaining the correct viscosity during a test. In a laminar flow, the flow has an orderly structure that gives the correct viscosity. While in turbulent flow, no structure is present and the molecules move freely, resulting in a falsely higher viscosity.

Due to the fact that the viscosity depends on many parameters and the relation of those parameters are only poorly understood, it is common to refer to the viscosity measured during experiments as *apparent* viscosity. The apparent viscosity means that this is the viscosity of the sample under the conditions that hold for that specific experiment. Still, this apparent viscosity can be used to give an indication of the viscosity and fuel's behaviour. Only comparisons to fuels described in literature should be made with caution as in the end, it is an apparent viscosity.

3.2. ALCOHOL BASIS

Based on the literature study performed at the start of this thesis, gelled fuels are among the most promising green fuels as they have energetic advances over solid and liquid propellants. As fuel, alcohols are very suitable because they are basic [1], non-toxic and can be gelled. Other benefits of alcohols are that they are in general cheap, storable, accessible, and have a low freezing point. Additionally, it was found that catalytic ignition with low percentages of catalyst would be a promising ignition technique. Therefore, the fuel has to be able to accommodate a catalyst. A catalyst can be suspended in organic compounds such as alcohols. Thus, gelled alcohols are the most promising green fuel to use. The requirements imposed on the fuel were already established during the literature study, but are listed below again;

- **PROP-FU-1:** The fuel shall be non-toxic
- **PROP-FU-2:** The fuel shall be in solid form or have characteristics of a solid
- **PROP-FU-3:** The fuel shall be miscible with the oxidizer (i.e. hydrogen peroxide)
- **PROP-FU-4:** The fuel shall be basic (pH > 7)
- **PROP-FU-5:** The fuel shall be able to accommodate a catalyst
- **PROP-FU-6:** The fuel shall have adequate mechanical properties such that a grain can be formed

When comparing the completely solidified ethanol fuel [22] with the gelled ethanol fuel [17], difference in performance can be observed. The gelled fuels have lower activation energies, which is beneficial for the ignition process. Solidified ethanol fuel has activation energies between 9.06 to 14.01 kJ/mol, while pure gelled ethanol fuel is around 7.1 kJ/mol. The benefits of the reduced activation energy can also be seen in the ignition delay times. Ignition delay times of solidified ethanol are between 49 ms to 307 ms, while that of the gelled ethanol are between 1 ms and 115 ms. Hence, the gelled fuels show better performance than completely solidified ethanol. However, the aim is to develop a solid fuel as the objective of this thesis is to design a hybrid bi-propellant system. Also, gelled ethanolamine [16] shows promising results. The amount of catalyst required is lower than that in gelled ethanol and the ignition delay times are very short, between 1.88 ms and 20.42 ms. The temperature profiles, however, are slightly lower than that of gelled ethanol. A temperature of 800 ^oC to 1200 ^oC for gelled ethanolamine vs 1000 ^oC to 1600 ^oC for gelled ethanol. Nevertheless, both temperature profiles are very high, which is promising. However, ethanolamine contains N-groups. As hydrazine, the traditional rocket fuel, also contains N-groups, this is an undesired similarity. To distinct more from those toxic fuels, ethanolamine is excluded from further research.

Additionally, research [23] showed that the enthalpy of combustion of only pure ethanol gel fuel is higher than that of pure liquid ethanol or metallized gelled ethanol. The enthalpy of pure gelled ethanol is around 36 kJ/g , while liquid and metallized gelled ethanol both have 28 kJ/g. Interestingly, this is not the case for other alcohol fuels, such as alcohols with a carbon chain length of propanol (C3H8O) to heptanol (C7H16O). For those alcohols, the enthalpy of combustion of the gelled and metallized fuels has an enthalpy lower than that of the liquid state. This does indicate that ethanol is a very interesting fuel and might be the best candidate to use for this thesis project.

Lastly, the miscibility of the fuel with the oxidizer is of great importance. The oxidizer has to penetrate the gelled fuel to maximize the contact area with the fuel and catalytic material. Hydrogen is highly miscible in ethanol due to its polar nature [17]. Furthermore, ethanol has already applications in the past as rocket fuel, hence proven its capabilities. Hence, ethanol (C_2H_5OH) will form the basis of the novel fuel. To investigate the influence of the carbon chain length, alcohol with a longer carbon chain will be studied as well. This then would be propanol (C_3H_7OH). As propanol is not available in the chemical lab of Aerospace Engineering, it is decided to use butanol (C_4H_9OH) instead. This comparative study will reveal the influence of the length of the molecule on the gelation process and the viscoelastic nature of the fuel.

3.3. GELLING AGENT

The basis of the fuel consists of ethanol or butanol and gelling technology will be used to solidify the fuel. A crucial step in gelling the alcohol is finding a suitable gelling agent. After the gelling agents are found, it is vital to find the critical concentration. A too low concentration results in a fuel that is too viscous and does not form a solid (does not possess the viscoelastic nature). On the other hand, a too high concentration of gelling agent results in more bonds. Stronger bonds are more difficult to break, which results in higher activation energy. This is undesirable for the ignition of the fuel.

3.3.1. SELECTION OF THE GELLING AGENT

By adding a gelling agent weak cohesive internal structures are formed in the substance. A gelling agent can be organic or inorganic, this is an important characteristic of the gelling agent. When gelling agents add positive heat of formation to the fuel, it can improve the performance of that fuel. As organic gelling agents participate in the combustion process, they positively influence the performance of the fuel [14]. Inorganic gelling agents do not participate in the combustion,

---

[1] Under basic conditions, hydrogen peroxide (the oxidizer) loses a proton and becomes less stable, this will ease the ignition process

therefore, they decrease the performance of the fuel. Especially when larger wt% of a gelling agent are added, this influence becomes more profound. The requirements imposed on the gelling agent required for the gelling technique were already founded during the literature study, but will be shown below again;

- **PROP-GA-1:** The gelling agents shall be organic
- **PROP-GA-2:** The gelling agents shall be green in nature
- **PROP-GA-3:** The gelling agents shall be non-reactive and compatible to the fuel

In previous published literature investigating solidified ethanol [22], two different organic gelling agents were tested; methylcellulose (MC) and hydroxypropyl methylcellullose (HPMC). Their results showed that cellulose-based gelling agents enhance the fuel characteristics by reducing the activation energy battier (hence, lowering the activation energy). However, which gelling agent lowers it the most can not be conducted as the MC13 and HPMC 13 both use 13% gelling agent, but the water content is different (10% vs 15%). Regarding the performance of the fuel, there is a difference based on the type of gelling agent. Since HPMC contain more active hydroxyl (-OH) groups, this results in a synergistic effect together with the catalyst particles in hydrogen peroxide decomposing reaction rates. Therefore, less catalyst is required to ignite ethanol solidified with HPMC than MC. Regarding the concentration of gelling agent, it was found that increasing the concentration of gelling agent decreases the ignition delay time because the gelling agent loading lowers the apparent activation energy of solidified ethanol fuel. In case of the HPMC, ignition delay time was reduced by 70% when the gelling agent concentration was increased by 3 wt%.

The only downside of the research was the fact that water was added to the fuel. Adding water has a negative effect on the final performance of the propellant. The reasoning for adding water to the fuel is not provided in the paper. It is known that adding water to ethanol influences the viscosity in a non-linear sense. The viscosity for different concentrations of water and ethanol are shown in Figure 3.1. Below a mole fraction of roughly 0.3 ethanol, the viscosity increases with increasing ethanol fraction. Above a mole fraction of roughly 0.3 ethanol, the viscosity decreases with increasing mole fraction of ethanol. In the previous study [22] a water content between 8 wt% and 15 wt% is used. Neglecting the presence of the thickening agent, the addition of water would result in a higher viscosity (pink area) compared to the case where no water (red line) would be added. Another aspect that can be observed in Figure 3.1 is the influence of the temperature. The higher the temperature the lower the viscosity. However, the temperature influence is less great at high or very low mole fractions of ethanol. It has to be noted, it is not yet investigated what the influence of the added water is on the thickening agent. Therefore, it can not yet be concluded if without the addition of water the sample would indeed have a lower viscosity.

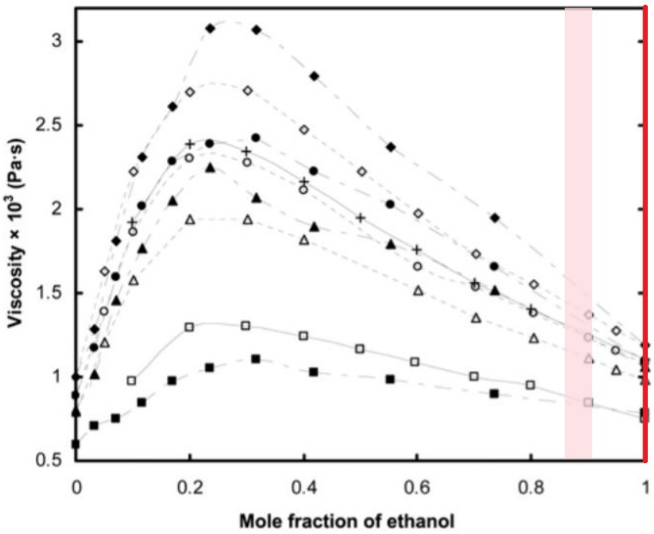

Figure 3.1: Experimental data of the viscosity of mixtures of water and ethanol at varying temperatures for different mole fractions of ethanol [1]

Another paper [17] also investigates gelled ethanol, however, this research focuses on gelled ethanol rather than solidified ethanol. During this research, propyl cellulose is used whereby no water is added to the samples. The concentration of thickening agent used is also lower than the concentrations used for MC or HPMC [22]. Yet another paper investigating gelled ethanolamine [16] whereby Polyvinylpyrrolidone (PVP) was used as a thickening agent. This is also an organic thickening agent as it consists of carbon atoms. However, the gelling agent used in this research is always a hybrid pair of PVP and SiO_2. This last substance is inorganic. As this is half of the hybrid combination, 50/50 PVP and SiO_2, this is not beneficial and also does not meet the requirements.

In Table 3.1 an overview of the thickening agents used in the literature and their associated concentrations are shown. Furthermore, other substances that are added, such as water, energizing particles, or a catalyst are also shown. In the table, a range of percentages is given for ethanol solidified with MC, but based on the ignition delay time the optimal catalyst concentration is 18%. For ethanol solidified with HPMC, the optimal catalyst is 16%. Furthermore, the energized particles indicated in the table are either aluminium, boron, or carbon. Although the viscosity of the fuel samples is not provided in the papers, all papers state that the percentages of gelling agent used are the critical values. These critical values are the ones at which the gel properties are maintained. A lower concentration would result in liquid-like behaviour which is undesirable. Hence, the values shown should correspond to the minimum concentrations.

Table 3.1: Overview of different types of gelling agents and associated percentages

Fuel			Thickening agent		Other	
Alcohol	Type	Percentage	Cellulose	Percentage	Type	Percentage
Ethanol [22]	Solidified	71 to 72 %	MC	13 to 14 %	Water	15%
Ethanol [22]	Solidified	54 to 66 %	MC	13 to 14 %	Water Catalyst (CCAT)	12% 8 to 21%
Ethanol [22]	Solidified	77 to 78 %	HPMC	10 to 13 %	Water	10%
Ethanol [22]	Solidified	60 to70 %	HPMC	12 to 13 %	Water Catalyst (CCAT)	8% 9 to 19%
Ethanol [17]	Gelled	93%	Propyl cellulose	6%	Catalyst (CCAT or MCAT)	1%
Ethanol [17]	Gelled	91%	Propyl cellulose	4%	Catalyst (CCAT or MCAT) Energizing particles	1% 4%
Ethanolamine [16]	Gelled	87%	PVP SiO2	6% 6%	Catalyst (CCAT or MCAT)	1%
Ethanolamine [16]	Gelled	86%	PVP SiO2	5.5% 5.5%	Catalyst (CCAT or MCAT) Energizing particles	1% 2%

Based on the requirements, propyl cellulose seems to be the most suitable thickening agent to use when comparing the options from Table 3.1. Proplyl cellulose is organic, it is likely that low concentrations would result in solidification, and it is green in nature. The only drawback is its lack of an -OH group that would have a synergistic effect with the catalyst. To overcome this, the gelling agent hydroxypropyl cellulose (HPC) will be used during this research. To compare the performance of hydroxypropyl cellulose, a second thickening agent is selected. This is hydroxypropyl methylcellulose (HPMC) as this also contains hydroxypropyl, so only the methyl part is different.

The literature study indicates that the percentage of gelling agent will be around 5% as this is the critical value for gelling ethanol [17]. However, the aim of this investigation is to obtain a solid system while also minimizing the concentration of the gelling agent. Hence, this critical concentration of HPC and HPMC will be determined in experimentally as shown in Subsection 3.3.2 and Subsection 3.3.3. As ethanol is the prime interest of this research, the critical concentration of gelling agent is investigated for ethanol. Then, the same concentration of gelling agent is used to make samples with butanol for the comparative study.

3.3.2. CRITICAL CONCENTRATION: HPC

To start, an arbitrary concentration of 3% thickening agent was used to gel the ethanol fuel. Firstly, only one sample (sample 1) with ethanol and 3.0 wt% of HPC was made. During the process of mixing, the ethanol and HPC were mixed by hand with a spatula. The use of a magnetic stirrer was not possible as only a small amount of fuel was produced. Therefore, the magnetic stirrer would not fit inside the bottle. Also, the fuel would stick to the magnetic stirrer when turned solid. Therefore, mixing by hand was preferred. The mixing was necessary to aid the dissolving of the gelling agent into the ethanol. Additionally, the kinetic energy released due to stirring helps the formation of bonds to form the 3D network. As the gelling process is a slow process, the stirring took roughly 30 minutes. During this time, some ethanol will evaporate which increases the effective concentration of HPC. Sample 1 still showed signs of liquid behaviour rather than of a solid. When the bottle is turned upside down, the fuel still tends to flow. This behaviour was only visible directly after mixing. After 24 hours the behaviour was different. The sample no longer tends to flow when the bottle is turned upside down.

However, when one shakes it firmly and abruptly stops, the fuel still deforms. Therefore, another sample (sample 2) was made, increasing the gelling concentration to 3.5 wt% HPC, this sample was also put to rest for 24 hours. This sample does show solid behaviour. It does not flow and only deforms very little upon a firm shake and sudden impact. To see if increasing the gelling agent further has an influence on its behaviour a sample with 4.0 wt% HPC was made. However, this sample did not perform better and still shifted slightly after a firm shake and abrupt stop. Therefore, it was believed that the critical concentration to gel an ethanol fuel is 3.5 wt% HPC.

Then, the same concentration of gelling agent was added to butanol fuel. For butanol, the chemical 1-Butanol anhydrous 99.8% was used. This resulted in sample 3 and sample 4. These samples behave differently than the ethanol samples (sample 1 and sample 2). After a resting period of 24 hours to allow the 3D network to form, these samples did not shift at all. Even when shaken firmly and put at an abrupt stop, they stayed in exactly the same shape. This behaviour can be explained based on the length of the carbon chain. As butanol has a longer chain, the internal network becomes stronger.

An overview of the samples can be seen in Table 3.2. More details of the samples can be found in Appendix A in Table A.1. Pictures of the samples taken after the formation of the 3D network are shown in Figure 3.2. It can be seen that air bubbles are trapped inside the fuel. This is due to the stirring process. It is clear that the samples all show solid behaviour and do not deform when the bottles are turned upside down.

Table 3.2: Composition of the samples containing HPC (samples 1, 2, 21, 3 and 4)

Sample number	Mass fraction gelling agent	Mass fraction alcohol
1	3.0 wt% HPC	97.0 wt% ethanol
2	3.5 wt% HPC	96.5 wt% ethanol
21	4.0 wt% HPC	96.0 wt% ethanol
3	3.0 wt% HPC	97.0 wt% butanol
4	3.5 wt% HPC	96.5 wt% butanol

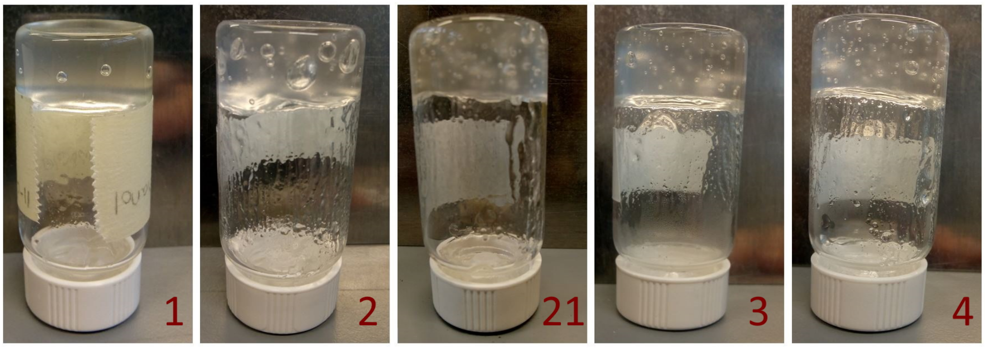

Figure 3.2: Solidification process of ethanol and butanol fuel gelled with HPC

3.3.3. CRITICAL CONCENTRATION: HPMC

In the literature, gelled ethanol was formed with HPMC and the addition of water. As water negatively affects the combustion performance of the propellant, it was tried to gel ethanol with only HPMC and no additional water. To compare the solidification of ethanol and butanol by different gelling agents, the concentration of gelling agent was kept the same. Therefore, the same concentrations as in Subsection 3.3.2 are used for HPMC. See Table 3.3 for the composition of the samples. More details of the samples can be found in Appendix A in Table A.2. Again, for butanol, the chemical 1-Butanol anhydrous 99.8% was used.

Table 3.3: Composition of the samples containing HPMC (samples 5, 6, 7 and 8)

Sample number	Mass fraction gelling agent	Mass fraction alcohol
5	3.0 wt% HPMC	97.0 wt% ethanol
6	3.5 wt% HPMC	96.5 wt% ethanol
7	3.0 wt% HPMC	97.0 wt% butanol
8	3.5 wt% HPMC	96.5 wt% butanol

The samples were produced in the same way as the samples consisting of HPC. Hence, the samples were mixed by hand with a spatula for approximately 30 minutes. However, it immediately became clear that no gelation occurred. The HPMC does not dissolve in ethanol nor butanol, rather a suspension is formed. This can also be seen in Figure 3.3 left and Figure 3.3 middle. After only a short amount of resting time (>5 minutes), the HPMC precipitate to the bottom. This can be seen in Figure 3.3 right. Although only sample 6 is shown here, it is representative of samples 5, 7, and 8. Hence, it can be observed that this gelling agent fails to solidify ethanol and butanol. The reason for the absence of solidification is due to the presence of the methyl groups, as this is the only difference between HPMC and HPC. The methyl groups prevent the connection between the OH-group of the alcohol to the gelling agent.

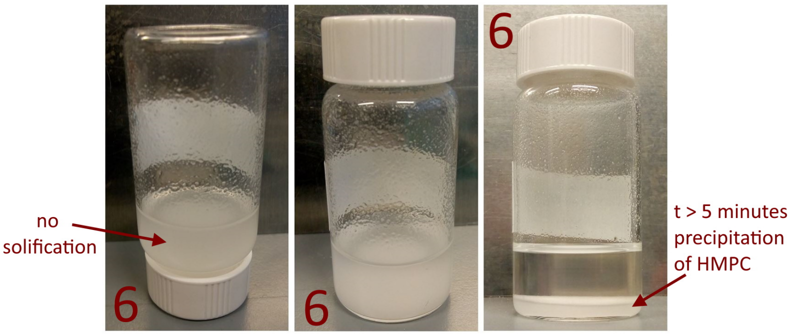

Figure 3.3: Solidification process of ethanol fuel gelled with HPMC

To still achieve solidification, water is added, just as was done in literature. By adding water, gelation can occur. The water acts as a connection between the OH-group of the alcohol and the gelling agent. Before, the OH-group tried to bind with the methyl group. However, this bond is very weak or can not exist. Therefore, that samples 3, 4, 5, and 6 failed to form a solid. By adding water, the OH-group of the alcohol forms a bond with water and the water also forms a bond with the gelling agent. This then results in a solidified system.

The concentration of water required to obtain a solid is unknown. As a starting point sample 9 was made consisting of 3.0 wt% of HPMC and ethanol. These two chemicals were taken as one part. Then water was added and mixed. To start, only 1 wt% of water was added. However, after a while of mixing, nothing happened. Then the water concentration was increased to 3 wt%, after mixing still nothing happened. This procedure was repeated with a water concentration of 5 wt%, still nothing happened. Then at 8 wt% water, the substance started to become more gelled. The water concentration was increased one final time to 10 wt%. At this concentration, the fuel's viscosity was raised to such an extent that the fuel started to behave as a solidified system. It still flows when the bottle was turned upside down, but a real change was visible compared to sample 5. As the process of adding water and stirring took over 1.5 hours, this sample is not very reliable. During this 1.5 hours, the bottle has been open constantly, which allowed the ethanol to evaporate. Especially as the 3D network had not yet formed at lower concentrations of water, the ethanol can easily escape the bottle during stirring. However, it did give a starting point for the new samples to be produced.

For the next sample (sample 10), the concentration of gelling agent was increased to 3.5 wt% of HPMC, but the water concentration was kept equal to that of sampel 9, so 10 wt% of water. This sample was stirred for around 30 minutes to keep it equal to the procedure of Subsection 3.3.2. In Figure 3.4, it can be seen that the viscosity of the fuel is still too low. When the bottle is turned upside down, the fuel immediately starts to flow towards the bottom. Therefore, a sample with a higher concentration of water was made, namely 13 wt% of water (sample 13). In Figure 3.4 it can be seen that sample 13 is already more viscous than sample 10, but that it is still not solidified enough. A new sample with again a higher concentration of water, namely 15 wt% water, was made (sample 14). This sample is found to be more promising, the fuel is gelled. In Figure 3.4 it can be seen that the fuel does still flow, but very slowly. An overview of the samples can be seen in Table 3.4. More details of the samples can be found in Appendix A in Table A.3 and Table A.4.

As adding high concentrations of water is undesirable, it has been desired to not further increase the water content, but rather increase the gelling agent. Adding more gelling agent will aid the formation of a 3D network to form a solid.

Table 3.4: Composition of the samples containing ethanol, HPMC and water (samples 9, 10, 13 and 14)

Sample number	Mass fraction test specimen		Mass fraction water
	Mass fraction gelling agent	Mass fraction alcohol	
9	3.0 wt% HPMC	97.0 wt% ethanol	10 wt%
10	3.5 wt% HPMC	96.5 wt% ethanol	10 wt%
13	3.0 wt% HPMC	97.0 wt% ethanol	13 wt%
14	3.5 wt% HPMC	96.5 wt% ethanol	15 wt%

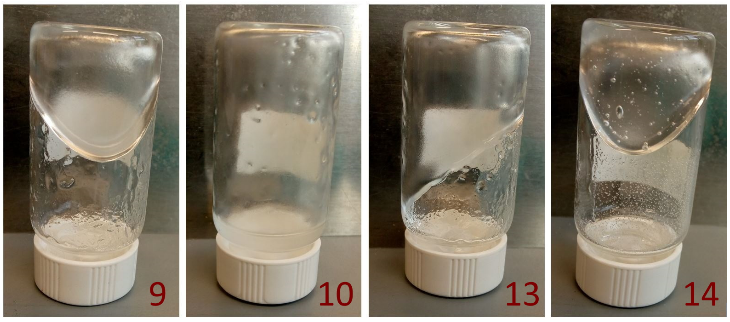

Figure 3.4: Solidification process of ethanol fuel gelled with HPMC and varying concentrations of water

Before, in Table 3.4 the mass fraction of the test specimen consisted of the gelling agent and the alcohol together. This was convenient to do at that time as for sample 9 the mass fraction of water could easily be increased. However, for the exact composition of the sample, it is not that handy because the actual concentration of gelling agent is lower as it is a fraction of a fraction. Therefore, the subsequently produced samples were constructed slightly differently. For these samples, the mass fraction of gelling agent was taken from the total mass, the same hold for the mass fraction of the alcohol.

The water concentration is held constant at a mass fraction of 15 %. The concentration of HPMC is increased in steps of 0.5 wt%. See Table 3.5 for all samples. More details of the samples can be found in Appendix A in Table A.5. Due to the different construction of the samples, sample 14 and sample 15 consists of the same composition. The first aspect that becomes clear, is that the gelling process goes faster for these samples. The addition of water increases the speed at which the 3D network is formed. Therefore, it is no longer needed to stir the samples for 30 minutes. Only 5 to 10 minutes of stirring is sufficient.

Table 3.5: Composition of the samples containing ethanol, HPMC and water (samples 15, 16, 17, 19 and 22)

Sample number	Mass fraction gelling agent	Mass fraction alcohol	Mass fraction water
15	3.0 wt% HPMC	82.0 wt% ethanol	15 wt% water
16	3.5 wt% HPMC	81.5 wt% ethanol	15 wt% water
17	4.0 wt% HPMC	81.0 wt% ethanol	15 wt% water
19	4.5 wt% HPMC	80.5 wt% ethanol	15 wt% water
22	5.0 wt% HPMC	80.0 wt% ethanol	15 wt% water

The critical concentration of gelling agent can be found by looking at the signs of solidification. For the samples gelled with HPMC and water, this deformation is visible more clearly. In Figure 3.5 the ethanol samples with increasing gelling concentration are shown. The samples with a concentration of 3.0 wt% and 3.5 wt% of HPMC (sample 15 and sample 16) clearly show signs of having a viscosity that is too low. A dome is formed when the bottle is turned upside down. This shows that the fuel already starts to flow towards the bottom. The pictures are taken one day after the mixing has occurred. Hence, enough time has passed to complete the formation of a 3D network. As the dome is still formed in sample 15 and 16, the solidification has not occurred. The sample with 4.0 wt% seems solid in the picture (Figure 3.5 sample 17) as no dome forms, however when the sample is shaken firmly and stopped abruptly, the fuel deforms. This shows that the fuel is still not solidified enough. The sample with 4.5 wt% ethanol does show solidified behaviour. In the picture (Figure 3.5 sample 19 and 22) it can be seen that no dome forms, even directly after mixing the fuel it is already solidified to such an extent that no dome forms. Additionally, after a firm shake and abrupt stop, it still holds its shape.

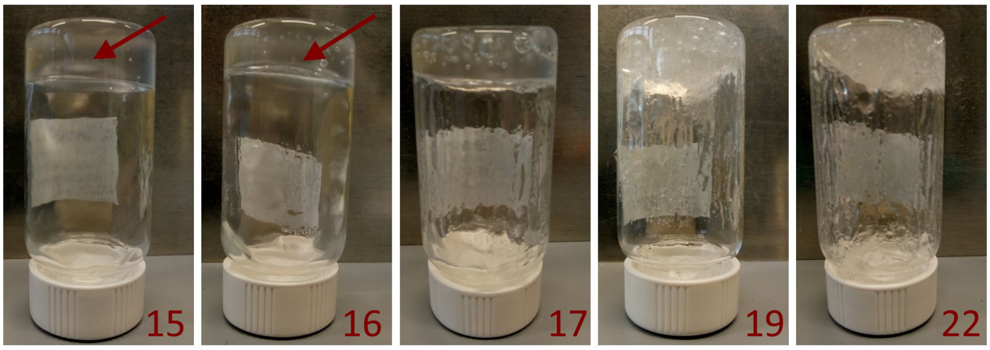

Figure 3.5: Solidification process of ethanol fuel gelled with HPMC and water

Then, the same concentrations of gelling agent and water used to make the butanol samples. This time the chemical 1-butanol 99.9% was used. On overview of the composition of the samples with butanol, HPMC and water can be seen in Table 3.6. More details of the samples can be found in Appendix A in Table A.6

Table 3.6: Composition of the samples containing butanol, HPMC and water (samples 11, 12, 18, 20 and 23)

Sample number	Mass fraction gelling agent	Mass fraction alcohol	Mass fraction water
11	3.0 wt% HPMC	82.0 wt% butanol	15 wt% water
12	3.5 wt% HPMC	81.5 wt% butanol	15 wt% water
18	4.0 wt% HPMC	81.0 wt% butanol	15 wt% water
20	4.5 wt% HPMC	80.5 wt% butanol	15 wt% water
23	5.0 wt% HPMC	80.0 wt% butanol	15 wt% water

Just as in the ethanol samples, the samples with 3.0 wt% and 3.5 wt% of HPMC show the formation of a dome. This can be seen in Figure 3.6. This dome indicates that the samples are not solidified and still flow. The sample with 4.0 wt% of HPMC (sample 18) is completely solidified. Even when shaken firmly and stopped abruptly, the fuel remains its shape. This is in contrast to the ethanol sample with 4.0 wt% HPMC (sample 17). Again, this can be explained by the length of the carbon chain of butanol. The carbon chain of butanol is twice as long as that of ethanol. The longer chain causes the fuel to become more viscous with the same concentration of gelling agent. The samples with a concentration of 4.5 wt% and 5.0 wt% HPMC are solidified even directly after mixing.

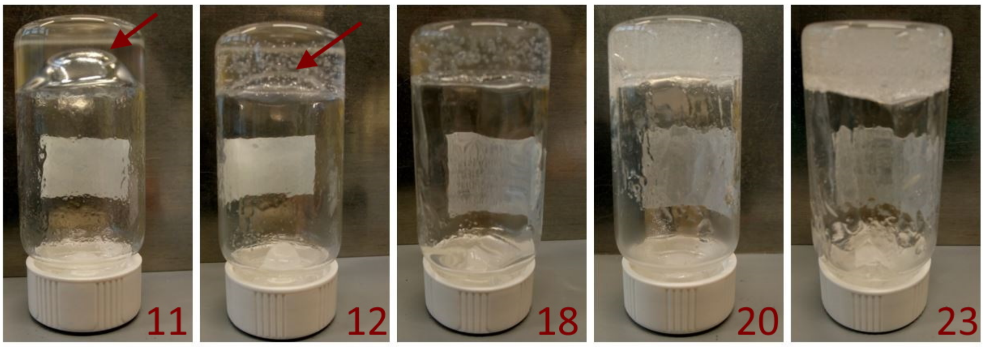

Figure 3.6: Solidification process of butanol fuel gelled with HPMC and water

3.4. CONCLUSION

Gelling technology is used to achieve a solidified fuel. Ethanol is the main compound for the green fuel and forms the basis of the fuel. To investigate the effect of the length of the carbon chain, fuel with butanol as a basis is also investigated. Via gelling technology, the viscosity of the alcohol is altered due to the formation of a weak cohesive internal structure. Literature revealed that propyl cellulose showed processing results and that presence of active hydroxyl (-OH) groups result in a synergistic effect with the catalytic particles in hydrogen peroxide. Therefore, hydroxypropyl cellulose (HPC) is used as a gelling agent during this research. To make it a comparative study, hydroxypropyl methylcellulose (HPMC) is also used as a thickening agent. The only difference between the two is the presence of methyl groups. The critical concentration for the ethanol fuel is found to be between 3.0 wt% HPC and 3.5 wt% HPC. These samples show solidified behaviour. For the butanol fuel, it is found that around 3.0 wt% HPC is the critical concentration to achieve solidification. Regarding the gelling agent HPMC, it was found that solidification does not occur with ethanol nor with butanol as the MC groups prevent the connection between the OH-group of the alcohol to methyl-group of the gelling agent. Water had to be added to obtain a solidified fuel as water acts as a bridge. The OH-group of the alcohol forms a bond with water and the water also forms a bond with the gelling agent. The ethanol fuel showed solidified behaviour at compositions of 15 wt% water and between 4.5 wt% and 5.0 wt% of HPMC. The butanol fuel showed solidification at a lower concentration of the gelling agent, namely at compositions of 15 wt% water and between 4.0 wt% and 4.5 wt% of HPMC. This difference can be explained based on the length of the carbon chain. Butanol has a carbon chain that is twice as long as the carbon chain of ethanol. This longer chain results in a packing of molecules that is more viscous.

4

ANALYSIS OF THE FUEL

To analyse and characterize the gelled fuel in terms of its viscoelastic nature, a rheology study is performed. Rheology is the study of the flow of a substance under conditions in which they respond with plastic flow rather than deforming elastically in response to an applied stress or force. Viscoelastic materials exhibit both elastic and viscous behaviour when deformed. The main characteristics to evaluate the viscoelastic nature are the Linear Viscoelastic Range of the fuel, the yield point of the fuel, and the loss factor which expresses the ratio between the elastic modules over the viscous modulus. These characteristics are described in Section 4.2, Section 4.3 and Section 4.4 respectively. Additionally, a stability study is performed to examine how the viscoelastic nature of the fuels changes over a period of one month as explained in Section 4.5. Also, a temperature study is performed to determine the effect of temperature on the viscosity of the fuel. Additionally, the activation energy of the fuel can be calculated based on the temperature study. These are provided in Section 4.6.

4.1. RHEOLOGY STUDY

During the literature study, it was found that multiple different tests are required to obtain all the above-mentioned characterstics. Firstly, the Linear Viscoelastic Range can be determined via a dynamic strain sweep study. Secondly, a shear stress ramp study can be done to find the yield point of the fuel. Also, the shear-thinning behaviour should become clear from this test. Thirdly, a temperature study reveals the effect of temperature on the study, but also the activation energy can be determined via this test. By using the Arrhenius equation, the natural log of the apparent viscosity can be plotted against the inverse of temperature. This will result in a linear relationship, the slope of the relationship equals the activation energy of the fuel. Lastly, a frequency sweep study reveals at which frequencies the viscous behaviour or the elastic behaviour is dominant.

4.1.1. TEST SET UP

The rheology study was performed at the Physics Lab (Hal 0.05) at the faculty of Aerospace Engineering. Since the fuel is gelled, it was possible to use the "HAAKE MARS III" device. Although it experiences difficulties with samples with a very low viscosity, this device is capable of measuring the flow properties of gelled fuels. A picture of the device can be seen in Figure 4.1. All specifics of the "HAAKE MARS III" can be found in Appendix C. Different shapes and sizes of the plate can be mounted on the device. As the fuel is in solid form, a parallel plate can be used. Furthermore, the lower the viscosity, the larger the plate should be. There are two parallel plates present, either an 80 mm plate or a 20 mm plate. Due to the solid appearance of the fuel, the parallel plate of 20 mm seemed fitting. All details of this plate can be found in Appendix C. The parallel plate needs to be screwed to the HAAK MARS III properly and securely. Otherwise, the plate will get loose during an experiment, resulting in false data.

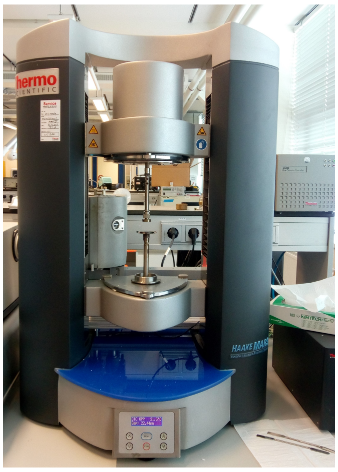

Figure 4.1: Rheometer Haake Mars III present at the Material Physics Lab

For every experiment, the sample has to be applied to the machine. The plate has to move upwards to make space to apply the fuel. The fuel is scoped out of its bottle with a spatula and placed exactly under the parallel plate. Then the plate is moved downwards to a gab size of 1.00 mm. This gab size is kept constant for all experiments. It is important that the fuel fills this entire gab and that there are no empty spaces near the edges. Also, additional material that consumes space outside the gab is removed. See Figure 4.2 for a visual presentation of the procedure. Although the ethanol evaporates less quickly due to the 3D network in the gel, it still evaporates. Hence, when experiments take a long time, the sample under the parallel plate shrinks. This is visible to the naked eye.

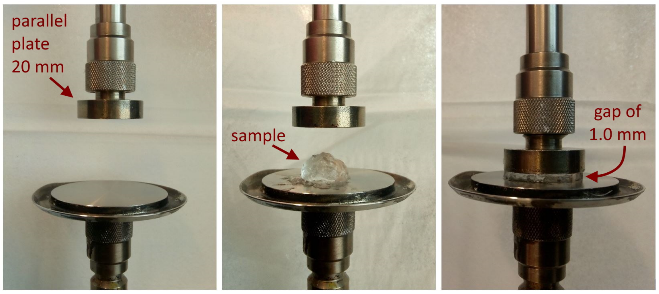

Figure 4.2: Test setup of the rheometer for the rheology study

The initial rheology study consisting of the amplitude sweep study, frequency sweep study, and ramp study, was executed over two days. On the first day, a lab supervisor was present to assist in the experiments. Therefore, all experiments were done only once that day. The tests are executed at t = 4 days after the sample was produced. This way, the samples have had enough time to completely form their 3D network and solidify to their maximum extent. The next day (t = 5 days) the experiments were repeated without the presence of a lab supervisor. The rheology study to investigate the stability was one month later at t = 35 days. All test and the testing order can be found in Appendix B in Table B.4.

4.1.2. PREPARATION OF THE SAMPLES

The samples analysed are based on the outcomes of Chapter 3. The aim of the research is to investigate ethanol fuel and additionally investigate butanol fuel as part of a comparative study. Therefore, the critical concentrations of the gelling agent of the ethanol fuels are analysed. For the butanol fuels, the same concentration of gelling agent will be analysed. This way, the only difference between the samples is the ethanol vs butanol rather than also using the critical concentrations of gellant of the butanol fuels as this introduces yet another variable.

Regarding the gelling agent HPC. The samples that showed solidified behaviour of the ethanol fuel were 3.0 wt% HPC and 3.5 wt% HPC. Therefore, these samples are further analysed. For the gelling agent HPMC a slightly higher concentration was required. The ethanol fuels that showed solidified behaviour were compost of 15 wt% water and 4.5 wt% HPMC and 5.0 wt% HPMC. To investigate the effect of the length of the carbon change, the butanol fuel with the same concentrations will be further analysed. This means that the 15 wt% water and 4.0 wt% HPMC of butanol, which also showed solidified behaviour, is not further tested.

For every experiment, a small volume of sample is required. According to the device, 1 to 2 mL of sample is required per test. However, this is very inaccurate as the diameters of the plates have a large range. To estimate the amount of volume required for the test, one can calculate the volume required to fill the gap. The diameter of the parallel plate is 20 mm and thus has a radius of 1.0 cm. This yields an area of ($A = \pi \cdot r^2 =$) 3.14 cm^2. The gab size is set to 1 mm or 0.10 cm. Then the required volume is equal to 0.31 mL. Every sample will undergo four different tests. The aim is to repeat each test at least three times to achieve sufficient scientific reliability. This would mean that at least 12 tests are executed on each fuel. Additionally, a stability study will be performed to determine the effects of storage on fuel quality. The total number of tests equals 24. This is then 24x3.14 = 7.5 mL in total. Obviously, one spills, but it does indicate an order of magnitude.

New samples are made for the rheology study. The sample number of Chapter 3 is reused, however, a hundred is added. This makes it more convenient to track the samples. To clarify, the previously named sample 1 is now sample 101. These new samples were all made on the same day to prevent any influence due to a difference in storage time. Also, the same technique to stir the sample is used. There was a learning curve present in the stirring technique, but at this moment the stirring technique is such that although the samples are stirred by hand, they are all produced in the same way. Furthermore, the bottles were pre-rinsed to eliminate foreign particles. Samples 101, 102, 103, and 104 were pre-rinsed with alcohol, and samples 119, 122, 120, and 123 were pre-rinsed with DL- water. After this, they were blown dry, to not alter the concentrations by leftovers of the pre-rinsing. An overview of the samples is shown in Table 4.1. More details of the samples can be found in Appendix A in Table A.7.

Table 4.1: Composition of the samples used for rheology study (samples 101, 102, 103, 104, 119, 120, 122 and 123)

Sample number	Mass fraction gelling agent	Mass fraction alcohol	Mass fraction water
101	3.0 wt% HPC	97.0 wt% ethanol	- - -
102	3.5 wt% HPC	96.5 wt% ethanol	- - -
103	3.0 wt% HPC	97.0 wt% butanol	- - -
104	3.5 wt% HPC	96.5 wt% butanol	- - -
119	4.5 wt% HPMC	80.5 wt% ethanol	15 wt% water
122	5.0 wt% HPMC	80.0 wt% ethanol	15 wt% water
120	4.5 wt% HPMC	80.5 wt% butanol	15 wt% water
123	5.0 wt% HPMC	80.0 wt% butanol	15 wt% water

The gelling process for the samples containing HPC is longer than the samples containing HPMC. Therefore, sample 101 and 102 were stirred for 15 minutes and sample 103 and 104 were stirred for 20 minutes. The samples 119, 122, 120, and 123 were all stirred for only 5 minutes. It has to be noted that this does have a small influence on the samples. Stirring the samples longer results in more evaporation of the alcohol. Although the formed 3D network will prevent rapid evaporation, it still occurs slowly.

Due to a limited amount of HPC that was present at the lab, the maximum amount of sample that could be made of samples 101, 102, 103, and 104 was 12 grams per sample. By then, the bottle of HPC was empty. As altering the total mass of a sample, could influence the test results, for the other samples the same amount was made. Hence, also samples 119 and 122 were made to be 12 grams per sample. Additionally, the amount of butanol was limited. Thus for samples 120 and 123 only 10 grams per sample could be made as there was no more butanol left. It was decided to use these amounts instead of ordering more chemicals, due to time constraints. Furthermore, it is deemed important to make the samples out of the same chemical bottles. All bottles used were already opened by someone else. What exactly happened to those bottles or when they were opened is unknown. Therefore, it was undesirable to use different bottles (even though they theoretically have the same content) as it is unknown how the different production dates, opening dates, and exposure conditions alter the performance of the fuel.

During the production of sample 120 (butanol fuel with 4.5 wt% HPMC and water) some strange behaviour was observed. At the start of the stirring process white flakes were formed, after a few seconds they disappeared and the rest of the stirring process went normally. Another observation was the trapped air bubbles in the samples. In all the samples, air bubbles were trapped due to the stirring process. However, the trapping of air was not the same for all samples. The sample gelled with HPC contained a lot of bubbles. The samples gelled with HPMC and water contained also a lot of air bubbles, but these were smaller. This observation was equal for the butanol and ethanol fuels. Figure 4.3 left shows gelled butanol with HPC and Figure 4.3 right shows gelled butanol with HPMC and water containing smaller air bubbles. In Figure 4.4 ethanol fuel is shown. Figure 4.4 left shows ethanol gelled with HPC and Figure 4.4 left shows ethanol gelled with HPMC and water containing smaller air bubbles.

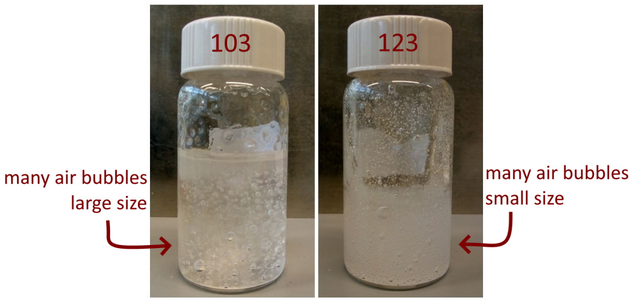

Figure 4.3: Air bubble size in the butanol fuel gelled using HPC (left) and gelled using HPMC (right) directly after mixing

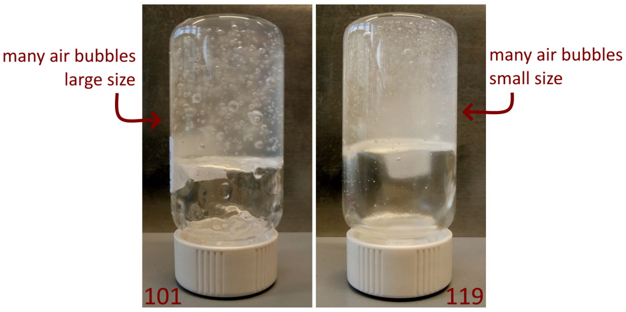

Figure 4.4: Air bubble size in the ethanol fuel gelled using HPC (left) and gelled using HPMC (right) directly after mixing

4.2. LINEAR VISCOELASTIC RANGE

Amplitude sweeps are used to describe the viscoelastic behaviour of gels. During an amplitude sweep study, the deflection of the measuring system is increased step-wise from one measuring point to the next, while keeping the frequency at a constant value. The frequency is chosen to be equal to the frequency used in literature [15]. It is typical to present the results of an amplitude sweep study in a diagram with the strain or shear stress shown on the x-axis and the storage modules (elastic modulus) G' and loss modules (viscous modulus) G" plotted on the y-axis. Both axes are on a logarithmic scale. Based on this graph, the Linear Viscoelastic Range of the sample can be determined.

4.2.1. SETTINGS OF THE AMPLITUDE STRESS SWEEP STUDY

The amplitude sweep was an oscillation amplitude sweep, whereby the amplitude of oscillation is equal to the maximum applied stress. The frequency used in the literature was equal to 5 Hz [15]. The frequency of 5 Hz represents the number of oscillations per second. The sample is approached in a controlled-stress (CS) mode. Hereby, the sample corresponds with a deformation. The starting value of the shear stress was set to $\tau = 0.1$ Pa and the ending value to $\tau = 1000$ Pa. These starting and ending values are found via trial-and-error. Furthermore, it is easier to have a higher ending value and to later not use the data, than to not have the data and having to redo tests to obtain missing data. The starting value is of importance as the sample is affected by the experiment itself. Hence, starting at a different point might yield other results. The starting point of 0.1 Pa is based on the capabilities of the HAAKE MARS III for gelled samples.

The amplitude sweep tests have the labels A, B, C, and E. On the first day (t=4 days), test A was executed, however, after the test of samples 101 and 102 the parallel plate was no longer properly attached to the device. Therefore, the results of all other samples were false. Hence, these samples were retested and labelled test B. The next day (t=5 days), the amplitude sweep test was repeated for all samples, labelled test C. By then, it was found that it would not be possible to repeat all studies for the third time as the sample quantity decreased faster than expected. Only the samples that showed large deviations or discrepancies were tested for the third time and labelled test E. The data that is not shown, can be found in Appendix B.

4.2.2. RESULTS

The results of the experiments can be seen in Figure 4.5 to Figure 4.12. To allow for a clear visual analysis of the results, the y-axis runs from 60 Pa to 1200 Pa for all samples. For the x-axis it has been decided to show the data from 0.5 Pa onward as at a lower shear stress the machine errors dominate and no reliable results are produced. As the main focus of this investigation is on the solid behaviour of the fuel, the exact crossing point of the G' and G" is not of interest. Rather, it is favoured to precisely compare the samples, which can be done more accurately when the axis are set to an equal range. The maximum is shear stress is set at 200 Pa, as after that the shear stress the weak internal structure is destroyed for most samples. Only for the samples containing butanol fuel with water and HPMC (sample 120 and 123) the range is set to 600 Pa.

In Figure 4.5 to Figure 4.8 it can be seen that the fuels gelled with HPC all show solidified behaviour. The G' graph is clearly located above the G" graph indicating that the fuel is highly structured. The wobbling line indicates that the fuel was not perfectly homogeneous. This can be caused by the mixing process of the fuel and gelling agent or by the trapped air in the fuel. Figure 4.8 does show a very homogeneous fuel as the lines are straight. Additionally, it can be seen that Figure 4.6 shows deviation between the first and second test. This could be caused by the alteration of the sample due to testing, which is further supported by the fact that the second test (test C) also shows less homogeneous behaviour. This will be further explained in Section 4.7.

In Figure 4.9 to Figure 4.12 it can be seen that the fuels gelled with HPMC all show solidified behaviour, but that this is closer to the critical case. The G' graphs only lie barely above the G" graph. In Figure 4.9 the G" of the first test (test B) is even located above the G' of the second test (test C). Also, the shear stress at which the internal structure of the fuel is destroyed is high for the butanol fuel gelled with HPMC compared to the other six samples.

Another aspect that can be seen from the graphs is that the G' of the first test (test A or B) are located above the G' of the second test (test C or E), except for Figure 4.7 and partly for Figure 4.5. Hence, the strength of the fuel during the first test is higher than that of the second test. This could be due to the alteration of the sample due to testing. When performing a test, a bit of fuel is scooped out of the sample. This motion might destroy some weak internal structure of the fuel, resulting in a lower strength for the second (and third) tests. A possible explanation that samples 101 and 103 form an exception to this trend, is the temperature. For all other samples, the second test (C or E) are performed at a slightly lower surrounding temperature than the first test (test A or B). However, for sample 101 and 103, the temperature increased, and the second test was performed at a slightly higher temperature (see Table B.2). However, due to the limited data, this can not be concluded for sure.

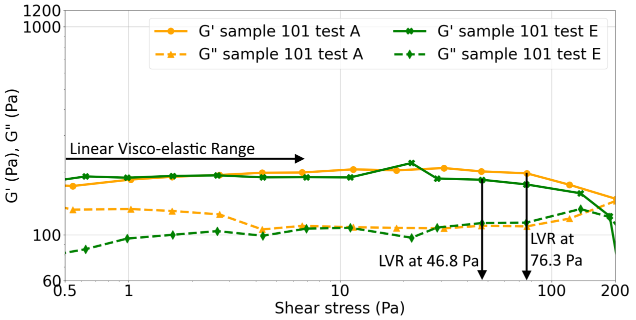

Figure 4.5: Amplitude stress sweep study of ethanol and 3.0 wt% HPC

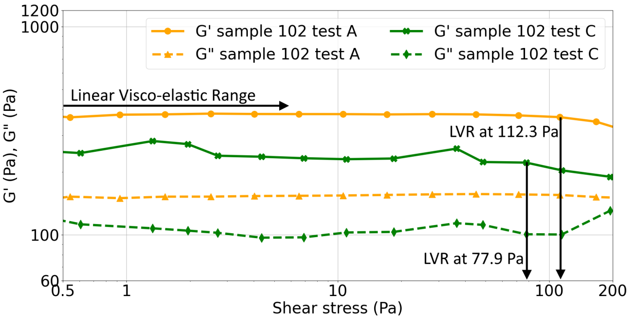

Figure 4.6: Amplitude stress sweep study of ethanol and 3.5 wt% HPC

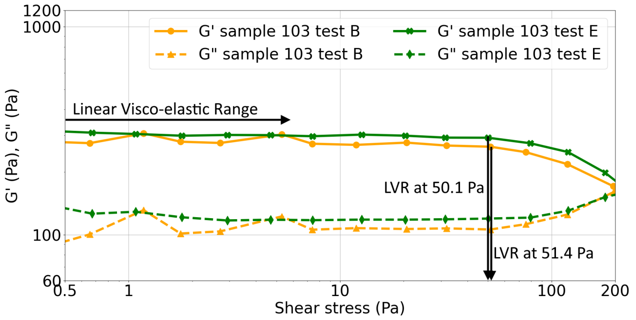

Figure 4.7: Amplitude stress sweep study of butanol and 3.0 wt% HPC

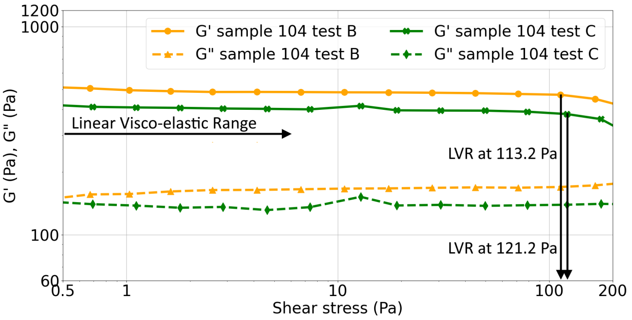

Figure 4.8: Amplitude stress sweep study of butanol and 3.5 wt% HPC

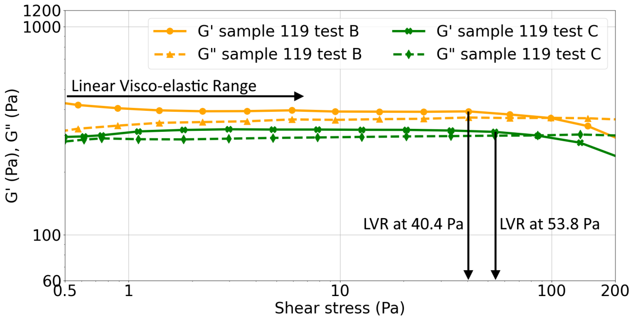

Figure 4.9: Amplitude stress sweep study of ethanol, water and 4.5 wt% HPMC

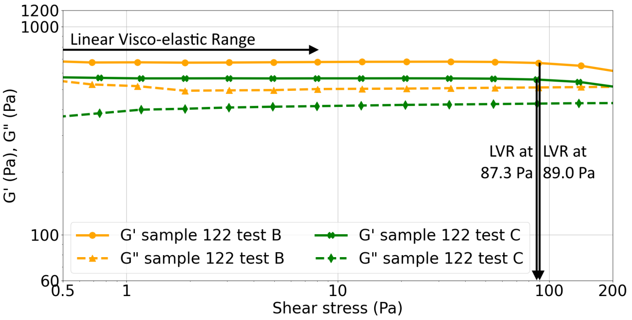

Figure 4.10: Amplitude stress sweep study of ethanol, water and 5.0 wt% HPMC

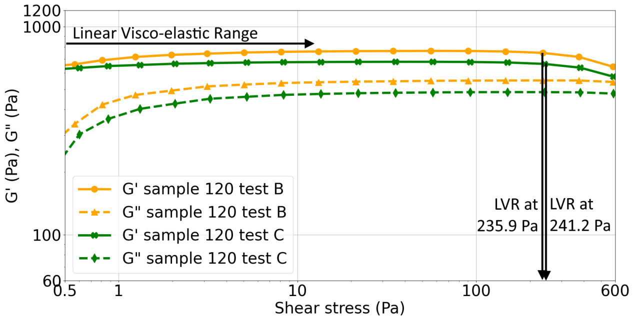

Figure 4.11: Amplitude stress sweep study of butanol, water and 4.5 wt% HPMC

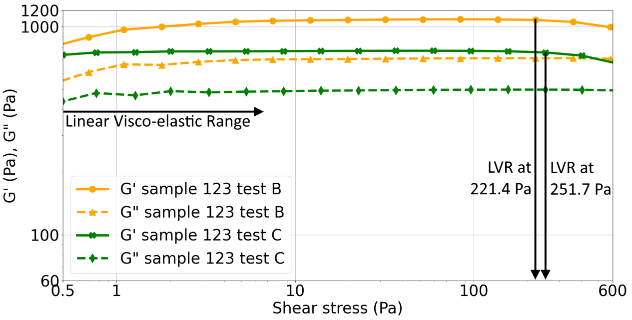

Figure 4.12: Amplitude stress sweep study of butanol, water and 5.0 wt% HPMC

In Figure 4.5 to Figure 4.12 the Linear Viscoelastic Range is determined with a ruler. An overview of the results can be found in Table 4.2. The Linear Viscoelastic Range indicates the range in which the test is executed without destroying the structure of the fuel. When G’ > G", the fuel shows a gel-like or solid structure and can be termed a viscoelastic solid material. However, when G" > G’, the fuel displays a fluid-structure and can be termed as a viscoelastic liquid. Keep in mind, this is only valid for the condition of a frequency of 5 Hz. In case the curve of the G’ function would drop continuously after leaving the Linear Viscoelastic Range, the sample would gradually break down the weak internal structure. However, this is not the case for these fuels. Rather, the fuels are destroyed shortly after leaving the viscoelastic range. Lastly, the G’ values in the Linear Viscoelastic Range represent the stiffness of the fuel or the strength of the gel.

Table 4.2: Overview of the Linear Viscoelastic Range

Sample number	Linear Viscoelastic Range (Pa)		
	Test A or B	Test C or E	Average
EtOH HPC low (101)	76.3	46.8	61.6
EtOH HPC high (102)	112.3	77.9	95.1
BuOH HPC low (103)	51.4	50.1	50.8
BuOH HPC high (104)	113.2	121.2	117.2
EtOH HPMC low (119)	40.4	53.8	47.1
EtOH HPMC high (122)	89.0	87.3	88.2
BuOH HPMC low (120)	235.9	241.2	238.6
BuOH HPMC high (123)	221.4	251.7	236.6

The before mentioned observation that the stiffness of the samples is higher for the first test compared to the second test does not affect the length of the Linear Viscoelastic Range. In half of the samples, the longest Linear Viscoelastic Range can be found in the first test (test A or B), and in the other half of the samples, the longest Linear Viscoelastic Range can be found in the second test (test C or E). Hence, no relation seems to exist between the Linear Viscoelastic Range and the stiffness of the fuel.

4.2.3. COMPARISON

From the results, multiple comparisons can be made. Firstly the effect of a high or low concentration of gelling agent can be used to verify the results. Secondly, the different types of fuel, ethanol vs butanol can be compared. Thirdly, the type of gelling agent used for gelation of the fuel, HPC vs HPMC with water can be compared. As it is difficult to make a comparison between Figure 4.5 to Figure 4.12, a new graph is made. See Figure 4.13. For this new graph, the average results of the tests per sample are taken. As both the x-values and y-axis vary, both are averaged. Furthermore, the layout of the graphs indicates the composition of the samples. The colour indicates the basis of the fuel. Red indicates ethanol based and blue indicates butanol based. The intensity of the colour indicates the concentration of the gelling agent. Light blue and light red indicate a low concentration and dark blue and dark red indicate a high concentration. The style of the line indicates the type of gelling agent. A solid line represents HPMC and a dotted line indicates HPC. The Linear Viscoelastic Range as shown in Table 4.2 is also made visible understandable as can be seen in Figure 4.14.

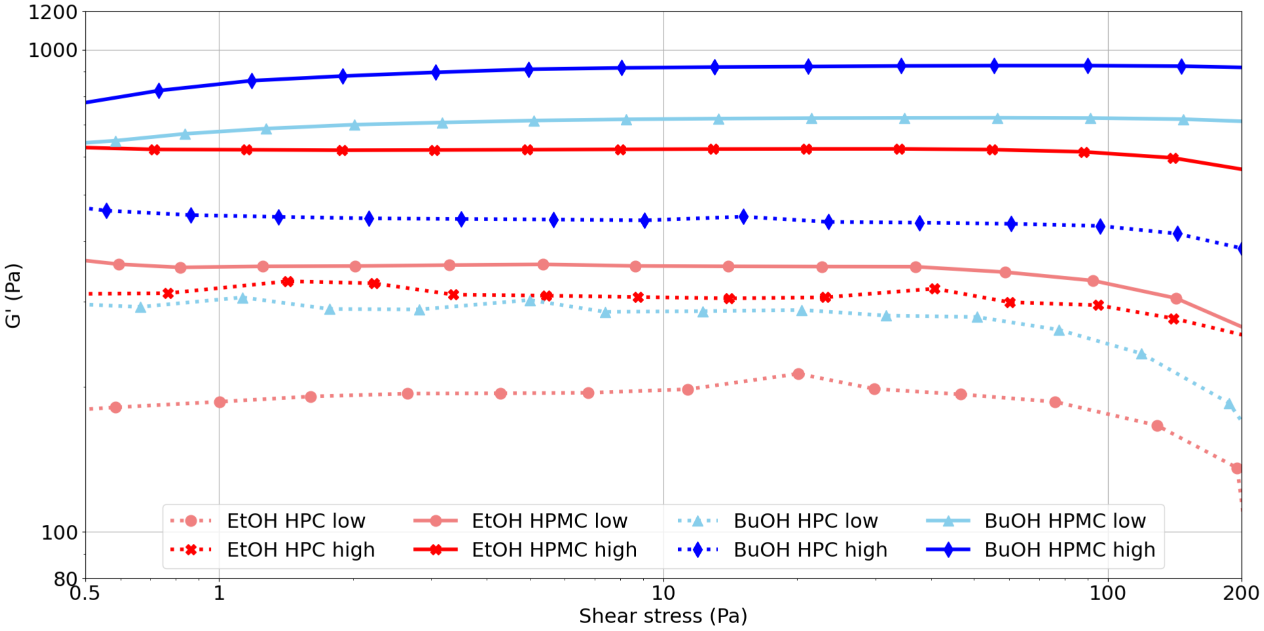

Figure 4.13: Amplitude stress sweep study comparison

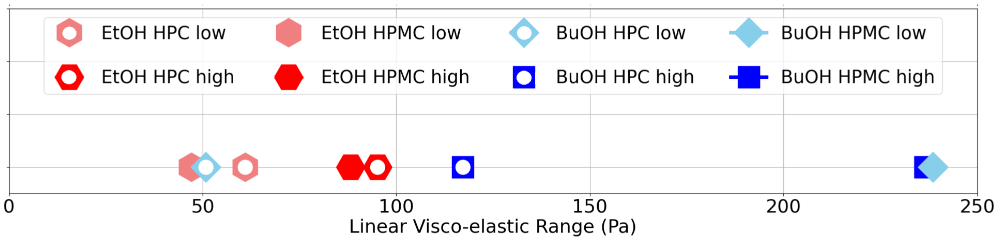

Figure 4.14: Linear Viscoelastic Range comparison

CONCENTRATION

In the graph (Figure 4.13) it can immediately be seen that the dark blue line is located above the light blue line and the dark red line is located above the light red line. This indicates that a high concentration of gelling agents result in a higher G' value. This relation is the case for all analysed fuels, so for the gelled ethanol fuels, the gelled butanol fuels, but also for both the HPMC and the HPC gelling agent. Hence, it can be concluded that the stiffness of the fuel or the strength of the gel increase with increasing concentration of gelling agent. This is also in line with physic laws, verifying the results.

Regarding the Linear Viscoelastic Range, no immediate trend is visible regarding the low concentrations and high concentrations of gelling agent. This can be seen in Table 4.2. Although a higher concentration seems to result in a longer Linear Viscoelastic Range, this is not the case for all samples. For the fuel gelled with HPC, both the ethanol and butanol fuel have a longer Linear Viscoelastic Range at higher concentrations of HPC. For the ethanol fuel, the range is increased with a factor of 1.5[1] and as for the gelled butanol fuel, the range is increased with a factor of 2.3 [2]. For the ethanol fuel gelled with HPMC the results are in the same trend as the Linear Viscoelastic Range is increased with a factor of 1.9 [3]. However, this was not the case for the butanol fuel gelled with HPC. For this sample, the Linear Viscoelastic Range decreased slightly (0.85%) for the higher concentration. This can be explained by the fact that the butanol fuel's critical gelling concentrations was found to be 4.0 wt% (see Subsection 3.3.3) and not the tested 4.5 wt% as shown in Figure 4.11. It could be that the Linear Viscoelastic Range does not increase further after a certain point of gelation, and that that point has been reached.

TYPE OF ALCOHOL

Regarding the stiffness of the fuel or the strength of the gel, the ethanol fuels are always weaker than the butanol fuels for the same concentration and the same gelling type. Additionally, the butanol fuel gelled with HPC is always stronger than ethanol fuel gelled with HPMC even independent of concentration. Hence, the length of the carbon chain influences the stiffness of the fuel. A longer chain results in a stiffer fuel.

There is no unambiguous trend visible for the Linear Viscoelastic Range between the ethanol fuels (represented by a red colour) and the butanol fuels (represented by a blue colour) as can be seen in Figure 4.14. Using HPC as gelling agent, the ethanol fuel with low concentration has a longer Linear Viscoelastic Range (61.6 Pa) than that of the butanol fuel with low concentration (50.8 Pa). However, for the ethanol fuel with high concentration, it is the other way around. There the ethanol fuels have a shorter Linear Viscoelastic Range (95.1 Pa) than that of the butanol fuel with a high concentration (117.2 Pa). Using HPMC as gelling agent does show a trend. There the butanol fuels have a longer Linear Viscoelastic Range than ethanol fuels.

TYPE OF GELLING AGENT

Regarding the stiffness of the fuel or the strength of the gel, the fuels gelled using HPMC are stronger than the fuels gelled with HPC independent of the alcohol type, but for the same concentration (low or high). In Figure 4.13 this can be seen by looking at the line style. The solid lines representing HPMC are always located above the dotted lines representing HPC, assuming the same concentration (low or high). However, one needs to keep in mind that the concentrations of gelling agent are not equal.

The Linear Viscoelastic Range of the ethanol fuels is lower for the fuel gelled with HPMC (47.1 Pa and 88.2 Pa) compare to the fuel gelled with HPC (61.6 Pa and 95.1 Pa). For the butanol fuels this is the other way around and the Linear Viscoelastic Range of the fuels gelled with HPMC are higher (238.6 Pa and 236.6 Pa) compare to the fuels gelled with HPC (50.8 Pa and 117.2 Pa). However, one needs to keep in mind that the concentrations are not equal to each other. This can be observed based on Figure 4.14 where the open symbols indicate HPC and the filled symbols indicated HPMC.

---

[1] Calculation: $\frac{95.1-61.6}{61.6} \times 100\% = 54\%$ or factor 1.5

[2] Calculation: $\frac{117.2-50.8}{50.8} \times 100\% = 131\%$ or factor 2.3

[3] Calculation: $\frac{88.2-47.1}{47.1} \times 100\% = 87\%$ or factor 1.9

4.3. YIELD POINT

The stress ramp study is the most frequently used technique to measure yield stress. The stress at the maximum viscosity provides a representative value for the yield stress. Structured fluids, like solidified fuel, do not flow unless they reach a critical stress level called yield stress. Below this yield stress, the material is elastic. Above the yield stress the structure of the fuel breaks down, and the fuel starts to flow. Structured materials have a viscosity that drops at higher rates of shear stress. This phenomenon is called shear thinning. This is due to the fact that the materials do not exhibit Newtonian flow after the yield. The viscosity decreases until a plateau is reached. It is typical to represent the results of a shear stress ramp study in a diagram with the shear stress (or velocity) shown on the x-axis and the apparent viscosity on the y-axis. Both axes are on a linear scale.

4.3.1. SETTINGS OF THE SHEAR STRESS RAMP STUDY

The shear stress ramp was a rotation ramp study. The time duration used was equal to 30 seconds, as this value is also used in the literature [15]. The sample was approached in a controlled-stress (CS) mode. The starting value of the shear stress was set to $\tau = 0.0\ Pa$ and the ending value to τ= 1000 Pa. This ending value is found by trial-and-error. As written before, it is easier to test for a longer range and not use the data, than to have to redo the test due to missing data. The distribution is set to linear and continuous.

The shear stress ramp tests are labelled C, D, and E. All tests are executed on the second day (t=5 days). It was found that it would not be possible to repeat the test again for a third time due to the fact that the sample quantity decreased faster than expected. Therefore, only the samples that showed deviations between test C and D are tested for the third time and labelled test E.

4.3.2. RESULTS

The results of the experiments can be seen in Figure 4.15 to Figure 4.22. To allow for comparison, the axes are kept equal as much as possible. The focus of this experiment is finding the yield point, and therefore, this point has to be shown clearly in the graphs. It can be immediately noticed that the range of shear stress is very different for the fuel gelled with HPC compared to the fuel gelled with HPMC, therefore the x-axis is not equal for all graphs. Rather, the x-axis for all fuels gelled with HPC (samples 101, 102, 103, and 104) runs from 0 to 400 Pa. For the fuels gelled with HPMC (samples 119, 122, 120 and 123) the x-axis runs from 0 to 700 Pa. Also, the maximum viscosity reached is varying between all the samples. Note that the y-axis is set optimal for every graph.

Another feature that becomes clear from the graphs is that the first test performed (test C) is always located below that of the second or third test (test D or E), except for sample 119. Hence, it seems that the viscosity of the sample increases due to the testing. An explanation for this could be due to the alteration of the samples as a result of the scooping. The visual change in the samples is explained in Section 4.7. Another explanation could be that during the scooping of the sample out of the bottle the internal structure is damaged. This allows a small amount of alcohol to evaporate, which then would results in an effectively higher concentration of gelling agent as less alcohol is present. This, however, is less likely as the bottles are only opened for a short amount of time. The temperature for experiment C is always below that of test D and E, so the temperature can not be the reason.

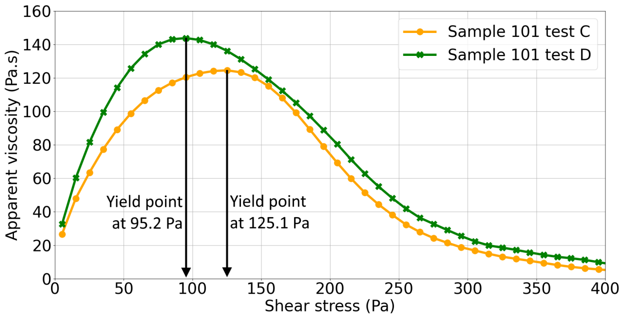

Figure 4.15: Shear stress ramp study of ethanol and 3.0 wt% HPC

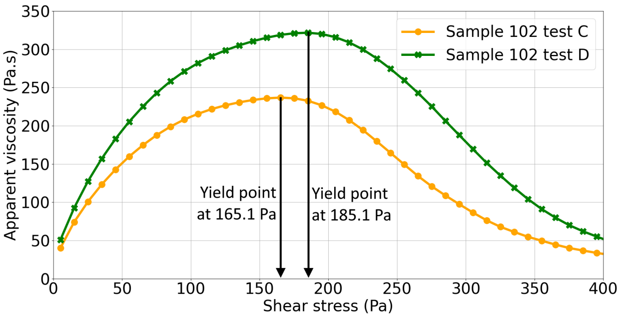

Figure 4.16: Shear stress ramp study of ethanol and 3.5 wt% HPC

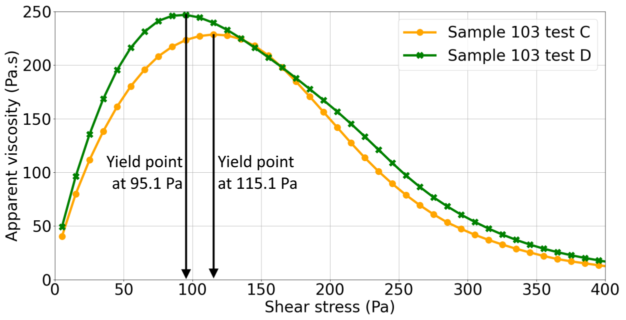

Figure 4.17: Shear stress ramp study of butanol and 3.0 wt% HPC

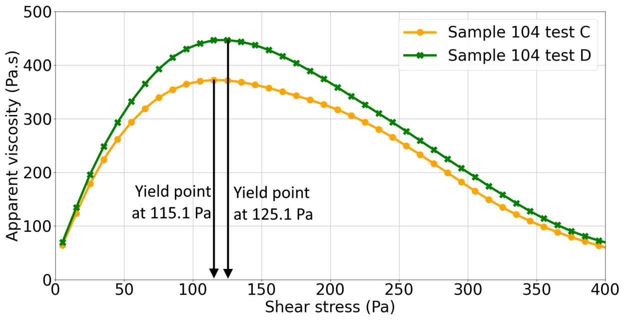

Figure 4.18: Shear stress ramp study of butanol and 3.5 wt% HPC

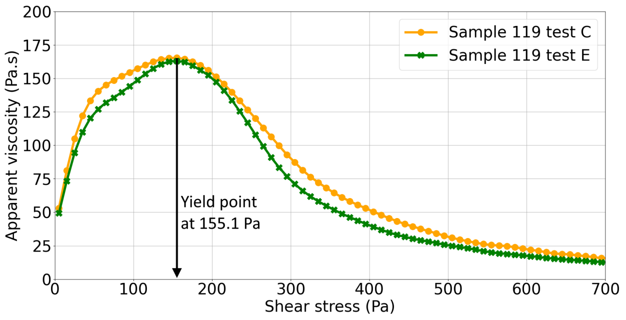

Figure 4.19: Shear stress ramp study of ethanol, water and 4.5 wt% HPMC

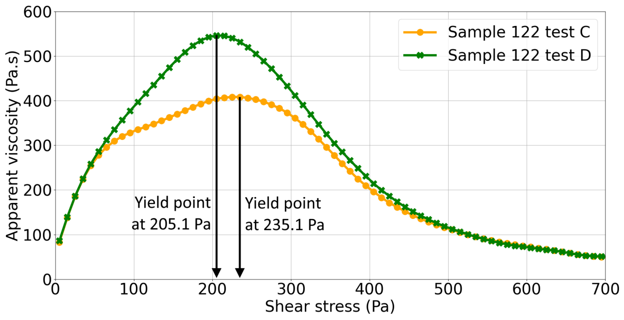

Figure 4.20: Shear stress ramp study of ethanol, water and 5.0 wt% HPMC

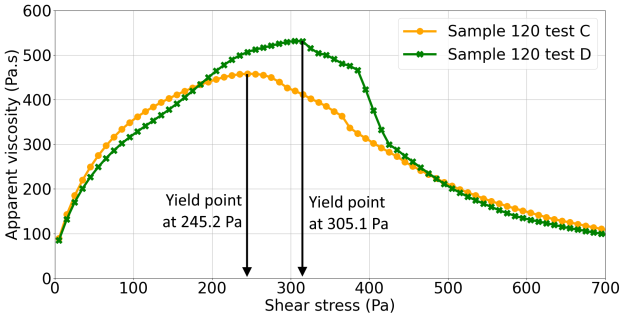

Figure 4.21: Shear stress ramp study of butanol, water and 4.5 wt% HPMC

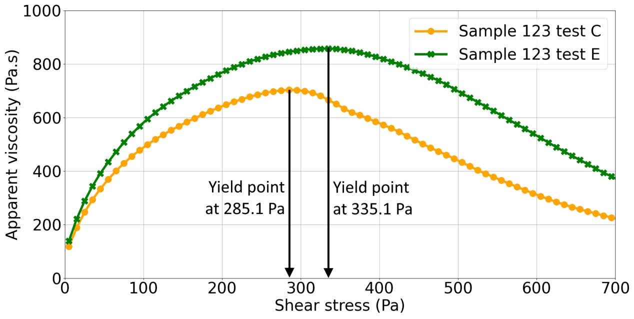

Figure 4.22: Shear stress ramp study of butanol, water and 5.0 wt% HPMC

The yield point of the fuel is equal to the shear stress at which the maximum viscosity is reached. An overview of the yield point per test and the average yield point per fuel can be found in Table 4.3. It can be seen that there is no relation between the maximum apparent viscosity and the yield point.

For Figure 4.15 to Figure 4.22 it can be seen that after the yield point is reached the fuel's viscosity decreases with increasing shear stress. This means that all fuels exhibit shear thinning behaviour. Shear thinning behaviour is a desirable property to possess as it will ease the mixing process between fuel and oxidizer. This also helps to overcome the low burn rate typically associated with hybrid rocket engines.

Table 4.3: Overview of the Yield Point

Sample number	Yield point (Pa)		
	Test C	Test D or E	Average
EtOH HPC low (101)	125.1	95.2	110
EtOH HPC high (102)	165.1	185.1	175
BuOH HPC low (103)	115.1	95.1	105
BuOH HPC high (104)	115.1	125.1	120
EtOH HPMC low (119)	115.1	155.1	135
EtOH HPMC high (122)	235.1	205.1	220
BuOH HPMC low (120)	245.2	305.1	275
BuOH HPMC high (123)	285.1	335.1	310

4.3.3. COMPARISON

From the results, multiple comparisons can be made; (1) the effect of the type of gelling agent HPC vs HPMC, (2) the effect of the different basis for the fuel, ethanol vs butanol fuels, and (3) the concentration of gelling agent, low vs high. To make a better comparison between Figure 4.25 to Figure 4.32 a new graph is made. See Figure 4.23. From this new graph, the average results of the test per sample are taken. As both the x-axis and y-axis vary, both are averaged. Furthermore, the lay-out of the graphs indicates the composition of the samples. The colour indicates the basis of the fuel. Red indicates ethanol based and blue indicates butanol based. The intensity of the colour indicates the concentration of the gelling agent. Diminished colours indicates a low concentration and dark colours indicates a high concentration. The style of the line indicates the type of gelling agent. A solid line represents gelling agent HPMC and a dotted line indicates gelling agent HPC.

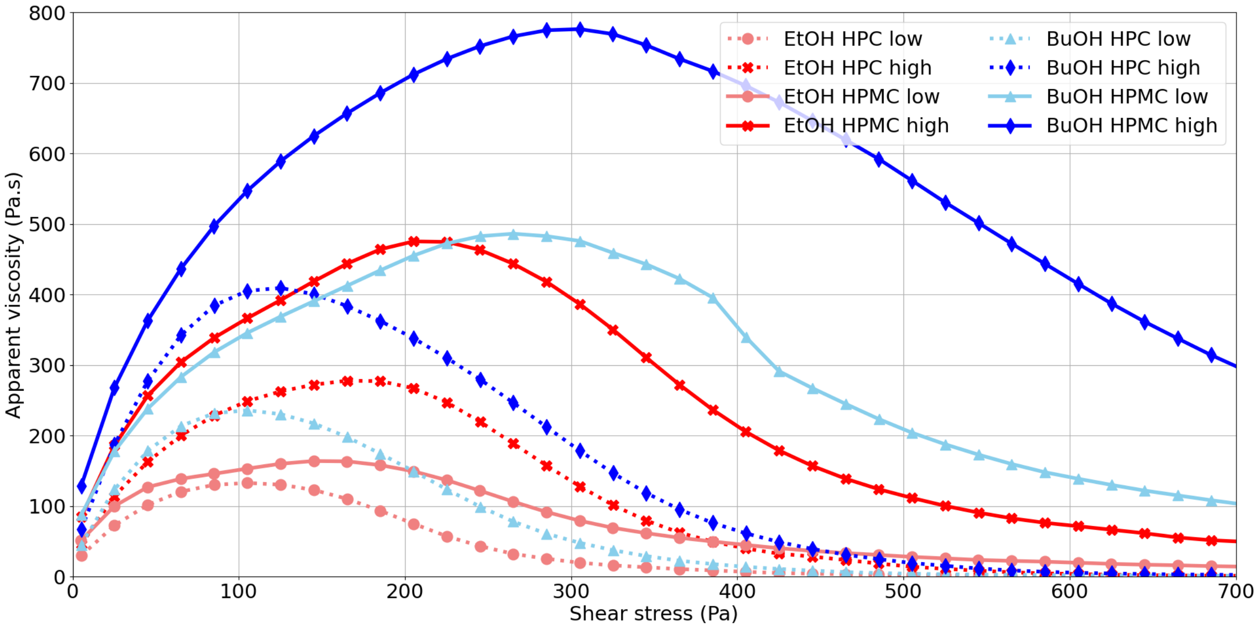

Figure 4.23: Shear stress ramp study comparison

The yield point as shown in Table 4.3 are visually represented in Figure 4.24. The type of gelling agent is represented by an open or filled symbol.

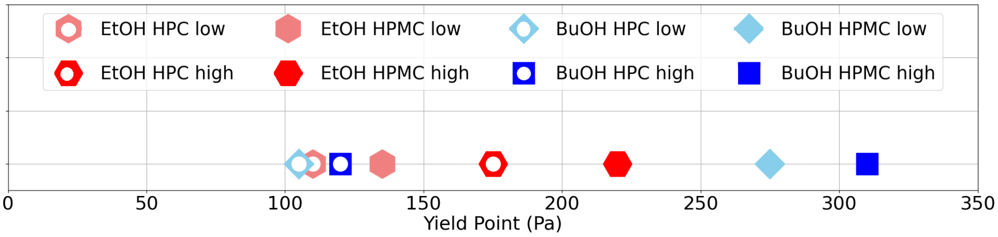

Figure 4.24: Yield point comparison

GELLING AGENT

In Figure 4.23 it can be seen that the viscosity of all fuels gelled with HPMC have a higher apparent viscosity, except ethanol fuel gelled with a low concentration of HPMC. It can also be seen that the ethanol fuel with low concentrations of HPC and HPMC (light red lines) are relatively close to each other compared with the other samples that have the same concentration and alcohol basis.

Regrading the yield point, the fuels gelled with HPMC have a higher yield point than the ones gelled with HPC, when taking the same concentration (low or high). On average, the yield point of the fuels gelled with HPMC is a factor of 1.9 higher[4] than the yield point of the fuels gelled with HPC. To be more specific, the yield point of the ethanol fuel gelled with HPMC is a factor 1.3 higher [5] than the yield point of ethanol gelled with HPC, independent of concentration. As for butanol, there is no such trend visible. The yield point of the low concentration is a factor 2.6 higher [6] while the yield point of the high concentration is only a factor 1.6 higher [7]. This, again, can be caused by the difference in critical gelation. For the butanol samples, the low concentration tested was 4.5 wt% while in Chapter 3 it was found that 4.0 wt% would already be sufficient. It could be that the yield point does not increase further after a certain concentration of the gelling agent.

CONCENTRATION

Figure 4.23 shows that the fuels with a high concentration of gelling agent have a higher viscosity than the fuels with a low concentration of the gelling agent. This is independent of the type of fuel or the type of gelling agent. This outcome verifies the result of this test, as physical laws also dictated that a higher concentration of gelling agents should result in a more viscous material.

Regarding the yield point, the higher concentrations of gelling agents always result in a higher yield point when comparing the same basis and same type of gelling agent. This can be seen in Table 4.3. For the ethanol fuels, the yield point increases with a constant factor of 1.6 [8], independent of gelling agent. For the butanol fuels, the yield point increases with a factor of around 1.1 [9], independent of gelling agent.

TYPE OF FUEL

The butanol fuels have a higher viscosity than the ethanol fuels when comparing only the different alcohol bases, but the same gelling agent and concentration. See Figure 4.23, where the blue lines (representing butanol) are always located above the red lines (representing ethanol).

Regarding the yield point, there is no trend. For the gelling agent HPC, the ethanol fuels have a higher yield point than the butanol fuels (when comparing the same concentrations). However, when looking at the gelling agent HPMC, it is the other way around. There the yield point of the butanol fuels is higher than that of the ethanol fuels, independent of concentration.

---

[4] Calculation: $\frac{(135+220+275+310)-(110+175+105+120)}{(110+175+105+120)} \times 100\% = 84\%$ or factor 1.9

[5] For low concentration $\frac{135-110}{110} \times 100\% = 23\%$ and for high concentration $\frac{220-175}{1755} \times 100\% = 26\%$, hence on average factor 1.3

[6] Calculation: $\frac{275-105}{105} \times 100\% = 162\%$ or factor 2.6

[7] Calculation: $\frac{310-120}{120} \times 100\% = 61\%$ or factor 1.6

[8] For HPC the increase is $\frac{175-110}{110} \times 100\% = 59\%$ or factor 1.6 and for HPMC the increase is $\frac{220-135}{135} \times 100\% = 63\%$ or factor 1.6

[9] For HPC the increase is $\frac{120-105}{105} \times 100\% = 14\%$ or factor 1.1 and for HPMC the increase is $\frac{310-275}{275} \times 100\% = 12\%$ or factor 1.1

4.4. TIME-DEPENDENT BEHAVIOUR

Frequency sweep studies are used to describe the time-depending behaviour of a sample in the non-destructive deformation range. This range is equal to the Linear Viscoelastic Range as found in Section 4.2. High frequencies simulate the fast motion on short timescales, whereas low frequencies simulate slow motion on long timescales. It is typical to present the results of a frequency sweep study in a diagram with the frequency shown on the x-axis and the storage modules (elastic modulus) G' and loss modules (viscous modulus) G" plotted on the y-axis. Both axes are on a logarithmic scale.

4.4.1. SETTINGS OF THE FREQUENCY SWEEP STUDY

The frequency sweep is an oscillation frequency sweep with constant shear stress. The shear stress was found via the amplitude sweep study (Section 4.2). As shear stress, it is advised to use a value in the middle of that Linear Viscoelastic Range measured on a logarithmic scale, hence shear stress of 10 Pa is chosen. This shear stress is kept constant in all experiments for all samples. The sample was approached in a controlled-stress (CS) mode. Hereby, the sample corresponds with a deformation. The starting value of the frequency was set to $f = 0.1\ Hz$ and the ending value to $f = 30\ Hz$. This ending value was found via trial-and-error. Furthermore, it is easier to test high frequencies now and later not used the data, than to not have the data and having to redo tests to obtain the missing data. The starting value of the sample is of importance as the sample is affected by the experiment itself. The starting point of f=0.1 is based on the time it takes to execute the experiment. Lower frequencies take longer to test, the longer the test takes, the more alcohol (butanol or ethanol) is evaporated while performing the test. Hence, a balance between experiment time and the quality of the data had to be found.

The frequency sweep tests have the labels A, B, C, and E. On the first day (t=4 days), test A and B were executed. Test A had the starting value of f=0.1 Hz. However, as the graphs did not cross, it was decided to see if this would happen at lower frequencies. Hence, tests labelled with B have a starting value of f=0.01 Hz. However, this increased the experiment time a lot, and therefore it was decided to just continue with the A-series. The next day (t=5 days), the frequency sweep test was repeated for all samples, labelled test C. By, then it was found that it would not be possible to repeat all studies for the third time as the sample quantity decreased faster than expected. As only sample 119 showed a very strange result in test B, this sample was tested for the third time and labelled test E. The data that is not shown can be found in Table B.

4.4.2. RESULTS

The results of the experiment can be seen in Figure 4.25 to Figure 4.32. To allow for a clear visual analysis of the results, the y-axis runs from 30 Pa to 1000 Pa. Only for the sample containing butanol with 5.0 wt% HPMC the range was set to 1500 Pa. For the x-axis, it has been decided to show the data from 0.1 Hz to 10 Hz. After 10 Hz the internal structure was destroyed to such an extent that machine errors dominate the results.

From the results (Figure 4.25 to Figure 4.32) it can be seen that for a shear stress of 10 Pa, the G' and G" are showing a more or less linear dependency on the frequency. At higher frequencies, this linear dependency is lost due to the destruction of the weak internal structure. Especially in the samples containing low concentrations of HPC (Figure 4.25 and Figure 4.27) it can be seen that the linear dependency is lost already well before the 10 Hz. In most samples (samples 101, 103, 104, 122 and 123) the G' is dominant over G" for the entire range of frequencies. Hence, these samples behave consistently like a perfect elastic gel. For the sample 102 and 119, the G" gets dominate above 8.5 Hz[10]. Although there is too little data to draw a conclusion, it seems like only some of the ethanol fuels have a crossing at 8.5 Hz, but that butanol does not show this behaviour (see Figure 4.26 and Figure 4.29).

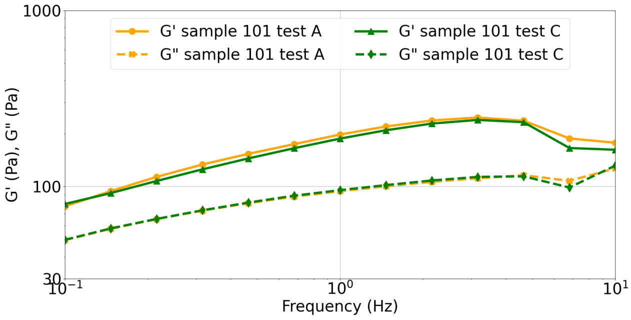

Figure 4.25: Frequency sweep study of ethanol and 3.0 wt% HPC

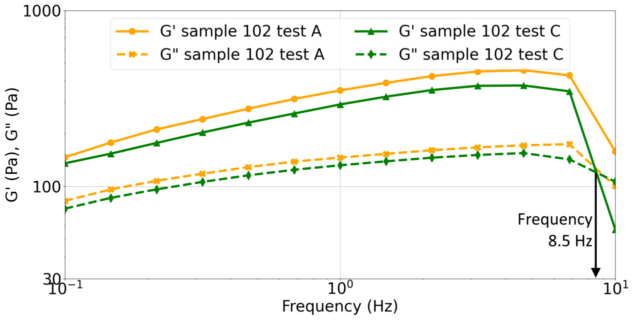

Figure 4.26: Frequency sweep study of ethanol and 3.5 wt% HPC

---

[10] For sample 119 the average of the two is $\frac{8.1+8.9}{2} = 8.5Hz$

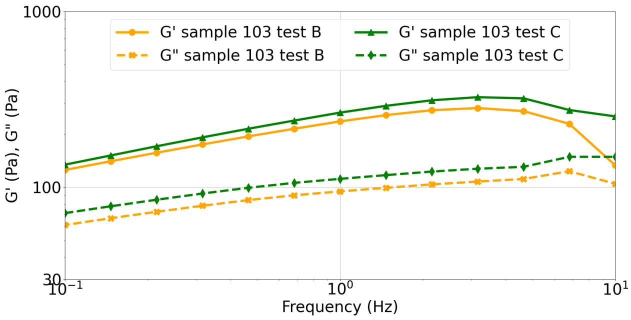

Figure 4.27: Frequency sweep study of butanol and 3.0 wt% HPC

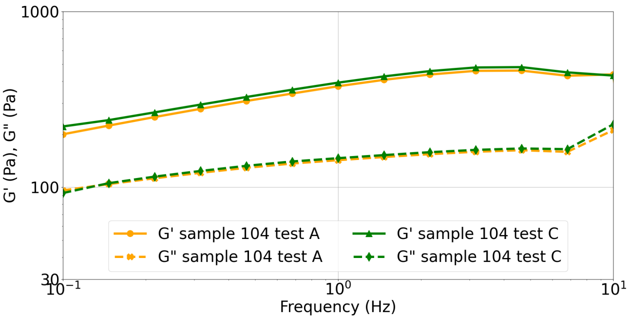

Figure 4.28: Frequency sweep study of butanol and 3.5 wt% HPC

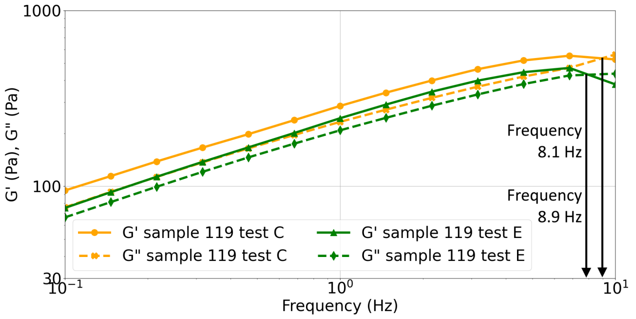

Figure 4.29: Frequency sweep study of ethanol, water and 4.5 wt% HPMC

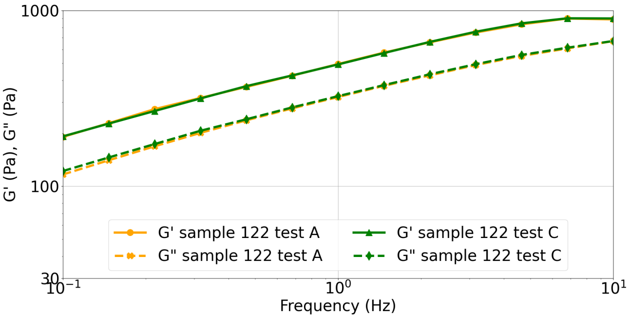

Figure 4.30: Frequency sweep study of ethanol, water and 5.0 wt% HPMC

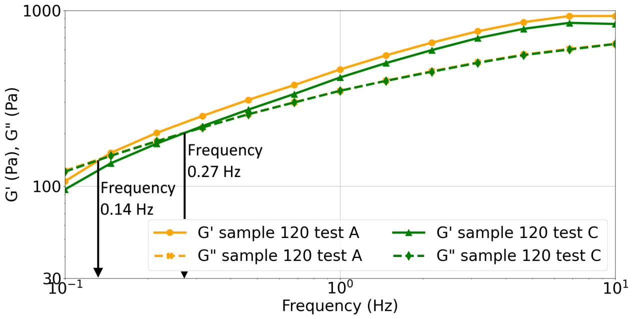

Figure 4.31: Frequency sweep study of butanol, water and 4.5 wt% HPMC

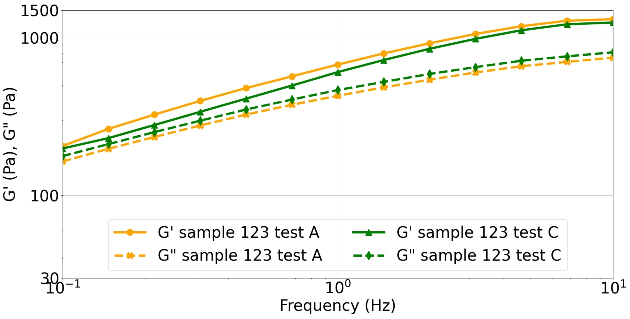

Figure 4.32: Frequency sweep study of butanol, water and 5.0 wt% HPMC

The fuel consisting of butanol, water, and 4.5 wt% HPMC is the only one that shows deviant behaviour from the others. See Figure 4.31. At low frequencies, the viscous behaviour reflected by G" is dominant, whereas at high frequencies, the elastic behaviour reflected by G’ is dominants. Hence, this sample seems to behave as a liquid viscoelastic material at low frequencies but behaves as an elastic material as the frequency increases.

Regarding the surrounding temperature at which the tests are performed. The first test (A or B) is always at a lower temperature than the second test (test C). The only deviation to this is sample 119, whereby test E is executed at a higher temperature. See Table B.2 for the average temperature during testing.

4.4.3. COMPARISON

From the results, multiple comparisons can be made. Firstly, the effect of a higher or lower concentration of the gelling agent. Secondly, the difference in basis for the fuel, ethanol vs butanol. Thirdly, the type of gelling agent used for gelation of the fuels, HPC vs HPMC with water. To make a better comparison between Figure 4.25 to Figure 4.32 a new graph is made, see Figure 4.33. From this new graph, the average results of the test per sample are taken. As both the x-axis and y-axis vary, both are averaged. Furthermore, the layout of the graphs indicates the composition of the samples. The colour indicates the basis of the fuel. Red indicates ethanol based and blue indicates butanol based. The intensity of the colour indicates the concentration of the gelling agent. Light blue and light red indicate a low concentration and dark blue and dark red indicate a high concentration. The style of the line indicates the type of gelling agent. A solid line represents gelling agent HPMC and a dotted line indicates gelling agent HPC.

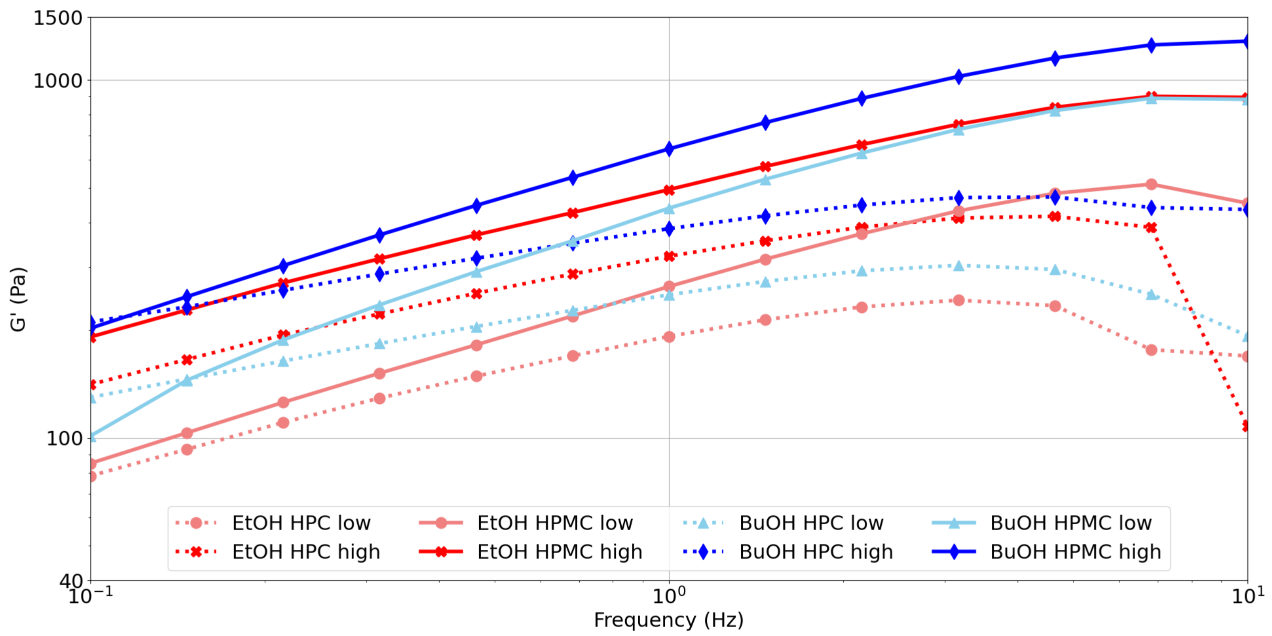

Figure 4.33: Frequency sweep study comparison

CONCENTRATION

In Figure 4.13 it can be observed that for high concentrations, the G' is above that of the low concentrations. All dark blue and dark red lines (representing a high concentration) are lying above the corresponding light blue and light red lines (indicating low concentration). This is independent of alcohol type or gelling agent type. Hence, it can be concluded that the stiffness of the fuel or the strength of the gel increases with the increase in the concentration of the gelling agent.

TYPE OF ALCOHOL

Regarding the type of fuel, ethanol fuels are always less stiff than butanol fuels (for the same concentration of gelling agent and the same alcohol basis). In Figure 4.33 both the dark and light blue lines representing butanol are always lying above the corresponding dark and light red lines representing ethanol. Hence, once again, this proves that the carbon chain influences the stiffness of the fuel. A longer chain results in a stiffer fuel.

TYPE OF GELLING AGENT

The graphs of the fuels gelled with HPC are flatter than those of the fuels gelled with HPMC. Hence, the fuel gelled with HPC shows less dependency on frequency than those gelled with HPMC. On the other hand, the samples gelled with HPMC have a higher stiffness than the once gelled with HPC. This can be seen in Figure 4.33 as the solid lines are above the dotted lines (when looking at the same alcohol basis and same gelling concentration). And lastly, it can be seen that the gap between the G' and G" of the fuel gelled with HPC is bigger (Figure 4.25 to Figure 4.28) then the ones gelled with HPMC (Figure 4.29 to Figure 4.32).

4.4.4. LOSS FACTOR TAN(δ)

The loss tangent or damping factor is important in oscillatory analysis. This ratio represents the ratio between the G"/G', hence the elastic modules over the viscous modulus. This ratio indicates whether a material behaves like an elastic, viscous, or viscoelastic material. For ideal elastic behaviour $\delta = 0$ and for ideal viscous behaviour $\delta = 90$, hence the fraction would approach infinity. Usually, for practical applications, a solid material is called ideally elastic if $\tan(\delta) < 0.01$.

In Figure 4.34 the graphs of all samples can be seen. These indicate that all samples behave like a viscoelastic solid at 10 Pa shear stress for most frequencies because the lines are located between 0.1 and 1. Furthermore, it can be seen that the ethanol fuel gelled with HPMC shows near frequency-independent behaviour as their lines are straight. Other aspects that can be noticed in the graph are that only the butanol fuel gelled with a 4.5 wt% (low) concentration of HPMC crosses the horizontal line of 1, due to the fact that the G'< G" at those frequencies. Also, the ethanol fuel gelled with a high concentration of HPC and ethanol fuel gelled with a low concentration of HPMC cross the horizontal line of 1, due to the fact that elastic modules dominate.

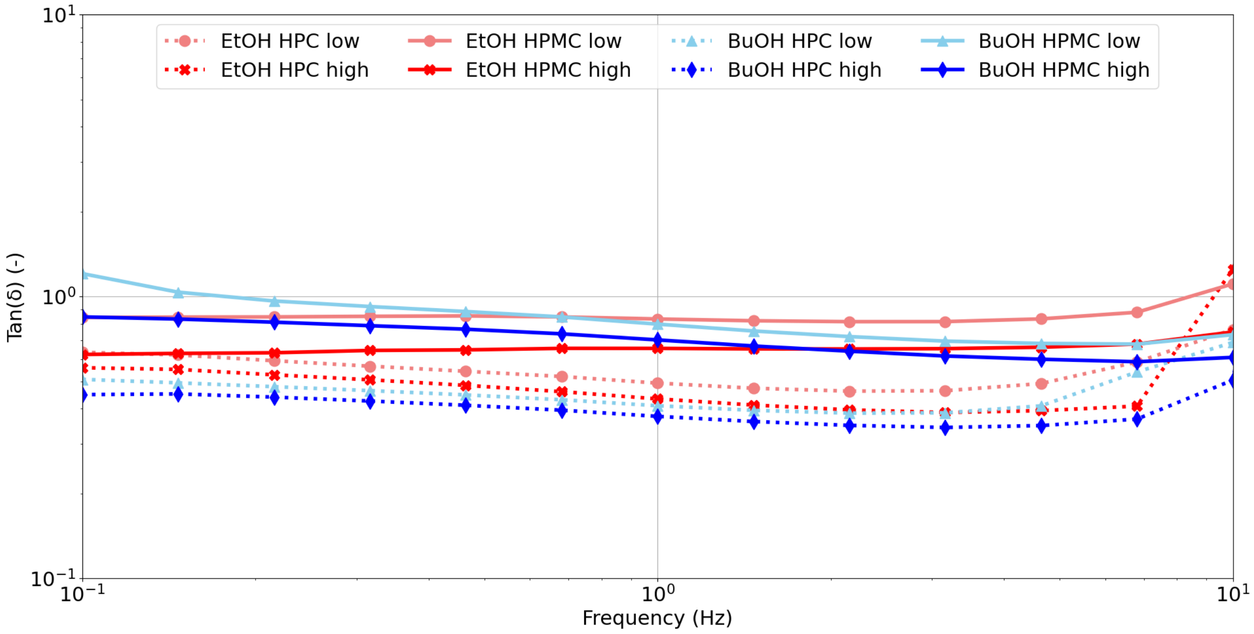

Figure 4.34: Loss factor of the different gelled fuels

This graph (Figure 4.34) shows clearly that all dotted lines (representing fuels gelled using HPC) are lying below the solid lines (representing fuels gelled using HPMC). This indicates that fuels gelled using HPC are showing a behaviour more closely to that of an ideally elastic material as they more closely to $\delta = 0$.

4.5. STABILITY STUDY

Stability studies are performed to determine the effects of environmental conditions on product quality. Environmental conditions can impact product shelf life and the viability of product formulation. To investigate the rheology characteristics over time, the amplitude stress sweep study, frequency sweep study, and shear stress ramp study are repeated. The initial study was performed at t=4 days or t=5 days. The stability study is performed at t=35 days. All settings of the experiments are kept to the same to allow for comparison. Two experiments are conducted for every study, these are sequentially labelled test K and test L.

The first noticeable change in the samples is already visible with the naked eye. The amount and size of the trapped air bubbles in the fuel samples have been reduced. For sample 101 (EtOH HPC low) the air bubbles have even completely disappeared. See Figure 4.4 and Figure 4.46 as a reference. Furthermore, there seems to be a relation between the concentration of gelling agent and the amount of air trapped. All high concentration samples have more air bubbles trapped compared to their associated low concentration samples. This is caused by the viscosity of the sample. The low concentration samples have a lower viscosity allowing the trapped air to move more freely to escape the fuel, while the high concentration samples have a higher viscosity hindering the movement of air bubbles. The change in trapped air can be seen in Figure 4.35 whereby the low and high concentrations are placed next to each other. Although this figure only shows the ethanol fuels, it is representative of the butanol fuels as well. The butanol samples can be seen in Figure A.1.

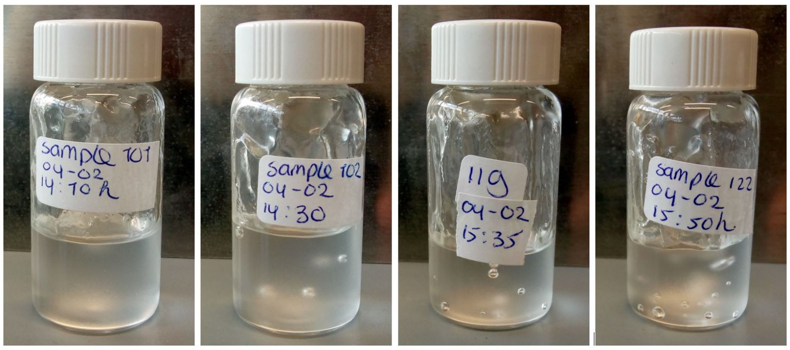

Figure 4.35: Visual appearance of the ethanol fuels during the stability study (at t=35 days)

4.5.1. LINEAR VISCOELASTIC RANGE

The Linear Viscoelastic Range is investigated by performing an amplitude stress sweep study. The settings are kept equal to that of Section 4.2. Hence, the sample was approached in a controlled-stress (CS) mode and the frequency was equal to 5 Hz. The results of the experiments can be seen in Appendix B in Figure B.8 to Figure B.15. The grey lines indicate the results of the previous test (Figure 4.5 to Figure 4.12). The first aspect that can be concluded from these graphs is that the strength of the fuels has stayed more or less equal over the timespan of one month. Furthermore, it can be seen that samples 101 and 103 still show a wobbling line. This indicates that the samples are not homogeneous. For sample 101, it can be concluded that the wobbling line (that was also already present at t=4.5 days) has to be caused by a lack of homogeneous mixing of the sample as no air was present in sample 101 (see Figure 4.35). However, other fuels such as samples 102 and 104 do now show a straight line, while at t=4.5 the line was wobbling. This indicates that the previously observed wobbles could be due to air trapped inside. Hence, the wobbling lines are caused by two aspects; trapped air in the fuel and a non-homogeneous mixing of the fuel. Note that this wobbling behaviour only occurs in the fuels gelled with HPC, the fuels gelled with HPMC are homogeneous.

The Linear Viscoelastic Range of the samples is again determined with a ruler. An overview of the Linear Viscoelastic Range can be seen in Table 4.4. Here, also the results of the initial rheology study are shown (Table 4.2). The change over time has been determined using $\frac{(average_{t=35})-(average_{t=4.5})}{(average_{t=4.5})} \times 100\%$. There is no clear trend visible over time. Most samples show an increase in Linear Viscoelastic Range, however, this is not always the case.

Table 4.4: Linear Viscoelastic Range during the stability study

Sample number	Linear viscoelastic Range (Pa)				Change of time
	Test K	Test L	Average at t = 35 days	Average at t = 4 or 5 days	
EtOH HPC low (101)	74.7	132.5	104	62	68 %
EtOH HPC high (102)	96.3	86.7	92	95	-4 %
BuOH HPC low (103)	144.0	79.7	112	51	120 %
BuOH HPC high (104)	151.3	192.6	172	117	47 %
EtOH HPMC low (119)	73.1	103.4	88	47	87 %
EtOH HPMC high (122)	143.7	144.6	144	88	64 %
BuOH HPMC low (120)	242.8	234.7	239	239	0 %
BuOH HPMC high (123)	222.9	225.4	224	237	-5 %

4.5.2. YIELD POINT

The yield point is investigated by performing a shear stress ramp study. The settings are kept equal to that of Section 4.3. Hence, the samples are approached in a controlled-stress (CS) mode and the time duration used equals 30 seconds. The results of the experiment can be seen in Appendix B in Figure B.25 to Figure B.32. A few aspects are immediately noticeable. First of all, the green line (test L) is always located above the orange line (test K). This can be due to the alteration of the sample caused by performing the test (see Section 4.7). Secondly, for most fuels, the maximum apparent viscosity is lower, except for samples 104 (BuOH HPC high) and 119 (EtOH HPMC low) which have a higher maximum apparent viscosity than before.

The yield point is determined again, an overview can be seen in Table 4.5. The average at t=4 days or t=5 days comes from Table 4.3. Two aspects are noticeable. First of all, sample 122 (EtOH HPMC high) is the only sample that has a lower yield point for test L (the second test). All other samples experience their highest yield point during test L, which is also the test that has the highest apparent viscosity. Previously (at t=4.5 days), no such relationship existed. Secondly, sample 104 (BuOH HPC high) is the only sample that shows an increase in yield point over time.

Table 4.5: Yield Point of the fuel during the stability study

Sample number	Yield Point (Pa)				Change over time
	Test K	Test L	Average at t= 35 days	Average at t= 4 or 5 days	
EtOH HPC low (101)	85.1	95.1	90	110	-18 %
EtOH HPC high (102)	115.2	125.1	120	175	-31 %
BuOH HPC low (103)	85.2	95.2	90	105	-14 %
BuOH HPC high (104)	125.1	135.1	130	120	8 %
EtOH HPMC low (119)	125.2	135.3	130	135	-4 %
EtOH HPMC high (122)	215.2	165.1	190	220	-14 %
BuOH HPMC low (120)	205.1	215.1	210	275	-24 %
BuOH HPMC high (123)	275.1	285.1	280	310	-10 %

4.5.3. TIME-DEPENDENT BEHAVIOUR

The time-dependent behaviour is investigated by performing a frequency sweep study. The settings are kept equal to that of Section 4.4. Hence, the sample is approached in a controlled-stress (CS) mode and the shear stress is equal to 10 Pa. The results of the experiment can be seen in Appendix B in Figure B.16 to Figure B.23. The grey lines show the results from the frequency sweep study at t=4 or t=5 days. It can be seen that at low frequencies the lines are almost completely on top of the grey lines, but that at higher frequencies deviations occur. Only sample 102 shows a bit less strength compared to a month ago and sample 122 shows a bit more strength.

A feature that has changed is the crossing point between G' and G". At t=4.5 only sample 102 (EtOH HPC high) had a crossing during one of its tests (Figure 4.26) and sample 119 (BuOH HPMC low) had a crossing point during both tests (Figure 4.29). At t=30 days the behaviour of the fuels containing HPMC as gelling agent is the same. Still, only sample 119 (BuOH HPMC low) shows a crossing point where G'=G", this time at 8.1 Hz and 10 Hz. Roughly, the same values as before (at t=4.5 the crossing were at a frequency of 8.1 Hz and 8.9 Hz). The other fuels gelled with HPMC still have no crossing points. Even sample 120 (BuOH HPMC low) that previously seemed to behave as a liquid viscoelastic material at low frequencies (Figure 4.31), now behaves as an elastic material for all frequencies. For the fuels gelled with HPC, more changes are visible. Sample 102 (EtOH HPC high) still shows a crossing at 8.1 Hz. However sample 101 (EtOH HPC low) now also shows a crossing at 7.9 Hz and sample 103 (BuOH HPC high) shows a crossing at 8.1 Hz and 9.5 Hz, while previously no crossing was present. At frequencies for which G" is dominant, the samples behave more like a liquid viscoelastic material. Hence, over time, the fuels gelled with HPC start to behave more like a liquid viscoelastic material for high frequencies. An overview can be seen in Table 4.6 and x means that no crossing was present (or at least not in the tested frequency range).

Table 4.6: Overview G"=G'

Sample number	G' equal G"				Change over time
	Intial study (t=4.5 days)		Stability study (t=35 days)		
	First test	Second test	Test K	Test L	
EtOH HPC low (101)	x	x	x	7.9 Hz	Yes
EtOH HPC high (102)	x	8.5 Hz	8.1 Hz	x	
BuOH HPC low (103)	x	x	9.5 Hz	8.1 Hz	Yes
BuOH HPC high (104)	x	x	x	x	
EtOH HPMC low (119)	8.9 Hz	8.1 Hz	10.0 Hz	8.1 Hz	
EtOH HPMC high (122)	x	x	x	x	
BuOH HPMC low (120)	G">G'	G">G'	x	x	Yes
BuOH HPMC high (123)	x	x	x	x	

The loss factor or tan(δ), which is the ratio between G"/G', is plotted for the stability study as well. The plot is shown in Appendix B Figure B.24. The grey lines indicate the graphs as they were at t=4.5 (Figure 4.34). The main focus of this plot is on the line tan(δ)=1. It can be seen that the BuOH HPMC low (solid light blue line) does not cross the tan(δ)=1 anymore and that all samples now behave as an elastic material at low frequencies. However, it can also be seen that more lines cross the tan(δ)=1 line at high frequencies. Previously, only EthOH HPMC low (light red dotted line) and EtOH HPC high (dark red solid line) crossed the tan(δ)=1 line, but now also BuOH HPC low (light blue dotted line) and the EtOH HPC low (light red dotted line) cross tan(δ)=1. This indicates that, over one month period, the viscoelastic nature of some fuels is more like a liquid viscoelastic material at high frequencies.

4.6. TEMPERATURE STUDY

A temperature study can be used to determine the effect of temperature on the viscosity of the fuel. The temperature range of interest is that between 0 ^oC to 45 ^oC. The bottle of HPC indicates that this gelling agent is insoluble at temperatures above 45 ^oC and therefore, this temperature is taken as the maximum. Although liquid ethanol already evaporates at 79 ^oC, this will not be the case for the gelled fuels. The (weak) internal structure will prevent the evaporation process of the alcohol. The same frequency as used in the amplitude sweep will be used during the temperature study, hence 5 Hz. Secondly, the activation energy of the fuel can be determined via a temperature study. This can be done using the Arrhenius equation (see Equation 4.1). In this equation $k[-]$ is the reaction rate constant, A [-] is the pre-exponential factor which is a particular constant to each reaction, E_a is the activation energy in J/mol, R is the universal gas constant which equals 8.3145 $J/Kmol$ and T is the temperature at which the reaction takes place in K. The temperature study will be executed with the MARS III rheometer with the CTC-MARS III to control the temperature.

$$k = A \cdot exp(\frac{-E_a}{RT}) \tag{4.1}$$

4.6.1. INITIAL TEMPERATURE STUDY

Literature [15] indicates the settings of rotation for the temperature study. However, the MARS III was unable to measure the samples via a rotation study. Also, a continuous temperature study was not possible due to limitations of the CTC-MARS III. Therefore, an osculation step-wise temperature study was performed instead. An experiment consists of three phases: (1) the cooling from room temperature to 0 ^oC, then (2) the actual data collection from 0 ^oC to 45 ^oC with ten steps, then (3) the cooling again back to room temperature. During the initial temperature study (t=25 days [11]) the sample was approached in a controlled stress (CS) mode with a shear stress of 10 Pa. These tests are labelled A. At t= 43 the test is repeated and labelled test Q. The data of this test can be seen in Appendix B in Figure B.33 to Figure B.36. Here it can already be observed that the results are strange. In Figure B.33 it can be seen that the low concentrations sample has a higher apparent viscosity than the high concentration sample. This is not in line with physical laws. In Figure B.34 it can be seen that the test results for sample 104 test A are completely different from that of test Q. Figure B.35 shows strange data as well, one expects more or less a smooth line and not the zigzag line as observed in this graph. Finally, Figure B.36 also shows that the low concentration sample has a higher apparent viscosity than the high concentration sample. Again, this is not in line with physical laws. Therefore, it is concluded that something went wrong during testing.

It was found that the MARS III was unable to accurately measure the samples. Looking at the data revealed that high axial forces were introduced during testing. In the samples gelled with HPC, the axial force was relatively low. The average normal force was roughly around -0.2 N with -0.7 N as the most extreme measurement. However, in the samples gelled with HPMC, the normal force was extreme. The average normal force was roughly around -3.4 N, with -8 N as the most extreme measurement. As the sample was approached with a constant gab of 1.000 mm this normal force means that a column has formed. This column was also observed during the opening of the machine after the experiment was finished. This can be seen in Figure 4.36. Keep in mind that this picture is taken during the opening of the rheometer, and hence shows an extremely large gab. During the experiment, the column was less thin. It is believed that this column formation is the reason for the strange results.

---

[11] Due to problems with the CTC-MARS III which controls the temperature, the temperature study was postponed. Therefore, the study was started on day 25 instead of day 4 or day 5.

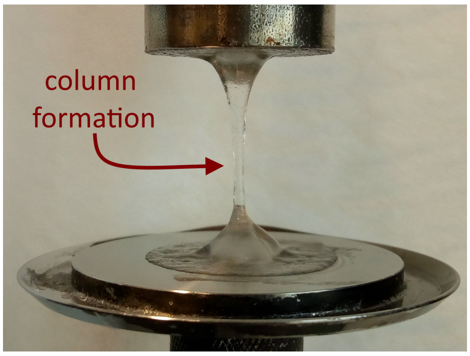

Figure 4.36: Column formation as observed during opening of the rheometer after the experiment

4.6.2. MEDIAL TEMPERATURE STUDY

As the results of the initial study were found to be wrong, a new temperature study was conducted. This was done on the day that the samples were t=43 days. The first focus was on reducing the huge axial force that was present during the previous executed experiment. Therefore, the settings were changed, and a controlled force was introduced (test R). This automatically means that the gab is no longer constant, but will decrease over time. Due to the normal force, the gab became around 30% smaller during phase 1 of the experiment. Therefore, it was decided to start with a bigger gab (test S). This resulted in a gap of 1.0 mm during the actual testing from 0 ^oC to 45 ^oC (phase 2 of the experiment). As it is sub-optimal to introduce an axial force, it was tried to reduce the force control to a smaller force (test T). However, then the MARS III was unable to preserve the constant normal force.

- **Test R:** Controlled stress (CS) mode with a shear stress of 10 Pa. Gab of 1.00 mm. Control force of 0.1 N.
- **Test S:** Controlled stress (CS) mode with a shear stress of 10 Pa. Gab of 1.30 mm. Control force of 0.1 N.
- **Test T:** Controlled stress (CS) mode with a shear stress of 10 Pa. Gab of 1.20 mm. Control force of 0.01 N.

This all did not have enough effect as the MARS III was still unable to measure the viscosity accurately. Therefore, it was decided to no longer try to approach the sample in a controlled stress (CS) mode, but rather use the controlled strain (DS) mode. Initially, a (random) strain of 5% was tested (test U) and this yielded an accurate measurement of the sample. Based on the amplitude stress sweep study a strain near the end of the Linear Viscoelastic Range was selected, namely a strain of 10% (test W). However, again, the MARS III was unable to measure the sample accurately. Lastly, the successful setting with 5% strain was repeated, but without the force control (test V). This resulted in a higher axial force (of around -0.5 N maximum) again.

- **Test U:** Controlled strain (DS) mode with a strain of 5%. Gab of 1.30 mm. Control force of 0.1 N.
- **Test W:** Controlled strain (DS) mode with a strain of 10%. Gab of 1.30 mm. Control force of 0.1 N.
- **Test V:** Controlled strain (DS) mode with a strain of 5%. Gab of 1.30 mm. No control force.

Hence, it was concluded that controlled strain (DS) mode was the way to go to achieve accurate results. Additionally, a force control of 0.1 N was required. This force control is high enough to not encounter machine errors but low enough that the sample is not squeezed. This can be seen in Figure 4.37. During phase 1 of the experiment, whereby the temperature is decreased from room temperature to 0 ^oC, the gab size already decreases a bit. Therefore, an initial gap of 1.30 mm is used as this roughly results in a gap of 1.0 mm during the data collection of the experiment (phase 2).

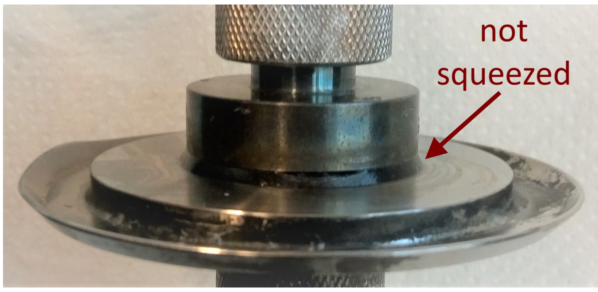

Figure 4.37: Visual appearance of a sample after an experiment with a normal force of 0.1 N

4.6.3. FINAL TEMPERATURE STUDY

The strain used during the experiment was eventually found in a scientific more sound approach. It was based on the results of the amplitude sweep study. There the strain associated with a shear stress of 10 Pa was found. It was found that per experiment (test A, B, C, E, K, or L) these values differ. Additionally, it was discovered that the associated strains for the samples gelled with HPMC are in general lower than the samples gelled with HPC. The average strain associated with a shear stress of 10 Pa was equal to around 3.0% for the HPC and to around 1.3% for the HPMC. The risk of using a high strain is that the plate will slip on the sample when the sample is unable to give enough resistance. Therefore, it is better to take the lower value. Hence, instead of taking the average of all samples, the average value of only the samples gelled with HPMC is used. Thus, the set strain is equal to 1%.

- **Test Y:** Controlled strain (DS) mode with a strain of 1%. Gab of 1.30 mm. Control force of 0.1 N. Test at t=44 days.
- **Test Z:** Controlled strain (DS) mode with a strain of 1%. Gab of 1.30 mm. Control force of 0.1 N. Test at t=48 days.

The experiments were conducted at t=44 days and t=48 days. For these experiments (test Y and test Z) the normal force was controlled correctly, except for the butanol samples gelled with HPC (samples 103 and 104). For those samples, the normal force was not preserved during the experiment.

RESULTS

The results of the temperature study are shown in Figure 4.40 to Figure 4.43. The first aspect that becomes clear is that the apparent viscosity is very different for all samples. It can be seen that sample 103 and 104 (Figure 4.41) have an extremely low viscosity. This is possible also the reason why the MARS III was unable to maintain the force control of 0.1 N. In Appendix B Table B.3 the measured normal force can be viewed. The low viscosity is furthermore visual after the experiment is over. The samples 103 and 104 looked different and more liquid-like compared to the other samples. The other samples looked almost like dried glue after the experiments were over (see Figure 4.38), but samples 103 and 104 were more liquid-like (see Figure 4.39). A possible reason for this could be the formulation of the fuel itself, but it is more likely that machine errors occurred with the temperature control. The temperature control reacts very aggressively and overshoots its target temperature greatly. This overshooting can have effects on behaviour of the fuel.

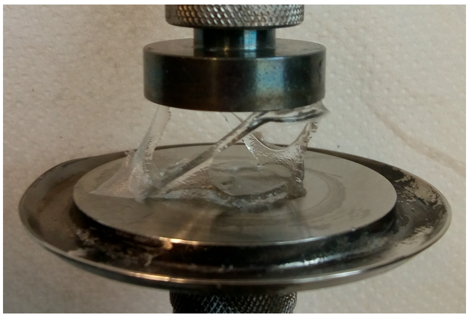

Figure 4.38: Typical behaviour of samples 101, 102, 119, 122, 120 and 123 after an experiment (with a normal force of 0.1 N)

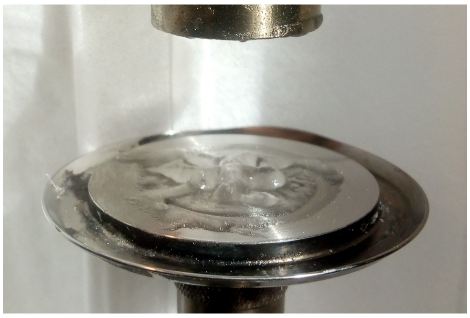

Figure 4.39: Typical behaviour of samples 103 and 104 after an experiment (whereby the force control was not maintained)

Secondly, it can be observed that in Figure 4.40 the high concentration (orange line) is located above the low concentration (green line). This is also expected as a higher concentration of gelling agent should result in a stiffer sample with a higher viscosity. In the other three figures, the lines are more in the same range, and there is not such a clear difference. This could be due to the limited amount of sample that is still left. Small amounts of the sample make the scooping of the sample out of the bottle more challenging. This disturbs especially the samples with low volumes, weakening the internal structure and causing the viscosity to change. Sample 101 and 102 were samples with relatively higher volumes still present.

Furthermore, it can be observed that the temperature dependency of the fuels varies. The ethanol fuels gelled with HPC show almost a linear dependency, while the butanol fuels gelled with HPC show a constant viscosity for the low temperatures, and only increase in viscosity at higher temperatures. Note that this last observation is most likely invalid due to incorrect measuring of the butanol fuels gelled with HPC. On the other hand, the ethanol fuel gelled with HPMC shows a higher viscosity at very low temperatures while increasing the temperature slowly decreases the viscosity, and around a temperature of 285 K the viscosity starts increasing. This initial higher viscosity could be caused by freezing of the water content in the sample. The MARS III sometimes overshoots its target temperature, resulting in an initial temperature of below 0 ^oC before the measurements start. The dependency of butanol fuel gelled with HPMC seems to have more of an S-shape. At first, the viscosity is quite constant, after which it suddenly increases rapidly. Near the end, it stabilizes again and even slightly decreases.

Lastly, it can be observed that sample 123 test Y is deviating from the other two tests. A possible explanation for this can be found inAppendix B Table B.3. In this table it can be viewed that the starting time is 21 minutes (while it was only 10 minutes for test Z and Z2). Additionally, the measurements were performed at a lower average gap of only 0.11 mm, while the other two were both 0.14 mm.

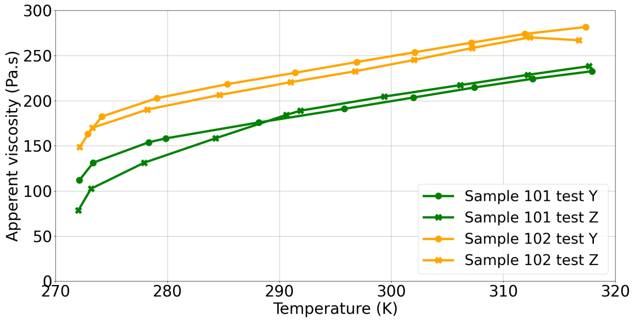

Figure 4.40: Temperature study of ethanol
and 3.0 wt% or 3.5 wt% HPC

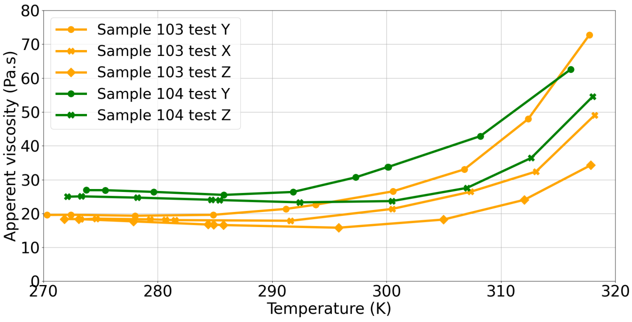

Figure 4.41: Temperature study of butanol
and 3.0 wt% or 3.5 wt% HPC

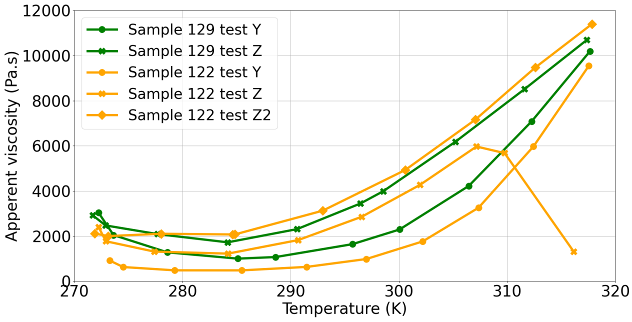

Figure 4.42: Temperature study of ethanol
and 4.5 wt% or 5.0 wt% HPMC

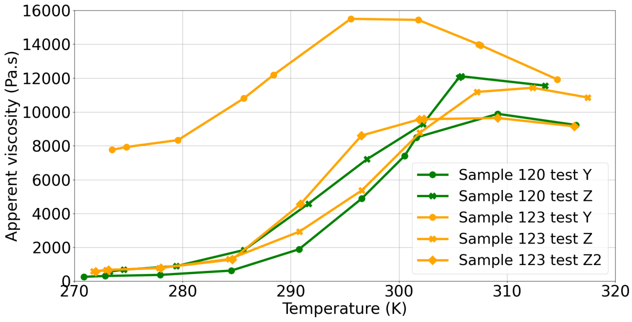

Figure 4.43: Temperature study of butanol
and 4.5 wt% or 5.0 wt% HPMC

4.6.4. COMPARISON

The apparent viscosity of the fuels gelled with HPMC (samples 119, 122, 120, and 123) have a high viscosity than the fuels gelled with HPC (samples 101, 102, 103, and 104). This is likely due to the different bonds that are present in these samples. In the fuels gelled with HPMC two types of bonds are formed as the water act as a connector between the OH-group of the alcohol and the gelling agent. Hence, there are (1) bonds between the OH-group of the alcohol and water and (2) bonds between the water and the gelling agent. These are strong bonds, which can be observed due to the high viscosity. The samples gelled with HPC only have one type of bond namely that between the OH-group of the alcohol and the gelling agent. This is a weaker bond, which can be observed due to the low viscosity.

To compare the results better, a new graph is made (Figure 4.44). To create this figure, the average results per sample are taken for both the x-axis and the y-axis. Furthermore, only the fuels with HPMC are shown as those have more reliable results. Two verticals dotted lines are plotted to indicate the 0 ^oC and the 45 ^oC clearly. It can be seen that the butanol has a higher apparent viscosity at temperatures above ± 12 ^oC. This is also expected as the butanol has a longer carbon chain resulting in a more viscous material.

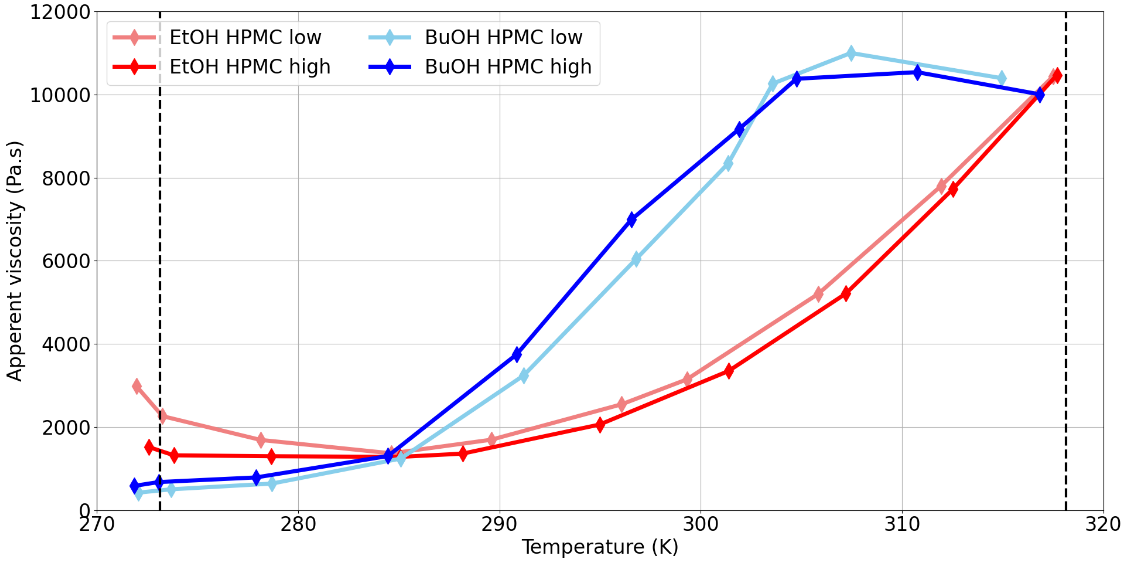

Figure 4.44: Temperature study comparison

4.6.5. ACTIVATION ENERGY

The activation energy is the minimum amount of energy that is required to result in a chemical reaction. The activation energy is of great importance for achieving ignition in the fuel. The higher the activation energy, the more difficult it becomes to ignite the fuel which eventually will result in poor performance of the propellant. The activation energy of the fuel can be found based on the temperature study. Therefore, the Arrhenius equation (Equation 4.1) needs to be rewritten to Equation 4.2.

$$ln(k) = \frac{-E_a}{R}\frac{1}{T} + ln(A) \tag{4.2}$$

This equation can also be viewed as $y = m\ x + b$, for which y is equal to $ln(k)$, m is equal to $(\frac{-E_a}{R})$, x is equal to $\frac{1}{T}$, and b is equal to $ln(A)$. The activation energy can then be found using Equation 4.3.

$$\frac{-E_a}{R} = slope \rightarrow E_a = -R \cdot slope \tag{4.3}$$

The activation energy can be found by changing Figure 4.40, Figure 4.42 and Figure 4.43 by taken the natural log of the apparent viscosity on the y-axis and the inverse of the temperature on the x-axis. This results in Figure 4.45. The average values are taken to create the plot. Furthermore, for sample 122 (EtOH HPMC high) test Z is excluded and for sample 123 (BuOH HPMC high) test Y is excluded. Also, the butanol samples gelled with HPC (samples 103 and 104) are excluded due to the axial forces affecting the results. The graphs in the form $y = m\ x + b$ are shown in the legend. Note that the m value has to be multiplied by 1000 due to the change in axis.

In Figure 4.45, it can be seen that the ethanol fuel gelled with HPC follows the trend line nicely. This is in contrast to the data point from the samples gelled with HPMC, which do not follow the trend line that well. A close up of all Arrhenius plot of all the different test are shown in Appendix B Figure B.37 and Figure B.38. However, this is also observed in literature ([15] *figure 9*). It is common for gelled systems to not precisely follow the trend line. Based on the slope of the graph, the activation energy can be determined. In Table 4.7 an overview of the activation energies can be found. Note that these activation energies are of the average test results.

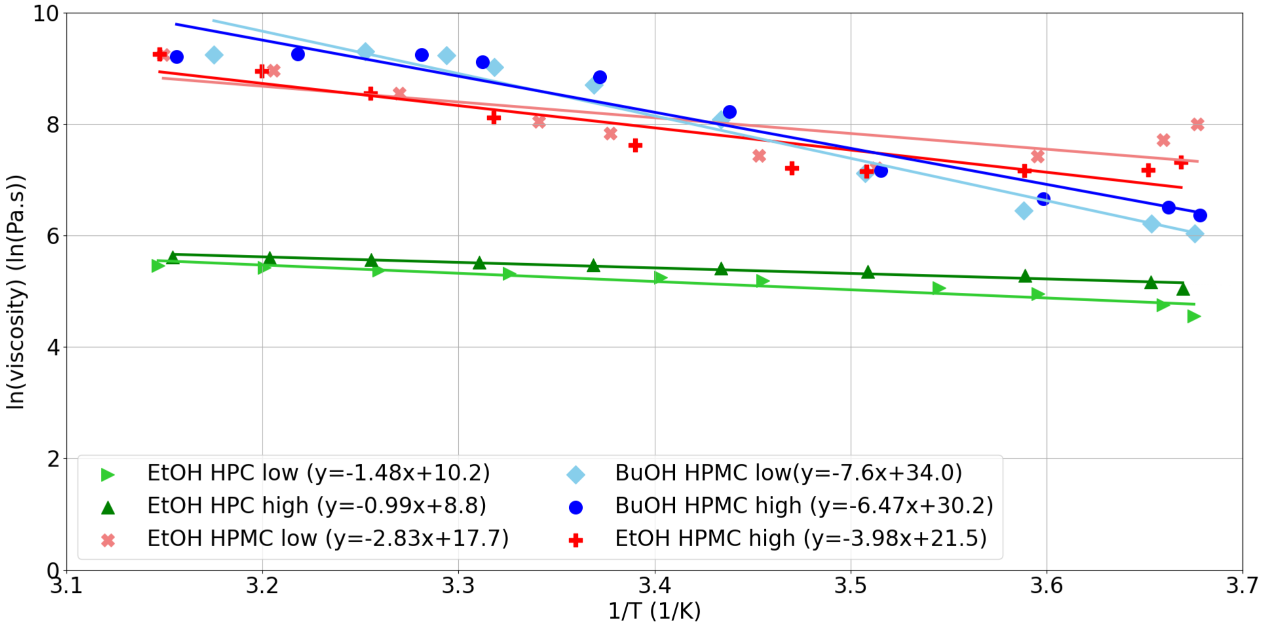

Figure 4.45: Arrhenius plot showing the viscosity–temperature relationship of gelled fuels

Multiple aspects become clear from Table 4.7. First of all, the activation energies are in line with literature [15], where it was found that gelled ethanolamine had activation energies between 21 kJ/mol and 76 kJ/mol. Secondly, it can be seen that the fuels gelled with HPC have a much lower activation energy than the fuels gelled with HPMC. This was expected based on the results of the Section 4.3 where the yield point was determined. The fuels gelled with HPC had a lower yield point, indicating that the activation energy would also be lower. Thirdly, it can be seen that the butanol fuels gelled with HPMC have a higher activation energy than the ethanol fuels gelled with HPMC. This is also expected, as butanol fuels are stiffer than ethanol fuels. Lastly, it can be seen that the ethanol fuel gelled with HPMC has a low activation energy (24 kJ/mol) for the low concentration of gelling agent and a higher activation energy (33 kJ/mol) for the high concentration gelling agent. This is also expected as a higher concentration of gelling agent should result in a stronger internal network and hence higher activation energy. This, however, is not the case for the ethanol fuel gelled with HPC and the butanol fuel gelled with HPMC. There, the fuels with a higher concentration of gelling agent have lower activating energy. The only parameter that can affect the activation energy of a sample is the presence of a catalyst. Parameter such as pressure and temperature can increase the reaction rate, but do not change the activation energy itself and hence can not be the explanation for this behaviour. The most likely reason for this abnormality is that the CTC-MARS III is unable to function properly.

Table 4.7: Overview of the activation energy of the gelled fuels

Sample	Slope from graph	Activation energy (J/mol)	Activation energy (kJ/mol)
EtOH HPC low	-1480	12305	12
EtOH HPC high	-990	8231	8
EtOH HPMC low	-2830	23529	24
EtOH HPMC high	-3980	33090	33
BuOH HPMC low	-7380	63186	63
BuOH HPMC high	-6470	53792	54

4.7. INFLUENCE OF TESTING

Performing a rheology study changes the characteristics of the sample. Taking the sample out of the bottle already disturbers the sample and by scooping the internal structure is weakened. This influences the test results, as the samples may appear weaker than they are. Performing multiple experiments increases the changes in the sample. For the initial rheology study at t=4 and t=5 days, at least six but sometimes even nine tests were executed. Every time some sample is scooped out of the bottle, weakening the internal structure. This weakening can be smelled as some alcohol is no longer trapped in the internal network and evaporates. Moreover, the changes in the sample are also noticeable in another way. By scooping some trapped air is moved upward and eventually moves out of the sample. This is the case for most samples as can be seen in Figure 4.46. Although this figure only shows sample 101, it is representative of all other samples except sample 104. One sample forms the exception, this is sample 104. In sample 104, the air bubbles are moved together to form one bigger air bubble. This is visible in Figure 4.47.

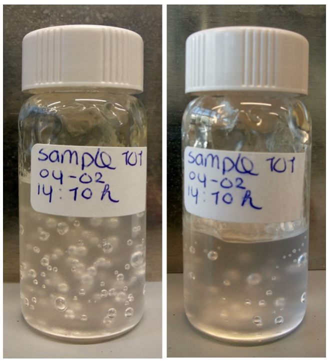

Figure 4.46: Air trapped in sample 101 (EtOH HPC low) before testing (left) and after testing (right)

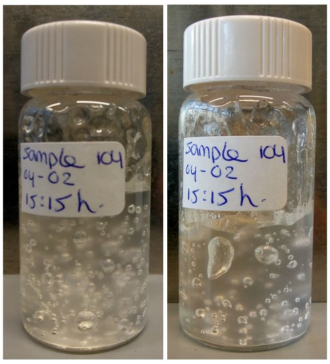

Figure 4.47: Sample 104 (BuOH HPC high) before testing (left) and after testing (right)

For the stability study, exactly the opposite happened. Almost no air bubbles were present before testing, but after testing the samples contained more and larger air bubbles. This can be seen in Figure 4.48. This could be caused by the limited amount of volume still left of the sample. It is harder to scoop the sample out of the bottle as so little is left.

Figure 4.48: Samples 104 (BuOH HPC high) and 123 (BuOH HPMC high) before and after testing

4.8. CONCLUSION

The viscoelastic behaviour of different types of fuels is investigated via a rheology study. This study confirmed that the novel fuel exhibits viscoelastic behaviour. Furthermore, a comparison study between two different alcohols (ethanol vs butanol) has provided inside into the influence of the carbon length of the alcohol on the fuel's behaviour. The most important parameters to evaluate the viscoelastic nature are; the Linear Viscoelastic Range, the yield point, and the loss factor (G' over G"). In total there were three variables in the experiments; the concentration, the type of gelling agent, and the alcohol that forms the basis of the fuel.

Concentration

The fuels are gelled with either a high or a low concentration of the gelling agent. The rheology revealed the following;

- Fuels containing a high concentration of gelling agent have a higher apparent viscosity than fuels containing a low concentration of the gelling agent. This is independent of the alcohol basis of the fuel or used gelling agent.
- Fuels containing a high concentration of gelling agent are stiffer or have a higher strength than fuels containing a low concentration of the gelling agent. This is independent of the alcohol basis of the fuel or used gelling agent.
- Fuels containing a high concentration of gelling agent have a higher yield point than fuels containing a low concentration of the gelling agent. This is independent of alcohol type or gelling agent.
- Fuels gelled with HPC containing a high concentration of gelling agent have a longer viscoelastic range than fuels gelled with HPC containing a low concentration of the gelling agent. This is independent of alcohol type.

The first three conclusions seem obvious, but it verifies that the experiments executed are in line with physical laws, and therefore, it confirms that the results from the experiments are reliable.

Type of alcohol
The effect of the length of the carbon chain is studied by comparing the ethanol fuel with the butanol fuel.

- Gelled butanol fuels are stiffer or have more strength than gelled ethanol fuels that have the *same* type and concentration of the gelling agent.
- Gelled butanol fuels have a higher viscosity than gelled ethanol fuels that have the *same* type and concentration of the gelling agent.
- Butanol fuels gelled with HPMC have a longer Linear Viscoelastic Range than ethanol fuels gelled with HPMC. This is independent of the concentration of the gelling agent.
- Butanol fuels gelled with HPMC have a higher yield point than ethanol fuels gelled with HPMC. This is independent of the concentration of the gelling agent.

The butanol fuel shows this behaviour due to its longer carbon chain, which results in a different stacking of the molecules. Hence, it can be concluded that a longer carbon chain results in a stiffer fuel with higher viscosity.

Type of gelling agent
To investigate the influence of the type of gelling agent, a comparative investigation into HPMC and HPC was executed. The difference between the two gelling agents is the presence of the methyl group and the addition of water.

- Fuels gelled with HPC show less dependency on frequency than fuels gelled with HPMC, independent of alcohol type.
- Fuels gelled using HPC show behaviour that is more closely to that of an ideally elastic material than fuels gelled using HPMC.
- Fuels gelled with HPMC have a yield point that is higher than fuels gelled with HPC. This is independent of concentration and fuel basis. It has to be noted that a higher yield point means that eventually, it will be harder to achieve ignition in the fuel.

Stability study
To determine the effect of environmental conditions on the fuel, the rheology study is executed again at t=35 days. This is one month after the initial rheology study.

- Regarding the Linear Viscoelastic Range, no clear trend is visible. Most fuels show a large increase in Linear Viscoelastic Range (>50%), however, the ethanol fuel gelled with a low concentration of HPC and the butanol fuel gelled with a high concentration HPMC show a small decrease in Linear Viscoelastic Range and the butanol fuel gelled with a high concentration HPMC remained constant.
- The time-dependent behaviour which was investigated using a frequency study revealed that the fuels gelled using HPMC remain more or less the same over time. The butanol fuel gelled with a low concentration of HPMC even improves as at t=35 days it behaves as an elastic material for all tested frequencies ($0.1\ Hz < f < 10\ Hz$). The fuels gelled using HPC do show changes for the high frequencies. The *low* concentrations of both the ethanol and butanol fuels seem to behave as a liquid viscoelastic material at high frequencies (G">G').
- The yield point decreases overtime for all tested fuels, except for the butanol fuel gelled with a high concentration of HPC. The average decrease is around 16%.

Also a temperature study was performed from a temperature of $0\ ^oC$ to $45\ ^oC$, but due to issues with the temperature control of the MARS III rheometer, these results are less reliable and should be evaluated qualitatively instead of quantitatively. The experiments showed that the apparent viscosity is dependent on temperature and shows a strong dependency, especially at higher temperatures.

5

ACHIEVING HYPERGOLICITY

Ignition by hypergolicity is the desired source of ignition. Hypergolic ignition means that the propellant combination consists of components that spontaneously ignite when coming into contact with each other. Current green bi-propellant do not have the combination to achieve hypergolicy naturally. To overcome this problem, a catalyst can be suspended to the fuel to achieve hypergolicity with a suitable oxidizer. This research will focus on investigating the influence of different catalysts on the ignition delay time of the gelled fuel. This chapter focuses on finding a suitable catalyst to achieve a hypergolic ignition of the alcohol-based gelled fuel. The potentially suitable catalysts are selected in Section 5.1 and the critical concentrations of the components of the fuel are discussed in Section 5.2. Then, the experiment used to investigate the hypergolicity is explained in Section 5.3. After that, the results of these experiments to evaluate the fuel's performance are provided in Section 5.4. Lastly, Section 5.5 provides the conclusion of which catalyst is most suited to achieve ignition.

5.1. SUITABLE CATALYST

Based on the literature study, it is found that the most active catalysts for hydrogen peroxide decomposition are some metal oxides and salts. Manganese, copper, and iron salts proved to be especially reactive towards 90% hydrogen peroxide [10]. Therefore, the most popular catalysts used for hydrogen peroxide are MnO and MnO_2 due to their elevated performance in comparison to their relatively low cost. However, also other catalyst can be used such as $CuCl_2$, $CuCl_2H_2O$, Ag, Pd, Co, $C_{10}H_{14}MnO_4$, Pt and Ir [24]. As cost is also an important criterion for this research, expensive catalysts such as silver are out of reach. Due to time limitations, it has been decided to inventory the catalysts present in the Chemical lab of the Aerospace Engineering faculty to avoid lengthy ordering procedures. Additionally, many interesting and suitable catalysts are already present, so it is also not required to buy new catalysts. The catalyst present were; iron(II, III)oxide, manganese(III)oxide, copper(II)oxide, manganese(II)acetylacetonate, copper(I)iode, copper(II)chloride, iron(III)chloride anhydrous and copper(II)bromide. The latter three did show some troubling features. The bottle of Copper(II)chloride consists of relatively large powder particles. Also, the bottle of Copper(II) bromide does not contain a powder, but rather contains small particles. Lastly, the bottle of iron(III)chloride anhydrous consists of black powder and large yellow particles, indicating that the bottle is either contaminated or that the substance has undergone a chemical reaction of some kind.

This research aims to develop a green fuel, therefore toxicity and other hazards of the catalyst are of importance. By simply looking at the HCS labels on the bottles, it can be seen which hazards are associated with the chemical. The only catalyst without an HCS label is iron(II,III)oxide. As iron salts are potentially a suitable catalyst, this catalyst is selected to be tested. Furthermore, manganese oxide is the second least hazardous chemical, as it only presents minor hazards (H315 Causes skin irritation, H319 Causes serious eye irritation, H335 May cause respiratory irritation) therefore this seems to be a suitable candidate as well. As it is also indicated that copper salts might be a suitable catalyst for high concentrations of hydrogen peroxide, a copper salt is selected as well. To compare the catalysts to the previously selected iron oxide and manganese oxide, also a copper oxide will be selected. Lastly, as literature ([22], [14], [17]) all used manganese(II)acetylacetonate as catalyst, it was decided to also test this catalyst to compare the results. Hence, the selected catalyst are;

- Iron(II,III)oxide
- Magnese(III)oxide
- Copper(II)oxide
- Manganese(II)acetylacetonate

The characteristics of these catalysts can be seen in Table 5.1. It has to be noted that the age of the catalyst is unknown, but it is likely that the catalysts are already present in the Chemical Lab of the Faculty of Aerospace Engineering for a few years. Therefore, the chemicals may be contaminated by other people. The chemicals appear normal, only the manganese(II)acetylacetonate has larger clumped particles in it.

Table 5.1: Characteristics of the catalyst

Catalyst	Empirical Formula	CAS number	Assay	Particle size	GHS symbol
Iron(II, III)oxide	Fe3O4	1317-61-9	97%	Back powder 50-100 nm	none
Magnese(III)oxide	Mn2O3	1317-34-6	99%	Black powder 325 mesh ($< 44\ \mu m$)	GHS07: Harmful
Copper(II)oxide	CuO	1317-38-0	98%	Black Powder <19 μm	GHS07: Harmful GHS09: Environmental hazard
Manganese(II) acetylacetonate	Mn(acac)2	14024-58-9	-	Brown powder	GHS08: Health hazard GHS07: Harmful

The first step of improving this ignition technique in green fuels has already been taken since gelling the fuel improves the suspensibility of the catalyst. Additionally, it is desirable to use a negligibly small amount of catalyst. This amount should be high enough to achieve hypergolicity, but be small enough to not negatively affect the performance of the fuel such as the poisoning of the fuel and catalyst due to extended periods of contact and the increase in molecular weight which decreases the specific impulse [24]. It has been decided to add 2.5 wt% of catalyst to the fuel, this is based on a trial-and-error process.

5.2. CRITICAL CONCENTRATIONS

The aim is to develop a novel green fuel with critical concentrations of gelling agent and catalyst. In general, additional elements added to the fuel decrease the performance of the fuel, and therefore it is vital to find the critical (or minimal) concentrations of gelling agent and catalyst. These critical concentrations should be sufficiently high to achieve viscoelastic nature and achieve ignition, but without effecting the permanence negatively. Chapter 3 already showed the critical formulation of the fuel and Chapter 4 revealed the viscoelastic nature.

5.2.1. CRITICAL GELLING CONCENTRATION

Due to time constraints it is not possible to further investigate all eight fuel combinations that were tested during the rheology study (Chapter 4). Rather, only the most promising fuels are further developed and investigated. For the research, it is interesting to test both gelling agents. To reduce the number of varying parameters only one basis of fuel is further investigated. So either ethanol fuels or butanol fuels.

Regarding the type of fuel to continue the study with. The rheology study revealed that the butanol fuel gelled with a low concentration of the gelling agent HPMC was not always behaving like a viscoelastic solid (Figure 4.34) and this is undesirable as the aim is to develop a fuel with viscoelastic behaviour. Additionally, the butanol fuels gelled with HPMC have a higher yield point than the ethanol fuels gelled with HPMC. A higher yield point indicates a stronger internal network. These stronger bonds require more energy to be broken and hence it is more difficult to achieve hypergolicty followed by ignition. The yield point is on average a factor 1.5 times higher for the butanol fuels compared to the ethanol fuels. Based on this, it is decided to not further investigate butanol but rather focus on ethanol fuels. Additionally, ethanol has a lower molecular mass what in the future will be beneficial for the combustion process.

Regarding the concentration of the fuel, it has been decided to further develop the high concentrations of gelling agents. This means the 3.5 wt% of HPC and the 5.0 wt% of HPMC. The focus of the investigation was finding the critical gelling concentration to achieve viscoelastic behaviour in the fuel. Based on the rheology study it was found the high concentration shows behaviour that is most in line with that of a solid. Additionally, it is essential to form a grain with the fuel. During the process of making a grain, it was found that ethanol fuel with 3.0 wt% of HPC was not strong enough to be shaped into a grain. Although adding a (solid) catalyst will make the system more rigid, it was still insufficient to be characterized as a solid. The high concentration of the gelling agent on the other hand is strong enough to be shaped into a grain and can be identified as a solid for this hybrid bi-propellant system.

5.2.2. FUELS CONSISTING OF CRITICAL CONCENTRATIONS

In total eight samples were produced with varying compositions. The constant among all eight samples is the basis of the fuel which is ethanol, while the variables are the type of gelling agent (HPC vs HPMC) and the type of catalyst. A total of 3.0 grams is made for every sample. All samples were produced in the same order. For the samples gelled with HPC, the steps were as follows; First, the catalyst was added to the bottle in the correct mass. Then the gelling agent was weighed in a separate box and added to the bottle. This was then gently mixed by lightly shaking the bottle. The third and final step was to add the ethanol to the bottle with a syringe. These samples were then stirred by hand for approximately 15 minutes. For the samples gelled with HPMC, the first step was also to add the catalyst to the bottle. Secondly, the gelling agent was weighed in a separate box and added to the bottle. Thirdly, the ethanol was added to the bottle with a syringe. These three components were then gently mixed by lightly shaking the bottle. Lastly, the DI water was added after which the solidification goes very quickly and only a few minutes of stirring is sufficient. It is very important to add the water after the ethanol, otherwise, it is impossible to achieve a homogeneous sample. Table 5.2 shows an overview of the compositions of the samples. The details of the samples can be found in Appendix A in Table A.8.

Table 5.2: Composition of the samples used for evaluating hypergolicity

Sample number	Mass fraction gelling agent	Mass fraction alcohol	Mass fraction water	Mass fraction catalyst
206	3.5 wt% HPC	94.0 wt% ethanol	- - -	2.5 wt% Mn(acac)2
208	5.0 wt% HPMC	77.5 wt% ethanol	15 wt% water	2.5 wt% Mn(acac)2
209	3.5 wt% HPC	94.0 wt% ethanol	- - -	2.5 wt% Fe3O4
210	5.0 wt% HPMC	77.5 wt% ethanol	15 wt% water	2.5 wt% Fe3O4
211	3.5 wt% HPC	94.0 wt% ethanol	- - -	2.5 wt% Mn2O3
212	5.0 wt% HPMC	77.5 wt% ethanol	15 wt% water	2.5 wt% Mn2O3
213	3.5 wt% HPC	94.0 wt% ethanol	- - -	2.5 wt% CuO
214	5.0 wt% HPMC	77.5 wt% ethanol	15 wt% water	2.5 wt% CuO

The production of these samples consolidates the findings that were already made in Chapter 3. The solidification process and hence the formation of a 3D network of the samples gelled with HPMC is very fast, already a few minutes after mixing and stirring the sample transforms to its solid form. The formation of the network in the samples gelled with HPC takes longer and therefore, it is required to stirrer these samples for at least 10 minutes and let "rest" for at least 12 hours to allow the further formation of the internal network to be built. Hence, the solidification process is slower with HPC.

Another observation that was made during the production of these samples is the colour change when producing samples 206 and 208 which had the catalyst Mn(aca)2. The samples both start with a sandy colour. For sample 208 (gelled with HPMC), this colour changes to dark brown colour in only a few minutes, however for sample 206 (gelled with HPC) the colour stays light brown. The next day, both the samples were further darkened to a very dark brown colour. The other samples, consisting of different catalysts, were black at all times. A picture of the samples can be seen in Figure A.2 and Figure A.3 in Appendix A.

5.3. MULTI DROP-TEST EXPERIMENT

The evaluation method for hypergolicity is important to determine correctly whether the propellant is a promising candidate. Hypergolic reactions between the fuel and oxidizer are typically measured using a drop-test. In a drop-test, small volumes of fuel and oxidizer are brought in contact with each other after which ignition occurs. The time interval between the moment of contact and the ignition, defined as the ignition delay time, can be measured. Up till today, there are no criteria to evaluate the ignition delay through a drop test and consequently, there are also no standardized drop-test conditions. Test conditions such as the droplet size, impact velocity of the droplet, and oxidizer-to-fuel ratio influences the ignition delay of a hypergolic propellant. Although the absence of a standardized drop-test makes it difficult to compare the results to literature, the results of the different fuels tested during this research can be compared to each other.

5.3.1. TEST SET-UP

A general schematic drawing of the test set-up of a drop test can be seen in Figure 5.2. Hence, five items are essential for this experiment. The high-speed camera available at TU Delft is the Photron High-Speed Camera (Photron FASTCAM Mini AX200) which has a maximum resolution of 1024 x 1024 and can provide 1 Megapixel image resolution at frame rates up to 64000 fps or 540000 fps at reduced resolution. The settings used for the drop-test experiment were 6400 fps with a resolution of 768 x 768 as this allowed for a film of around 6 seconds. It was found that 6 seconds would be sufficient to capture the entire ignition process. As a syringe pump, the NE-1000 from the company "New Era Pump Systems INC" was used. The flow rate is set to 2.8 mL/min. As an external light source, the GS Vitec SN Multiled QT is used. The power can be set to any desired percentage. During the experiments, the light is set to 28%. The experiment is executed in a large fume hood. This size is required to be able to position the high-speed camera inside the fume hood as well. Additionally, a dark environment is required to keep the external light source as the only light source. To create a dark environment, all windows and the lighting of the fume hood are covered with a black curtain. Furthermore, aluminium foil is placed on top of the table to protect the table from highly concentrated hydrogen peroxide. Lastly, a white paper is placed behind the test set-up. This reduces the reflection of light by the aluminium foil. This reflection results in bright light on the film which makes it harder to see the exact time of ignition. Therefore, it is of great importance that this piece of paper is placed properly. A picture of the test set up can be seen in Figure 5.1.

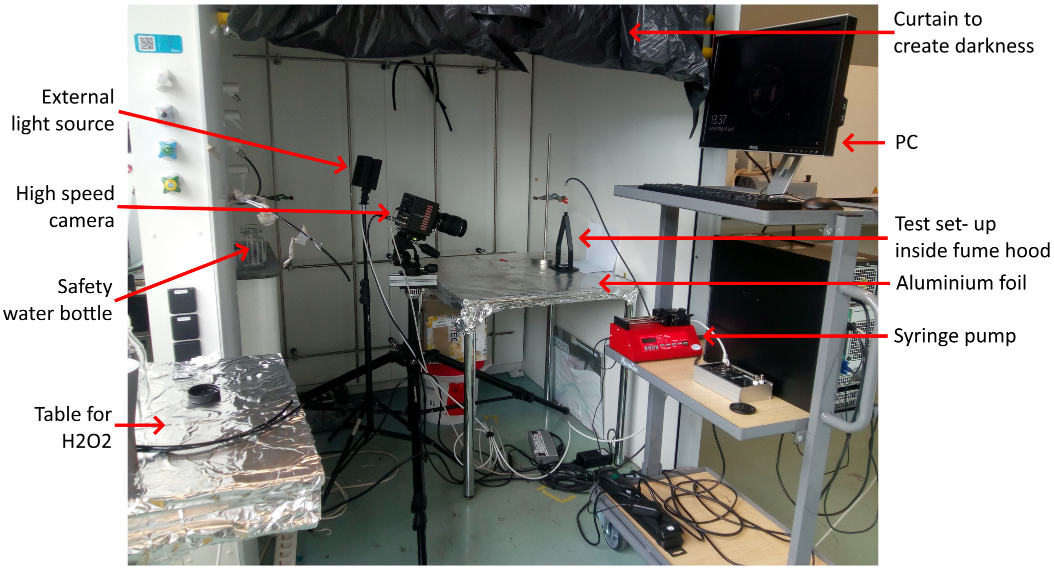

Figure 5.1: Overview of the test setup of the multi-drop test

To make sure the hydrogen peroxide droplet impacts the fuel exactly in the centre, a test setup has been designed. This test setup makes sure that the watch glass where the fuel is placed, is at a fixed location. The tube at the top of the test setup makes sure that the glass tube that holds the hydrogen peroxide is aligned with the centre of the watch glass. Also, the height is fixed this way, which should result in a constant drop velocity at impact. The test setup is printed using 3D printers of DASML. The technical drawings of this test setup can be found in Appendix C Figure C.2. A picture of the test set-up can be seen in Figure 5.3.

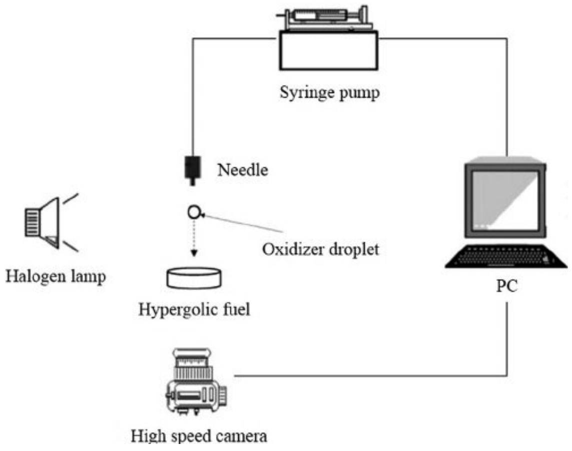

Figure 5.2: Schematic drawing of the test setup of the drop test

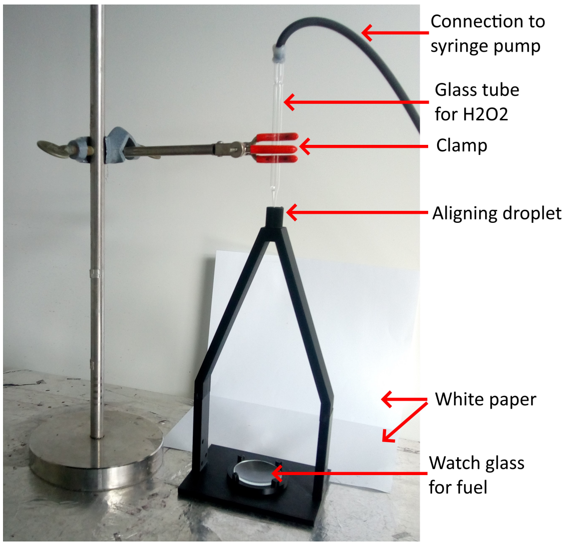

Figure 5.3: Close up of the test setup of the multi-drop test

5.3.2. TEST PROCEDURE

Before the experiments can be executed, all items and devices should be placed in position. The high-speed camera, external light source, the test setup that directs the droplet should be placed in the fume hood. Then the exact concentration of hydrogen peroxide is measured using a Brix Refractometer. After all these steps are taken the actual experiment can be executed in the following manner. The glass tube is filled with hydrogen peroxide. Then the fuel is shaped into a grain and placed on the watch glass (at the desk). The watch glass with fuel is then positioned in the test setup (in the fume hood). The camera is activated and started. Three droplets are released using the syringe pump. The camera stops automatically after a few seconds after which the video is saved to an external storage unit. This can take up to 20 minutes. During this time the watch glass can cool down. The remaining residue is rinsed and cleaned above a waste bottle. The watch glass is dried with a paper towel and the desk is diluted with water and wiped dry with a paper towel as well. The detailed experiment procedure can be found in Appendix C under the title "*Test Procedure for Multi-Drop Test*".

5.3.3. SAFETY

Safety is always an important part of performing experiments. However, when executing experiments with hypergolic substances, safety is even more crucial as the components ignite spontaneously upon contact. The safety measurements taken are listed below:

- Personal safety
  - Wear cotton cloths
  - Wear resistant shoes that are not easily penetrable
  - Wear a lab coat
  - Wear safety glasses at all times
  - Hair tied in a ponytail
- The fuel and hydrogen peroxide should be handled at different places to avoid accidental contact. There is one table assigned for handling the H2O2 and a second desk, at some distance, is assigned for handling the fuel. The location of this desk and table can be seen in Appendix C Figure C.1.
- Two water bottles of at least 500 mL should be present to allow for quick dilution of the hydrogen peroxide in case of an accident. One bottle should be located inside the fume hood, the other bottle should be located at the desk where the fuel is prepared.
- Gloves should be worn at all times. However, it is also important that the gloves are clean. When they are contaminated with H2O2 or with fuel (and thus catalyst) new gloves should be put on. When only a slight amount of catalyst comes in contact with highly concentrated hydrogen peroxide, the gloves will ignite.
- Make sure to not look into the external light source as this device is labelled as a Laser safety class 2M. Secondly, if the fan of the external light sources stops working, turn off the light.
- The test procedure as given in Appendix C under the title "*Test Procedure for Multi-Drop Test*" is mounted visibly to read such that it can be easily followed during the experiment.
- The testing area is clear such that in case of emergency an escape route is available.
- Small amounts of chemicals are present. Hence, only 3 grams of fuel is located at the desk, and only a small bottle of (maximum) 10 mL of H2O2 is located at the table. Additionally, the glass tube for H2O2 is filled for a maximum of three experiments. Redundant chemicals should be placed in storage.

5.4. EVALUATION OF THE HYPERGOLICITY

To investigate which type of catalyst results in hypergolic ignition of the fuel, its performance has to be evaluated. In order to investigate the ignition process, a multi drop-test study is executed with three drops. The experiments are conducted around 24 hours after the production of the samples. SolvGE produces the high concentration of hydrogen peroxide used for the experiments. The Brix% of this hydrogen peroxide was 43.5% which equals an H2O2 concentration of 98.2%. The camera settings were set to 6400 frames per second to be able to capture the ignition very accurately. A resolution of 768x768 then gives a film of around 6 seconds. The syringe pump was set to a rate of 2.8. The intention was to execute a multi drop-test three times for every sample. However, the amount of highly concentrated hydrogen peroxide was limited, and therefore it was not possible to repeat the experiment three times for samples 206 and sample 208. An overview of the results can be found in Table 5.3. During the execution of the experiment, it was found that is challenging to generated exactly three drops. Therefore, some experiments are executed with four drops.

Table 5.3: Results of the multi-drop test to evaluate hypergolicity of different catalysts

Experiment	Sample number	Catalyst type	Droplets	Observation
44	209	Fe3O4	3	No ignition
45	209	Fe3O4	4	No ignition
46	209	Fe3O4	3	No ignition
47	210	Fe3O4	3	Drops were misaligned No igntion
48	210	Fe3O4	4	No ignition
49	210	Fe3O4	3	No ignition
50	211	Mn2O3	3	No ignition
51	211	Mn2O3	4	No ignition
52	211	Mn2O3	3	No ignition
53	212	Mn2O3	3	No ignition
54	212	Mn2O3	3	No ignition
55	212	Mn2O3	4	No ignition
56	214	CuO	3	No ignition
57	214	CuO	3	No ignition
58	214	CuO	4	No ignition
59	213	CuO	3	No ignition
60	213	CuO	4	No ignition
61	213	CuO	3	No ignition
62	206	Mn(acac)2	3	Ignition after the first droplet
63	206	Mn(acac)2	3	Leakage of the glass tube Ignition occured
64	208	Mn(acac)2	4	Slight misalignment of the first droplet Ignition after the fourth droplet

There were three different types of phenomena visible after a drop of hydrogen peroxide impacted the fuel consisting of different catalysts. The first phenomenon was that nothing happened. The visualization could be described as plain water impacting a normal gel, hence absolutely nothing happened. This was the case for all experiments with the catalysts iron(II)oxide, manganese(III)oxide, and copper(II)oxide. The visualization of the phenomena is shown in Figure 5.4. These photos are of experiment 54 but are representative of experiments 44 to 61. Based on these experiments, it can be concluded that a 2.5 wt% of catalyst is insufficient to ignite the fuel with any of these three catalysts. There is also no potential visible that suggest that a slightly higher concentration would result in ignition. Signs of the fuel having the potential to ignite would be fizzing of the hydrogen peroxide, sparkling of the fuel, and smoke formation. However, these signs were not observed during the experiments.

The only catalyst that resulted in successfully achieving a hypergolic ignition was manganese(II)acetylacetonate. This is also the type of catalyst that is studied in literature and that has shown it potential to achieve hypergolic ignition of a gelled fuel. Although only one experiment could be executed per sample, this is sufficient to prove its ability to ignite ethanol fuel. The analysis of the films made from experiments 62 and 64 did reveal that the behaviour of the fuel's ignition with the hydrogen peroxide is different.

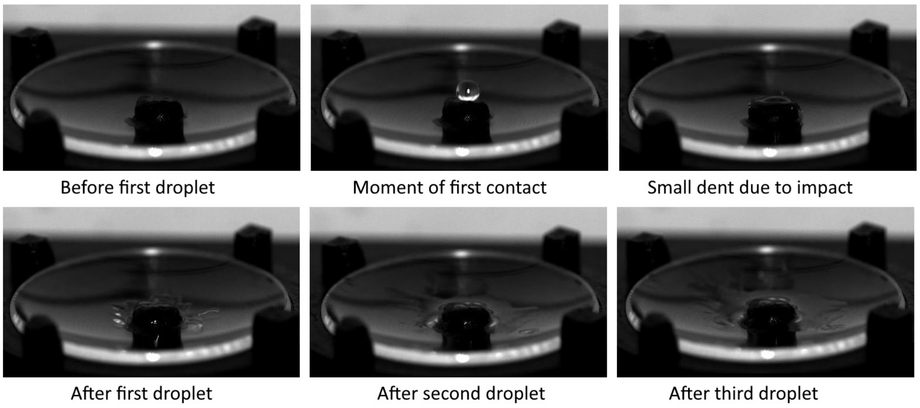

Figure 5.4: Experiment 54: ignition process of ethanol fuel gelled with 5.0 wt% HPMC, 15 wt% DI water and 2.5 wt% Mn2O3

A detailed analysis of experiment 62 with ethanol fuel gelled with HPC yielded the following observations. The start of the ignition process is when the bottom of the droplet of hydrogen peroxide contacts the top of the fuel. After around 60 ms[1] fizzing of the hydrogen peroxide starts, followed by sparkling of the fuel. A clear small white dot of light is visible 178 ms after the first contact. This dot of light indicates the fuel has the potential to ignite, however, the auto-ignition temperature of the fuel is not yet met causing the ignition to delay. At 247 ms after the first contact ignition occurs. During the burning of the fuel a crackling sound can be heard, this is caused by the catalyst particles. Then 474 ms after the first droplet, the second droplet hits the fuel which results in a larger explosion of the fuel. Then at 961 ms the third droplet contact the fuel, resulting again in a larger explosion of the fuel. Also, a very small amount of foam is formed on top of the fuel and this foam is later airborne. The visualization of this experiment is shown in Figure 5.5.

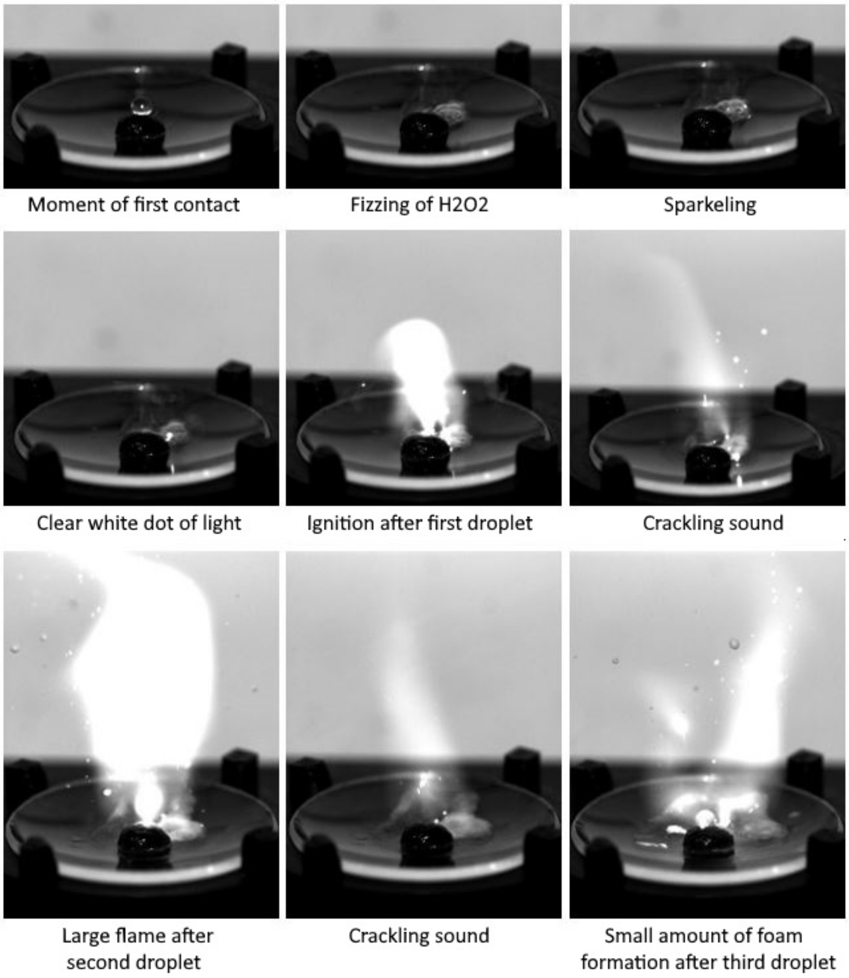

Figure 5.5: Experiment 62: ignition process of ethanol fuel gelled with 3.5 wt% HPC and 2.5 wt% Mn(acac)2

---

[1] All times indicated are measured from the moment of the first contact between the hydrogen peroxide and fuel

The ignition process of the fuel gelled with HPMC is different. Similar to what is being described in literature, a lot of foam is formed during the ignition process. A detailed analysis of experiment 64 yielded to the following observations. After the first contact of hydrogen peroxide with the fuel tinny sparkles are visible. It has to be noted that the first droplet of hydrogen peroxide is impacting the fuel slightly of centre. After 296 ms a small amount of foam is formed on top of the fuel. Then, also fizzing is visible. The second droplet impacts at 468 ms. After this second droplet, more tinny sparkles and fizzing are observed, also more foam is formed covering one side of the fuel completely. The third droplet impacts at 972 ms. Again, more foam is formed, and tinny sparkles are visible inside and on the foam. Also smoke starts to form. At 1532 ms a clear small white dot of light is visible. This indicates the fuel's potential to ignite. At 1534 ms the fourth droplet impacts the fuel after which ignition occurs at 1569 ms. The visualisation of this experiment is shown in Figure 5.6.

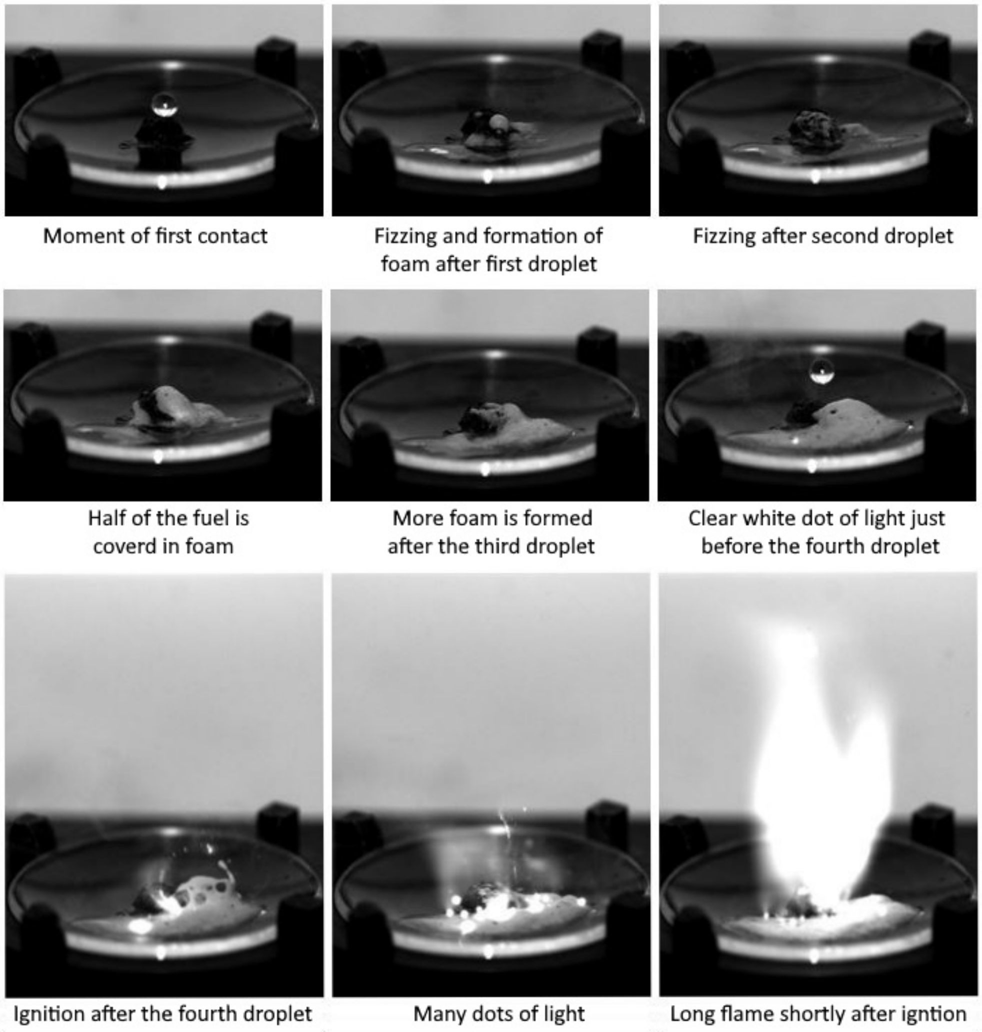
Moment of first contact

Fizzing and formation of foam after first droplet

Fizzing after second droplet

Half of the fuel is coverd in foam

More foam is formed after the third droplet

Clear white dot of light just before the fourth droplet

Ignition after the fourth droplet

Many dots of light

Long flame shortly after igntion

Figure 5.6: Experiment 64: ignition process of ethanol fuel gelled with 5.0 wt% HPMC, 15 wt% DI water and 2.5 wt% Mn(acac)2

The ignition delay is caused by many reasons. First, the mixing of the fuel and oxidizer is more challenging because the fuel is in a solid-state. This phase difference complicates the mixing of the fuel and oxidizer. The ethanol fuel has a viscoelastic nature with elastic dominance (see Chapter 4). Hence, the fuel has to overcome its elastic behaviour by breaking the 3D network to form a viscous system. Then, this viscous system can mix with the bi-products of H2O2 to initiate ignition. An additional reason for the long delay has to do with the testing environment, which are atmospheric conditions (atmospheric pressure and temperature). The fact that a clear small white dot of light is formed during the experiments with both HPC and HPMC as gelling agents indicates that there is already potential to ignite at that point in time. However, the auto-ignition temperature of the fuel is not yet met due to heat losses to the surroundings. In an actual pressurized propulsion system, this loss of heat will be less, resulting in shorter ignition delay times. Furthermore, pressure plays an important role in the ignition delay time, so, in a pressurized propulsion system, the ignition delay time will decrease even further.

Another observation made in these experiments was the leakage of the glass tube that holds the H2O2. Initially, it was believed that the hose itself or the connections between the hose and the glass tube or syringe pump were not sufficiently airtight. However, after inspection, it was found that this was not the case. Another explanation would be that the hydrogen peroxide is decomposing inside the glass tube. This decomposing results in the formation of oxygen gas increasing the pressure in the tube, which leads to the release of a droplet. The intensity of the light of the external light source likely accelerates the decomposing process. Although it is an inconvenience to have occasional leakage, it does not form much harm. The only aspect that has to be taken into consideration is that the concentration of hydrogen peroxide might be lower than measured at the start of the experiment. Nevertheless, to limit the decomposition of hydrogen peroxide in the glass tube, the external light source will be switched off between experiments to limit the decomposition of hydrogen peroxide.

5.5. CONCLUSION

By performing a multi drop-test with three to four drops the hypergolicity of eight different fuels consisting of different catalyst and gelling agents was evaluated. All investigated fuels had an ethanol basis and were gelled with either HPC or HPMC. The investigation focuses on hybrid propellants whereby the fuel is in a solid-state. The ethanol fuels gelled with 3.5 wt% HPC or 5.0 wt% HPMC and 15 wt% water exhibit this solid behaviour and are stiff enough to be moulded in the shape of a grain. The catalysts that were investigated are iron(II,III)oxide, manganese(III)oxide, copper(II)oxide, and manganese(II)acetylacetonate. The concentration of this catalyst was equal to 2.5 wt%. The amount of catalyst should be high enough to sufficiently lower the activation energy of the fuel to achieve hypergolic ignition with a high concentration of hydrogen peroxide, without compromising its performance. The multi-drop test was executed with 98.2 % H2O2 and the syringe pump was set to a flow rate of 2.8 mL/min. The results of the three multi drop-test revealed that 2.5 wt% of iron(II,III)oxide, manganese(III)oxide or copper(II)oxide were insufficient to achieve hypergolicity in the fuel. Also, no potential to ignite or fizzing of the hydrogen peroxide was observed. Therefore, these catalysts are considered unsuitable for this application. On the other hand, the experiments with the catalyst manganese(II)acetylacetonate did show promising results. Ignition was achieved with the 2.5 wt% catalysts in the ethanol fuel gelled with 3.5 wt% HPC and ignition was achieved with the ethanol fuel gelled with 5.0 wt% of HPMC. The ignition process of the two differs. The ignition of the fuel gelled with HPMC shows the formation of a lot of foam before ignition. On the other hand, almost no foam is formed during the ignition process of fuel gelled with HPC.

As it is established which catalyst can be used to achieve ignition by hypergolicity, a detailed analysis of its performance is shown in the next chapter. Accordingly, more experiments are executed to obtain a more reliable ignition delay time and additional experiments are conducted to obtain more performance characteristics.

6

ANALYSIS OF THE PERFORMANCE OF THE PROPELLANT

A detailed analysis of the performance of the propellant is performed. During this analysis, only the catalyst manganese(II)acetylacetonate is studied as this was the only catalyst with lowered the activation energy sufficiently to result in ignition of fuel. During this analysis, the main focus is on the critical concentration, which is equal to 2.5 wt% catalyst for atmospheric test conditions. The analysis consist of three parts; (1) the Ignition Delay Time (Section 6.1), (2) the regression rate (Section 6.2), and (3) the energy content of the fuel (Section 6.3).

The critical catalyst concentration for the conditions present during testing in atmospheric conditions is 2.5%. However, for the actual fuel, the critical concentration will be between 2.0 % and 2.5% as in the propulsion system less heat is lost to the environment. To compare the results also samples with 2.0 % and 3.0% catalyst are analyst. However, the main focus of the research is on the 2.5% catalyst, and therefore, this fuel is tested most extensively. The details of the sample can be found in Appendix A in Table A.9.

Table 6.1: Composition of the samples used to analyse the performance of the novel propellant

Sample number	Mass fraction gelling agent	Mass fraction alcohol	Mass fraction water	Mass fraction catalyst
201	3.5 wt% HPC	94.5 wt% ethanol	- - -	2.0 wt% Mn(acac)2
217	5.0 wt% HPMC	78.0 wt% ethanol	15 wt% water	2.0 wt% Mn(acac)2
206 & 206A	3.5 wt% HPC	94.0 wt% ethanol	- - -	2.5 wt% Mn(acac)2
208 & 208A	5.0 wt% HPMC	77.5 wt% ethanol	15 wt% water	2.5 wt% Mn(acac)2
215	3.5 wt% HPC	93.5 wt% ethanol	- - -	3.0 wt% Mn(acac)2
216	5.0 wt% HPMC	77.0 wt% ethanol	15 wt% water	3.0 wt% Mn(acac)2

6.1. IGNITION DELAY TIME

A good indicator of the hypergolicity of a fuel is its Ignition Delay Time (IDT). The Ignition Delay Time is the interval between the first contact between the oxidizer and fuel and the start of combustion. It consists of the physical delay (including atomization, vaporization, and mixing) and pre-combustion reactions. The Ignition Delay Time depends on the environmental temperature, fuel-to-oxidiser ratio, and pressure. It is typical to determine the Ignition Delay Time experimentally. To achieve a reliable result, all experiments are repeated at least three times. However, since the gelled ethanol fuel with 2.5 wt% catalyst is of main interest, these samples are tested 10 times to better understand the ignition process. Since the Ignition Delay Time could also be retrieved from the regression rate experiment (Section 6.2) and the temperature profile experiments (Section 6.3), there is even more data available.

6.1.1. ETHANOL FUEL WITH 2.5% CATALYST

The Ignition Delay Time is studied in a multi-drop test including three drops. The test results of sample 206, which consists of ethanol, 3.5 wt% HPC and 2.5% catalyst, are shown in Table 6.2. Not only the results of the experiments specifically for the Ignition Delay Time are shown here, but also the Ignition Delay Time of the temperature profile and regression rate experiments are shown. The temperature profile testing includes four drops sometimes, but this is not a problem as ignition occurred already at or before the third droplet. Therefore, it can simply be seen as a multi-drop test with three drops. Of the 18 executed experiments, only three failed to ignite. Including in those three failures is experiment 32 which could be eliminated as there was an error in the experiment due to a lack of hydrogen peroxide droplets. Hence, 88% of the test resulted in successful ignition. In Chapter 5 it was already described that the ignition process of ethanol fuel gelled with HPC differs from that of ethanol fuel gelled with HPMC. This is further confirmed by these experiments. The ignition process is also very constant. After the first droplet, the hydrogen peroxide starts fizzing indicating its potential to ignite. Then sparkling starts and smoke begin to form. Typically, a clear white dot of light is observed. This firmly shows the potential of the fuel to ignite, however, the auto-ignition temperature of the fuel is not yet reached resulting in some delay before ignition occurs. The fact that it takes a relatively long time to achieve the auto-ignition temperature of the fuel has to do with the energy loss to the surroundings. As becomes clear in Section 6.3, the temperature decreases 20% to 30% over a length of only 1 cm. Hence, it can be expected that the Ignition Delay Time will decrease when the propellant is placed in an actual propulsion system where the energy is more contain inside. Based on Table 6.2, it takes on average 1.5 droplets of hydrogen peroxide before ignition occurs and the average Ignition Delay Time is equal to 538 ms.

Table 6.2: Ignition Delay Time of ethanol fuel gelled with HPC and 2.5wt% catalyst

Experiment	Sample number	Total amount of drops	Concentration H2O2	IDT (ms)	Drops before ignition	Observations
30	206	3	94.9	-	-	No ignition
31	206	3	94.9	177	1	A small ignition occures after the first drop, however, true ignition of the entire fuel grain does not seem to happen. Also no loud sound
32	206	2	94.9	-	-	Glass tube was empty only two drops fell. After the second drop, fizzing of the H2O2, some smoke and sparkling. Also a single light dot for a short time. No ignition
38	206	3	98.2	912	3	Fizzing, sparkling and smoke, already clear white dots of light after the first drop.
39	206	3	98.2	-	-	Fizzing, sparkling and smoke, no ignition
40	206	3	94.9	1003	1	Fizzing, sparkling and smoke, no real ignition of the fuel, more a short flame and no igntion of the entire grain
41	206	3	94.9	140	1	Fizzing, sparkling and smoke and clear white dots of light.
62	206	3	98.2	240	1	Fizzing, sparkling and smoke and clear white dots of light.
63	206	3	98.2	ND	ND	Leakage of the glass tube results in a small first spatter before the test begins. Ignition occures
75	206	3	97.1	125	1	A small ignition occures after the first drop, however, true ignition of the entire fuel grain does not seem to happen untill the second drop. Also no loud sound
76	206	3	97.1	291	1	Fizzing, the foam is formed after the third drop impacts
69	206	3	98.2	961	2	Regression rate test
70	206	3	98.2	386	1	Regression rate test
86	206A	3	96.7	196	1	Regression rate test
65	206	3	98.2	215	1	Temperature test
66	206	4	98.2	1660	3	Temperature test
98	206A	3	96.7	1135	3	Temperature test
100	206A	4	96.7	90	1	Temperature test

The test results of sample 208, which consists of HPMC, DI water, and 2.5% catalyst, are shown in Table 6.3. The intention was to achieve a reliable result by executing 10 drop test. It can be seen that experiments 35, 36, and 37 all resulted in no ignition. When analysing the data this was found to be suspicious as experiments executed with even lower concentrations of hydrogen peroxide did result in ignition. It was found that experiment 35 was the first experiment of that day and that the day prior an experiment with water was executed using the same glass tube. Hence, it is believed that small droplets of water were still present in the glass tube when it was filled with hydrogen peroxide, instantly reducing its concentration. Experiments 35, 36, and 37 were executed with the same fill and hence, this dilution would have affected all three experiments. The next experiment (experiment 38 and 39) was executed after refilling the glass tube. Although these did not have such a strong effect, it can be seen in Table 6.2 that also these tests resulted in bad performance of the fuel.

Table 6.3: Ignition Delay Time of ethanol fuel gelled with HPMC and 2.5wt% catalyst

34	208	3	94.9	ND	ND	Ignition occurred, no movie due to camera issues with saving the movie
35	208	3	98.2	-	-	No ignition. Absent of ignition is likely caused by an experimental error. It is hypothesised that the the hydrogen peroxide was diluted.
36	208	3	98.2	-	-	
37	208	3	98.2	-	-	
42	208	3	94.9	994	2	Fizzing of the H2O2, sparkling, and a lot of foam is formed, already after the first drop
43	208	3	94.9	1270	2	Fizzing of the H2O2, sparkling and a lot of foam is formed, already after the first drop
64	208	4	98.2	1569	4	Accidentally four drops, fizzing of H2O2, sparkling, and foam is formed after the second drop
77	208	3	97.1	1240	2	Fizzing of the H2O2, sparkling, and a lot of foam is formed already after the first drop. Foam covers entire fuel
78	208	3	97.1	965	2	Fizzing of the H2O2, sparkling and a lot of foam is formed already after the first drop
33	208	2	94.9	-	-	no ignition, glass tube was empty, sparkling and foam formation
73	208	3	98.2	1871	3	Regression rate test
80	208 A	3	96.7	1457	3	Regression rate test
82	208A	3	96.7	-	-	Regression rate test, no ignition
83	208A	3	96.7	-	-	Regression rate test, no ignitrion
84	208A	3	96.7	-	-	Regression rate test, no ignition
67	208	3	98.2	2078	3	Temperature test
68	208	4	98.2	1568	3	Temperature test
99	208A	4	96.7	1125	3	Temperature test
101	208A	4	96.7	635	2	Temperature test

In Table 6.3 also the Ignition Delay Times as could be obtained from the regression rate drop test (Section 6.2) and temperature profile test (Section 6.3) are included. The temperature profile testing includes four drops sometimes, but this is not a problem as ignition occurred already at or before the third droplet. Hence, it can be seen as a multi-drop test with three drops. Of the 19 executed experiments, three failed due to diluted hydrogen peroxide and one test includes only two drops due to an empty glass tube (experiment 33), resulting in 15 reliable experiments. From these 15 experiments only three failed, hence, 80% of the experiments resulted in successfully ignition. Furthermore, the process of ignition is quite constant. After the first droplet the hydrogen peroxide starts fizzing, very small little sparkles are visible and foam is formed. Then after the second droplet more foam is formed, sometimes completely covering the fuel, after which ignition occurs. The formation of foam can be seen as a 3D network. Since this foam is not observed in sample 206, it can be reasoned that foam forms due to either the presence of water in the system or by the fact that a methyl group is present. In any way, the formation of foam is an undesirable feature for a propellant. Based on Table 6.2, it takes on average 2.6 droplets of hydrogen peroxide before ignition occurs and the average Ignition Delay Time is equal to 1320 ms.

As one can imagine, there is a strong relationship between the number of droplets required to ignite the fuel and the Ignition Delay Time. The fuel already shows potential to ignite, but has to "wait" for the next droplet to achieve ignition. It is therefore likely, that the flow rate at which the hydrogen peroxide is released influences the Ignition Delay Time strongly. The average time between two droplets is 0.6 seconds, but it deviates between 0.5 seconds and 0.7 seconds. In Figure 6.1 the relationship between the Ignition Delay Time and the number of droplets required to achieve ignition is shown. The first aspect that becomes clear from this graph is that the slope of the trend line is quite similar, both are steep slopes. The gradient of the lines indicates a strong relationship between the number of droplets and the Ignition Delay Time. Additionally, it can be seen that the Ignition Delay Times of ethanol fuels gelled with HPC are lower than ethanol fuels gelled with HPMC. Moreover, ethanol fuels gelled with HPC require fewer drops to achieve ignition compared to ethanol fuel gelled with HPMC as can be seen in Figure 6.3. This difference in Ignition Delay Time can be caused by the formation of foam in the ethanol fuels gelled with HPMC. The foam acts as a heat sink, see Section 6.3 for a further explanation. Another aspect that plays a vital role in achieving ignition is the yield point of the fuel. The yield point of the ethanol fuel gelled with HPMC is higher than the yield point of the ethanol fuel gelled with HPC. The yield point can be seen in Chapter 4 and Section 6.4.

Furthermore, there is also a relation between the concentration of hydrogen peroxide and the Ignition Delay Time. This relationship is not that strong, but can still be seen in Figure 6.2. Here only the data of the ethanol fuel gelled with HPC is shown, whereby ignition was achieved with one droplet. This is done to eliminate the effects of the flow rate associated with a multi-drop test.

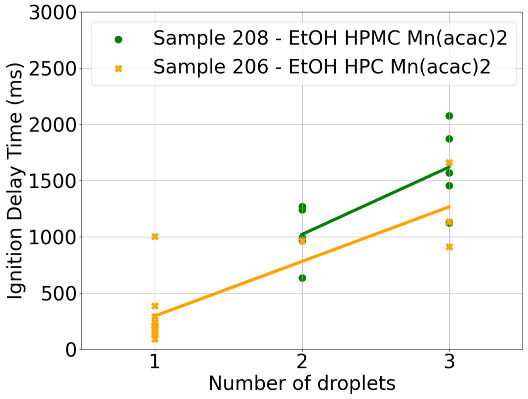

Figure 6.1: Relation between the number of droplet to achieve igntion and the Ignition Delay Time

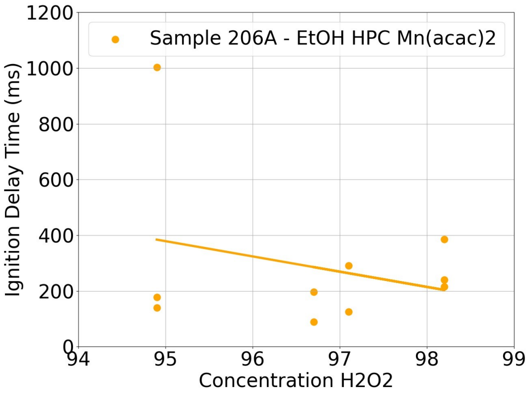

Figure 6.2: Relation between the concentration of hydrogen peroxide and the Ignition Delay Time

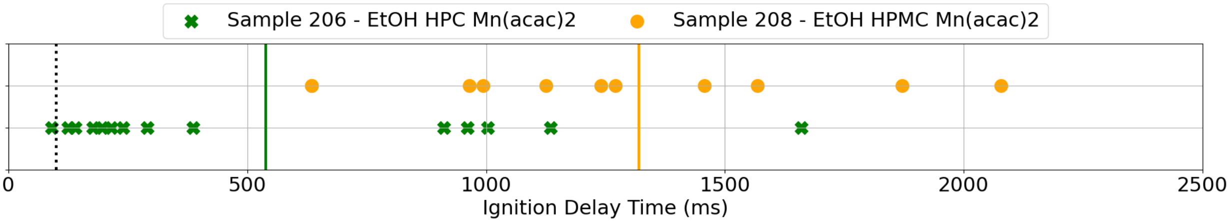

Figure 6.3: Overview of the Ignition Delay Time of gelled ethanol fuels with 2.5 wt% catalyst

6.1.2. ETHANOL FUEL WITH 3.0% CATALYST

The results of the multi-drop test with three drops with the gelled fuel containing 3.0 wt% of catalyst are shown in Table 6.4 and Table 6.5. The Brix% of the hydrogen peroxide was 42.8%, which equals an H2O2 concentration of 96.7%. The concentration of hydrogen peroxide was the same for all experiments. During the experiments it is noticed that the flame is more white, indicating a higher temperature of the flame. Additionally, it can be seen that for sample 215 all experiments resulted in successfully achieving ignition. While in sample 206 (with 2.5 wt% catalyst) the success rate was still at 88%, this has now increased to a 100 %. A higher concentration of catalyst lowers the activation energy of the fuel more. The lower the activation energy of a fuel, the lower its Ignition Delay Time will be as less energy is required to achieve ignition. This trend is not that clearly visible in sample 116, where the successfully achieved ignitions increased from 80% to 83 %. Hence, due to the limited amount of testing, this can be considered as remaining constant.

Table 6.4: Ignition Delay Time of ethanol fuel gelled with HPC and 3.0 wt% catalyst

Experiment	Sample number	Total amount of drops	Concentration H2O2	IDT (ms)	Drops before ignition	Observations
95	215	3	96.7 %	540	2	After the first drop already clear white dots of light are visible, fizzing of the H2O2 and some smoke. No wind.
96	215	3	96.7 %	597	2	After the first drop, clear white dots of light are visible, fizzing of the H2O2 and some smoke. Bubbles are forming after the second drop. No wind.
97	215	3	96.7 %	211	1	After 103 ms a clear white dot of light is visible, this dot eventually ignitions as well.
79	215	3	96.7 %	435	1	Regression rate test
87	215	3	96.7 %	187	1	Regression rate test
88	215	3	96.7 %	80	1	Regression rate test

Table 6.5: Ignition Delay Time of ethanol fuel gelled with HPMC and 3.0 wt% catalyst

Experiment	Sample number	Total amount of drops	Concentration H2O2	IDT (ms)	Drops before ignition	Observations
89	216	3	96.7 %	1073	2	After the first drop, some bubbles form, a bit of smoke, a bit of fizzing of the H2O2. After the second drop, a lot more foam is formed that covers almost the entire fuel. No wind.
90	216	3	96.7 %	1619	3	The first drop is slightly of centre, fizzing and smoke are visible, after second drop formation of a lot of foam.
91	216	3	96.7 %	843	2	First drop slightly of centre, fizzing and smoke, after second drop formation of foam. The flame is very white, rendering the fuel invisible. Windy.
92	216	3	96.7 %	897	2	Regression rate test
93	216	3	96.7 %	-	-	No ignition, regression rate test
94	216	3	96.7 %	1601	3	Regression rate test

6.1.3. Ethanol fuel with 2.0% catalyst

To find the critical concentration of catalyst, also the 2.0 wt% of catalyst was tested. The results of these test can be seen in Table 6.6 and Table 6.7. The Brix% of the hydrogen peroxide was 42.5% which equals an H2O2 concentration of 96.0%. The concentration of hydrogen peroxide was constant for all experiments. It has to be noted that sample 201 is 15 days old by now and changes are already visible in the fuel. The fuel had, at t=0, a colour that can be best described as the colour of Coca-Cola. Black but under certain light more brown. However, now, at t=15 days, the colour is more orange-like.

In these experiments, another feature became more visible. Especially in experiment 105, it can be seen that the fuel deforms slightly under the impact of the droplet of hydrogen peroxide. Hence, it seems that the ethanol fuel gelled with HPC (sample 201) deforms under the impact of the droplet of hydrogen peroxide. As stated before, this could be due to the age of the sample. The motion can be described as the motion of a pudding cake. The ethanol fuel gelled with HPMC (sample 217) does not show this behaviour.

Table 6.6: Ignition Delay Time of ethanol fuel gelled with HPC and 2.0 wt% catalyst

Experiment	Sample number	Total amount of drops	Concentration H2O2	IDT (ms)	Drops before ignition	Observations
104	201	2	96.0 %	-	-	The glass tube was empty, so only two drops fell. No ignition. The fuel deforms a bit under the impact of the droplet. Fizzing and sparkling visible, also a bit of smoke.
105	201	3	96.0 %	915	2	Deformation of fuel under impact droplet. Fizzing and smoke after the first droplet, more fizzing after the second droplet, also foam formation.
106	201	3	96.0 %	1320	3	A small amount of fizzing and smoke after the first droplet, more fizzing after the second droplet, and not wind present. Watch glass breaks during the experiment.
110	201	3	96.0 %	774	2	The fuel deforms under the impact of the droplet. Fizzing, sparkling, and smoke are visible and bubble formation and quite some foam formation.

Table 6.7: Ignition Delay Time of ethanol fuel gelled with HPMC and 2.0 wt% catalyst

Experiment	Sample number	Total amount of drops	Concentration H2O2	IDT (ms)	Drops before ignition	Observations
107	217	3	96.0 %	2	780	Fizzing of the fuel, a lot of foam formation, and no wind
108	217	3	96.0 %	2	1007	Fizzing of the fuel, after the second drop the foam covers almost the entire fuel.
109	217	3	96.0 %	-	-	Fizzing of the fuel, no wind, sparkling but no light dot, foam formation. No ignition.

6.1.4. Comparison

To compare the results of all samples, an overview is made which can be seen in Table 6.8. Here, the average amount of droplets and average Ignition Delay Time is taken based on the experiments where ignition was achieved. It can be seen that the samples gelled with HPC behave just as expected. With increasing concentration of catalyst, the average amount of drops before ignition and the average IDT decrease. This is expected as the catalyst lowers the activation energy of the fuel, easing the process of ignition. However, this behaviour is not directly clear from the sample gelled with HPMC. It seems that sample 217 has an extremely low Ignition Delay Time and requires the least amount of droplets to achieve ignition. However, this can be easily explained by the fact that only the successful ignitions are included in this table. For sample 217, 30% of the test failed to ignite, but these failures do not appear in this table. Hence, this value of 894 ms is not representative, and an IDT of round 1400 to 1450 ms would be more fitted.

Table 6.8: Comparison between average IDT of ethanol fuels with different wt% of catalyst

Sample number	Content	Average amount of drops before ignition	Average Ignition Delay Time (ms)
201	3.5 wt% HPC + 2.0 wt% catalyst	2.3	1003
206(A)	3.5 wt% HPC + 2.5 wt% catalyst	1.5	538
215	3.5 wt% HPC + 3.0 wt% catalyst	1.3	342
217	5.0 wt% HPMC + 2.0 wt% catalyst	2.0	894
208(A)	5.0 wt% HPMC + 2.5 wt% catalyst	2.6	1320
216	5.0 wt% HPMC + 3.0 wt% catalyst	2.4	1207

Another observation is that there is a difference in Ignition Delay Time based on the type of gelling agent used to transform the fuel into a solid. Multiple aspects contribute to the longer Ignition Delay Time of the fuels gelled with HPMC. First, to achieve solidification with HPMC water had to be added as well. Water acts as a heat sink, absorbing energy from the system. All energy taken by the water can not be used to achieve hypergolicity in the fuel, therefore delaying ignition. Secondly, a higher critical concentration of HPMC was required to transform the ethanol in a solid system compared to HPC (4.5 wt% HPMC vs 3.0 wt% HPC, see Chapter 3). According to Table 4.3 the yield point of fuels gelled with a critical concentration of HPMC is higher than the yield point of fuels gelled with a critical concentration of HPC. This higher yield point also results in a longer Ignition Delay Time. Lastly, HPMC consist of two methyl groups, these groups increase the length of the molecule. This long chain might influence the Ignition Delay Time, however, a chemical engineer should investigate this aspect further.

6.2. REGRESSION RATE

The regression rate of a fuel is the rate at which the surface of the fuel recedes during the entire burn time of the fuel. For a hybrid rocket fuel, the average regression rate is one of the most important parameters to determine to predicate its performance. To determine the regression rate experimentally, the fuel has to be shaped into a grain. This process is explained in Subsection 6.2.1. Furthermore, the camera settings have to be changed to be able to have sufficient filming time. The frame rate of 1000 fps provides a filming time of almost one minute, while still achieving a photo interval accuracy of 1 ms. The regression rate ($\dot{r}$) of the fuel is equal to the height of the grain (h) divided by the burn time (t_{burn}), see Equation 6.1. The burn time is defined as the time interval between ignition and the last moment the fuel is white-hot. The main focus of this investigation is on the fuels with 2.5 wt% catalyst. Therefore, these fuels are investigated most extensively. However, to allow for a comparison, also regression rate of fuels with 3.0 wt% catalyst are investigated.

$$\dot{r} = \frac{h}{t_{burn}} \tag{6.1}$$

The regression rate of the ethanol gelled fuel is determined experimentally. The experiment consisted of a multi-drop test with three drops. An average volume of a droplet is around 0.036 mL. This means that in total an oxidiser volume of 0.1 mL is added to the system. Unfortunately, the concentration of hydrogen peroxide was not constant during the experiments. The fuel is moulded in the shape of a grain. This assures that the shape is kept as constant as possible, however, due to the sticky nature of the gelled fuel, some deviations in shape are inevitable. To verify the shape of the grain, the grains are weighed on a scale just before the experiment starts.

6.2.1. PROCESS OF FORMING THE GRAIN

Multiple options were considered to mould the fuel into a grain. One critical aspect of the grain is its size. The size of the grain has to be very small to stay within the tight safety limits of performing a drop test. Large amounts of fuel present could lead to a big explosion. The first option was to make a mould and print this with the 3D printer. However, as the fuel is very sticky, it would be challenging to retrieve the grain from the mould. Applying baking paper to the mould to ease pushing the grain from the mould is not possible due to the small dimensions. Therefore, a simple syringe was used to suck up the fuel (or fuel is pushed into the syringe). This way, a very small grain could be made. The syringe is cut open at the top to allow for a wider opening. See Figure 6.4 for clarification. The syringe has a diameter of 4.6 mm, however, the fuel collapses a bit due to the pressure from pushing the fuel out of the syringe. Therefore, the diameter of the fuel is equal to around 4.8 mm. The height of the fuel is equal to around 4.6 mm. To make verify the size of the grain, the fuel is weighed before the experiment. Typically, the mass of the grain is around 83 mg.

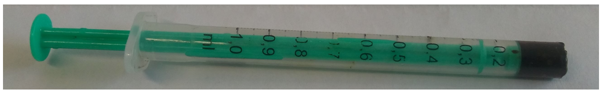

Figure 6.4: Syringe with cut open top to make the grain

6.2.2. ETHANOL FUEL WITH 2.5% CATALYST

The experiments are executed with two different concentrations of hydrogen peroxide, because of a limited amount of hydrogen peroxide. The concentrations used are 96.7% hydrogen peroxide (a Brix% of 42.8) or 98.2 % hydrogen peroxide (a Brix% of 43.5). Additionally, the amount of sample 206 and sample 208 was insufficient and therefore more of this sample is produced and named sample 206A and sample 208A respectively. An overview of the results are shown in Table 6.9. The regression rate is based on a grain height of 4.6 mm. The number of drops before ignition is included as it was believed that it might influence the burn time. As one can imagine, adding hydrogen peroxide to the already burning fuel would maybe increase the intensity of the burning which then would decrease the burn time. However, due to the limited amount of tests performed, this could not be determined. One does need to keep in mind that the total volume of H2O2 that is added to the system is kept constant.

Table 6.9: Regression rates of ethanol fuels with 2.5 % catalyst

Experiment	Sample number	Total amount of drops	Concentration H2O2	Mass of the fuel (g)	IDT (ms)	Drops before ignition	Burn time (s)	regression rate (mm/s)
69	206	3 drops	98.2 %	0.087	961	2	47.220	0.10
70	206	3 drops	98.2 %	0.084	386	1	43.961	0.10
86	206A	3 drops	96.7 %	0.086	196	1	40.731	0.11
73	208	3 drops	98.2 %	0.086	1871	3	35.809	0.13
80	208 A	3 drops	96.7 %	0.087	1457	3	50.870	0.09
82	208A	3 drops	96.7 %	0.085	-	-	-	-
83	208A	3 drops	96.7 %	0.083	-	-	-	-
84	208A	3 drops	96.7 %	0.086	-	-	-	-

A visual representation of the experiment can be seen in Figure 6.5. The shape of the grain is shown in the first picture. During ignition and the adding of additional droplets of hydrogen peroxide, the grain is not visible due to the extensive light that is released during those times. When the flame reduces in intensity, it can be seen that the grain becomes more narrow as the fuel is consumed on all exposed areas of the grain and not only from the top. Over time, the grain becomes smaller and smaller until only one dot of clear white light remains. When also this light goes out the burn is considered over. The residue left is only a limited amount, brown and dried.

All experiments were executed under windy circumstances, except for experiment 86 where no wind was present. The influence of wind on the flame is very obvious, as can be seen in Figure 6.6. The presence of wind increases the heat loss to the environment. This also forms a possible reason why the burn time of experiment 86 is short compared to experiments 69 and 70 even though the concentration of hydrogen peroxide is lower. Due to the absence of wind during experiment 86 less heat was lost to the environment.

The intention was to repeat all experiments three times. However, as sample 208A failed to ignition during three experiments, only two experiments were successfully executed. This indicates that the performance of ethanol fuel gelled with HPMC is less predictable and less constant. This is in contrast to ethanol fuel gelled with HPC (sample 206). It can be seen that the burn time of ethanol fuel gelled with HPC is relatively constant. This is a favourable characteristic of this type of fuel.

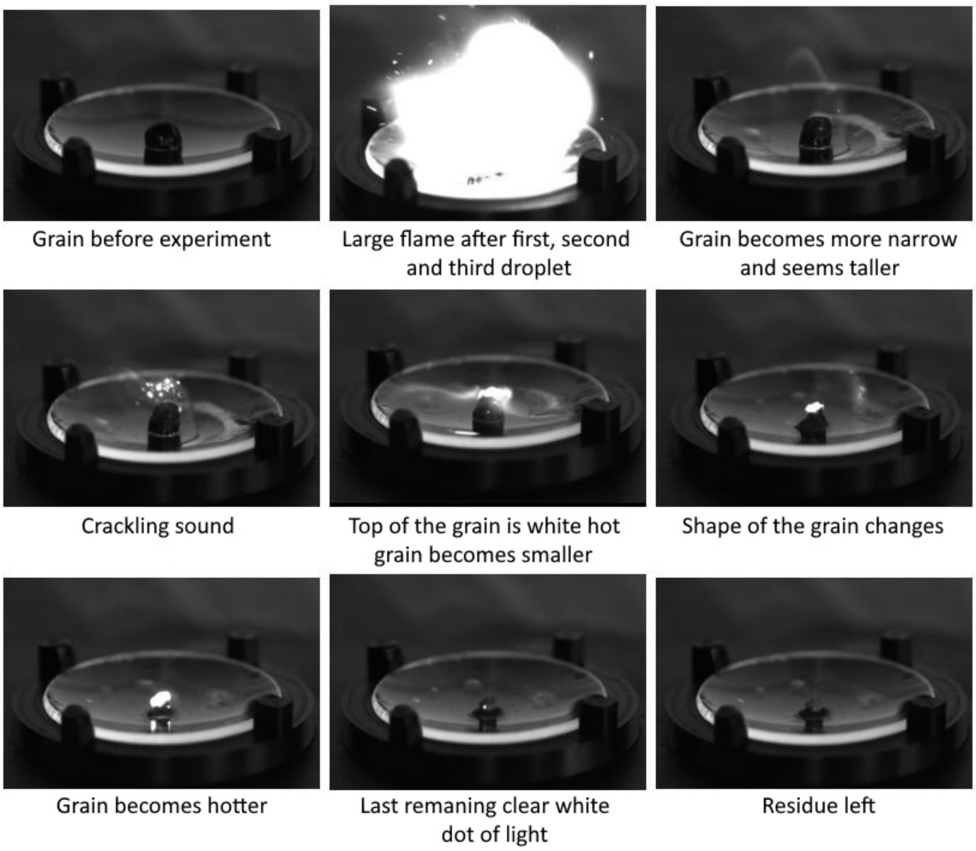
Grain before experiment
Large flame after first, second and third droplet
Grain becomes more narrow and seems taller
Crackling sound
Top of the grain is white hot grain becomes smaller
Shape of the grain changes
Grain becomes hotter
Last remaning clear white dot of light
Residue left

Figure 6.5: Experiment 70: regression rate of ethanol fuel gelled with 3.5 wt% HPC and 2.5 wt% Mn(acac)2

REGRESSION RATE TEST WITH FOUR DROPS

It was challenging to precisely release three droplets during the experiments to obtain the regression rate. Therefore, also some experiments were (accidentally) executed with four drops. The results can be found in Table 6.10. The amount of hydrogen peroxide that is added to the system increased due to the fourth droplet. Therefore, one can expect that the regression rate would increase compared to the experiments with only three droplets (as in Table 6.9). This is also precisely what is happening for ethanol fuel gelled with HPC (sample 206). However, this does not happen for the ethanol fuel gelled with HPMC (sample 208), which again shows that the performance of this type of fuel is hard to predict. One possible explanation could be that for experiment 74, no additional droplets (which would increase the regression rate) are released after ignition because ignition still occurs at the last released drop. Another possible explanation is that the concentration of hydrogen peroxide is lower during these four multi-drop experiments than during the three multi-drop experiments. An overview of the average burn time and regression rates are shown in Table 6.12.

Table 6.10: Regression rates of ethanol fuel with 2.5 % catalyst (multi drop test with four drops)

Experiment	Sample number	Total amount of drops	Concentration H2O2	Mass of the fuel (g)	IDT (ms)	Drops before ignition	Burn time (s)	Regression rate (mm/s)
71	206	4	98.2 %	0.086	250	1	31.522	0.15
85	206A	4	98.2 %	0.085	139	1	36.212	0.13
74	208	4	96.7 %	0.081	2578	4	41.215	0.11
81	208A	4	96.7 %	0.083	843	2	42.077	0.11

6.2.3. ETHANOL FUEL WITH 3.0% CATALYST

The regression rate was also determined for the samples which consist of 3.0 wt% of catalyst. The results of the experiments are shown in Table 6.11. As the scale was in use by someone else during experiments 92 and 93, these fuels were weighted with another, less accurate scale.

Table 6.11: Regression rates of ethanol fuel with 3.0 % catalyst

Experiment	Sample number	Total amount of drops	Concentration H2O2	Mass of the fuel (g)	IDT (ms)	Drops before ignition	Burn time (s)	Regression rate (mm/s)
79	215	3	96.7 %	0.082	435	1	38.099	0.12
87	215	3	96.7 %	0.086	187	1	34.993	0.13
88	215	3	96.7 %	0.082	80	1	41.505	0.11
91	216	3	96.7 %	0.085	843	2	34.569	0.13
92	216	3	96.7 %	0.08	897	2	50.095	0.09
93	216	3	96.7 %	0.08	-	-	-	-
94	216	3	96.7 %	0.077	1601	3	> 51.456	< 0.09

In experiment 94 the burn time could not be determined as the film already ended before the fuel stopped burning. Due to the limited memory of the camera, only a restricted amount of seconds can be stored. Therefore, it could only be determined that the burn time was longer than 51 s. Additionally, experiment 93 did not result in the ignition of the fuel. Other observations were that for experiment 91, the first droplet was slightly off-centre. This could be the reason why the fuel required two droplets to ignite. However, this did not seem to affect the burn time. Lastly, experiment 87 was the only experiment without wind. All other experiments were executed in windy conditions. The influence of wind can be seen in Figure 6.6.

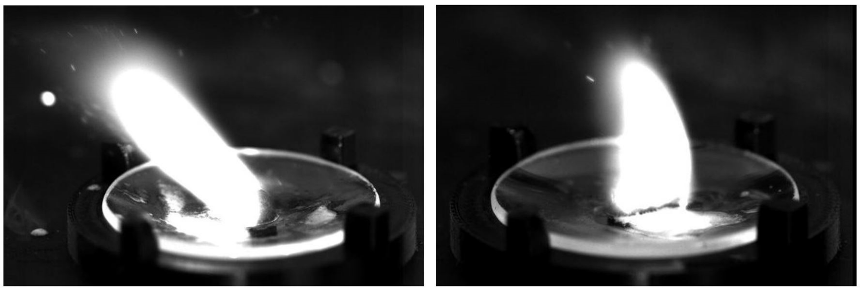

Windy conditions - experiment 79

No wind - experiment 87

Figure 6.6: Wind conditions influencing the direction of the flame

As already is shown in Section 6.1, the Ignition Delay Time decreases with the increasing concentration of catalyst. Due to this decrease in Ignition Delay Time, also the number of droplets to achieve ignition decreases. This consequently results in more droplets of hydrogen peroxide being released after ignition already occurred. All droplets that are added to the system after ignition result in a more intense and hotter flame, increasing the regression rate. Hence, one can expect the regression rate to decrease in the samples with 3.0 wt% catalyst compared to the samples with only 2.5 wt% catalyst. An overview of the average burn times and regression rates can be seen in Table 6.12. It is clear that the regression rate of the ethanol fuel gelled with HPC increase with the increasing concentration of catalyst (sample 206 and sample 215). The regression rate increases from 0.10 mm/s to 0.12 mm/s. However, no such trend is visible for the ethanol fuel gelled with HPMC (sample 208 and sample 216). There the regression rate decreases from 0.1 mm/s to <0.1 mm/s. This could be a consequence of the fact that only "successful" measurements are included in this overview. When the fuel failed to ignite, no burn time or regression rate could be obtained and hence, these are not taken into account when calculating the average values as shown in Table 6.12. The number of successful experiments did increase when comparing sample 208 with sample 216. Anyhow, it again shows the unpredictability of the performance of ethanol fuels gelled with HPMC.

Table 6.12: Overview of average burn times and regression rates

Sample number	Content	Burn time (ms)	Regression rate (mm/s)	Burn time (ms)	Regression rate (mm/s)
		3 drops		4 drops	
206(A)	3.5 wt% HPC + 2.5 wt% catalyst	44	0.10	34	0.14
208(A)	5.0 wt% HPMC + 2.5 wt% catalyst	43	0.11	42	0.11
215	3.5 wt% HPC + 3.0 wt% catalyst	38	0.12	-	-
216	5.0 wt% HPMC + 3.0 wt% catalyst	>46	<0.10	-	-

6.3. ENERGY CONTENT

TThe energy content of the propellant is an important property as it defines the fuel's primary energy. The energy content is the amount of heat produced by the burning of one gram of a substance, and it is measured in joules per gram. It is common to measure this energy based on the calorific value or the heat generation from the complete combustion of one unit of fuel under well-defined conditions. The easiest way to experimentally determine the energy content is with a calorimeter (or bomb calorimeter). This device measures the amount of heat liberated when the reaction goes to completion. The principle behind the calorimeter is based on the temperature change of a constant volume of water that is sealed in the calorimeter. See Equation 6.2, whereby H is the heat released by combustion, m is the mass in grams of the water used as a heat collector, C is the specific heat of water (4.184 J/g ^{o}C) and ΔT is the temperature change in ^{o}C. Unfortunately, no such calorimeter is available. Therefore, another way to obtain inside into the energy content has to be found.

$$H = m \cdot C \cdot \Delta T \tag{6.2}$$

A temperature profile also indicates the amount of heat that is released during the ignition process and burning of the fuel. The temperature of the fuel is measured using omega thermocouples. Based on the expected temperatures the k-type, unsheathed, with a diameter of 0.125 mm and length of 300 mm is chosen. In the test setup (Figure 5.3) holes are present to mount the thermocouples. The precise location of these holes can be seen in Appendix C Figure C.2. The initial idea was to measure the temperature at the top of the grain and at the bottom of the grain. As the grain is only a few mm long and the predefined holes are quite large, the thermocouples are located at different sides of the grain. Hence, one thermocouple is positioned at the top front side of the grain, and another thermocouple is located at the rear bottom side of the grain. Experiment 65 also had this configuration. However, as both thermocouples melted due to the high temperature, it was decided to relocate the lowest thermocouple. In the remaining experiments, the second thermocouple was placed 11 mm above the first thermocouple.

In Table 6.13 and Table 6.14 the experiments and results are shown. As both bottles of sample 206 and sample 208 were empty, new samples were produced and labelled sample 206A and208A respectively. The experiment was repeated four times per sample. The intention was to perform a three multi-drop experiment, but sometimes four drops fell. This only might have affected the results of experiment 68 as here the wires break after the fourth droplet. For the other experiments (66, 99, 100, and 101) this additional fourth drop did not have any influence on breaking the thermocouples as they were already broken before the fourth drop fell or did not break at all.

Due to the breaking of the thermocouples, the temperature profile could not be determined for most of the experiments. However, the fact that the thermocouples broke did indicate a minimum temperature that was achieved during the ignition of the fuel. The thermocouples can withstand temperatures up to 1260 °C. Although there is a deviation in this breaking point, it can be assumed that this temperature is reached. For experiment 99 and experiment 100 temperature data was collected from the thermocouples. The graphs of the temperature profile can be seen in Figure 6.7 and Figure 6.8. For the other experiments, no data from the thermocouples could be collected due to incorrect calibration or failure of the data acquisition box to collect data.

Table 6.13: Temperature profile of ethanol fuel gelled with HPC and 2.5 wt% catalyst

Experiment	Sample number	Total amount of drops	Concentration H2O2	Temperature low thermal couple (°C)	Temperature high thermal couple (°C)	Observation
65	206	3	98.2 %	>1260	-	Ignition occurs after the first droplet (IDT: 215 *ms*). This experiment had two thermal couples at the grain, both broke. The first one broke shortly after the second drop at 734 *ms*. The second wire snaps after the third drop at 1364 *ms*
66	206	4	98.2 %	>1260	<1260	Ignition occurred after the third droplet (IDT: 1660 *ms*). The low thermocouple broke after the fourth droplet at 2739 *ms* The high thermocouple survived Wind present
98	206A	3	96.7 %	>1260	>1260	First drop was misaligned. The ignition occurred after the third drop (IDT: 1135 *ms*). The thermocouples broke at 1247.3 *ms* and 2405.8 *ms*. No wind
100	206A	4	96.7 %	max 1159	max 928	Ignition occurred after the first droplet (IDT: 90 *ms*). The thermocouples became white of the heat but both survived. No wind

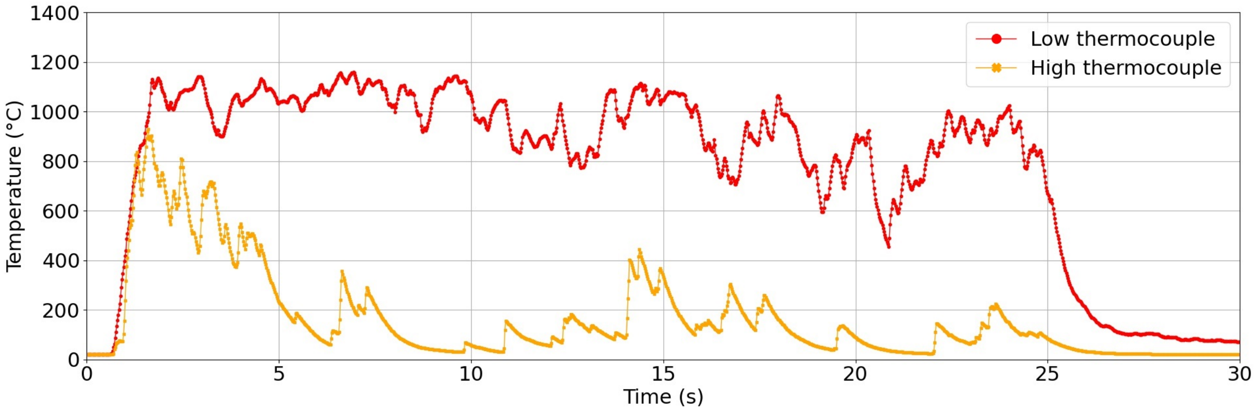

Figure 6.7: Temperature profile of ethanol fuel gelled with HPC and 2.5wt% catalyst (experiment 100)

Table 6.14: Temperature profile of ethanol fuel gelled with HPMC and 2.5 wt% catalyst

Experiment	Sample number	Total amount of drops	Concentration H2O2	Temperature low thermal couple (°C)	Temperature high thermal couple (°C)	Observation
67	208	3	98.2	>1260	>1260	Ignition occurs after the third drop (IDT: 2078 *ms*). The low thermocouple broke at 2291 *ms* and the high thermal couple broke at 2409 *ms*, No wind present
68	208	4	98.2	>1260	>1260	Ignition occurred after the third droplet (IDT: 1568 *ms*). The low thermocouple broke after the fourth droplet at 2147 *ms* shortly followed by the high thermal couple which broke at 2392 *ms*. There is no wind
99	208A	4	96.7	max 1317	max 844	Ignition occurred after the third droplet (IDT: 1125 *ms*). The lower thermocouple became white hot, but both thermocouples survived. There is some wind present
101	208A	4	96.7	>1260	<1260	Ignition occurred after the second droplet (IDT: 635 *ms*). The lower thermocouple breaks also after the second droplet (at 835 *ms*). High thermocouple became white hot. There was wind present

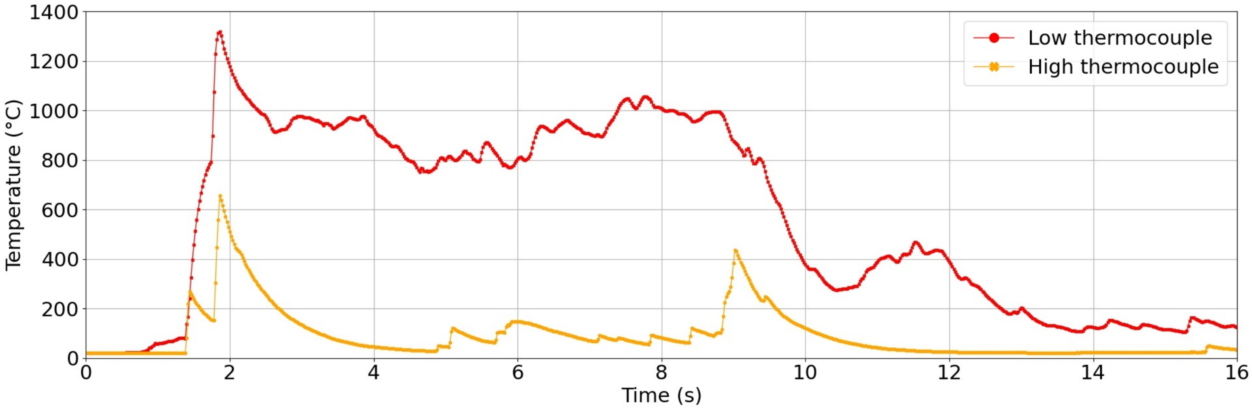

Figure 6.8: Temperature profile of ethanol fuel gelled with HPMC and 2.5wt% catalyst (experiment 99)

During experiment 100, the maximum achieved temperature of the low thermocouple (which is located at the grain) equals 1159 °C, while the high thermocouple, located 11 mm above the low thermocouple, achieved a maximum temperature of 929 °C. This indicates a temperature decrease of already 20% over 1 cm. During experiment 99, the maximum achieved temperature of the low thermocouple (which is located at the grain) equals 1317 °C, while the high thermocouple, located 11 mm above the low thermocouple, achieved a maximum temperature of 844 °C. This indicates a temperature decrease of more than 30% over 1 cm. This shows the great amount of heat that is dissipated into the environment. Hence, this confirms the statement that was made in Section 6.1 and that the IDT will likely decrease in an actual propulsion system where heat is contained inside the engine much more.

The fluctuation of the temperature, which is visible in the temperature profiles, is likely caused by the movement of the flame. The thermocouples are located slightly off-centre to the fuel which would result in a higher fluctuation of heat even though almost no wind was observed.

Although only one temperature profile could be made containing both thermocouple measurements, Figure 6.8 does show one characteristic of ethanol fuel gelled with HPMC very clearly; namely the formation of foam. The visual representation of this phenomenon can be seen in Figure 6.9. The small increase in temperature of the low thermocouple is caused by the formation of the foam. This covers the thermocouple and some heat is already generated inside the foam. The foam reaches a temperature of around 80 °C before ignition occurs. This indicates that the foam acts as a heat sink, absorbing heat that therefore can not be used by the ignition process. The formation of the foam is likely a contributing factor for the longer Ignition Delay Time of ethanol fuel gelled with HPMC compared to ethanol fuel gelled with HPC.

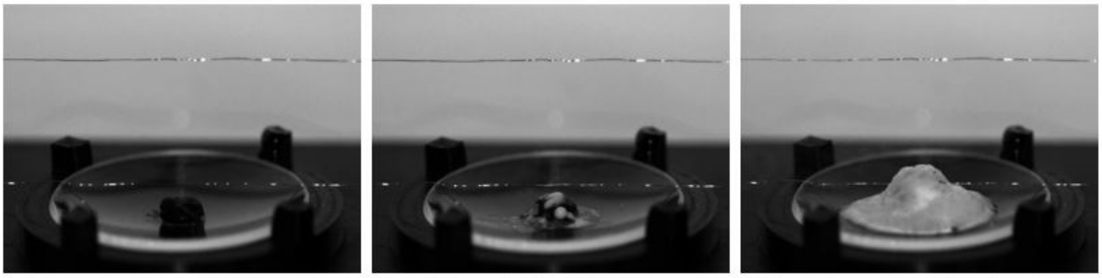

Low thermocouple and high thermocouple

After the first droplet formation of foam on the fuel

After the second droplet foam touches low thermocouple

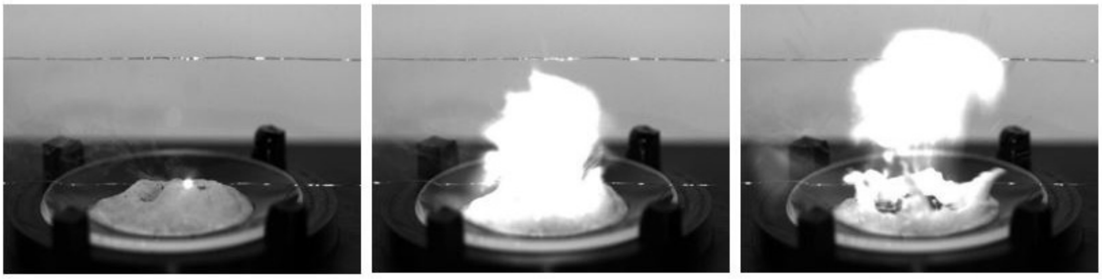

First sign of ignition (t=0)

Ignition process (t= 4 ms)

Ignition process (t=6 ms)

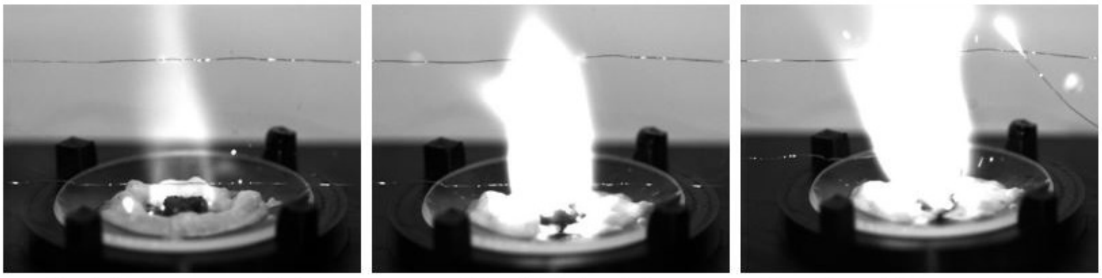

Straight flame, no wind

After third droplet More intense flame

Breaking of thermocouple

Figure 6.9: Experiment 67: Multi-drop test with thermocouples of ethanol fuel gelled with 5.0 wt% HPMC, 15 wt% DI water and 2.5 wt% Mn(acac)

6.4. VISCOELASTIC NATURE OF THE FUEL

The rheology characteristics of the ethanol fuel gelled with HPMC or HPC including the catalyst Mn(acac)2 are determined using the same experiments as explained in Chapter 4. The experiments are executed when the samples were 3 days old. Furthermore, each experiment is repeated three times. The average results of the shear stress ramp study can be seen in Figure 6.10. The yield points are also included. It can be seen that the yield point of sample 206A equals 125 *Pa*, and that the yield point of sample 208A equals 225 *Pa*. Fuels with a higher yield point are more challenging to ignite, something that also became clear from Section 6.1 as the fuels gelled with HPMC have a longer Ignition Delay Time than the fuels gelled with HPC. Another aspect that becomes clear from this study is that the apparent viscosity of sample 208A is high. This was also observed when working with the sample, as the sample already felt stiffer. The apparent viscosity has also almost doubled compared to the same sample without catalyst (see Figure 4.23). The apparent viscosity with catalyst is almost 1000 *Pa.s*, while without catalyst it was only around 500 *Pa.s*. Furthermore, the average results of the amplitude stress sweep study can be seen in Figure 6.11. The Linear Viscoelastic Range of the fuels are more or less the same as without catalyst, and also have roughly the same length as without catalyst (see Table 4.2 as a comparison).

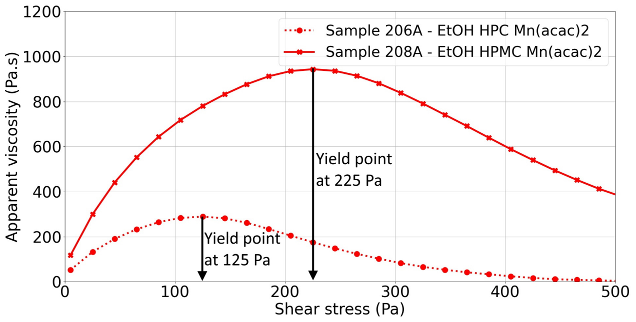

Figure 6.10: Shear stress ramp study of ethanol fuel with 2.5wt% catalyst

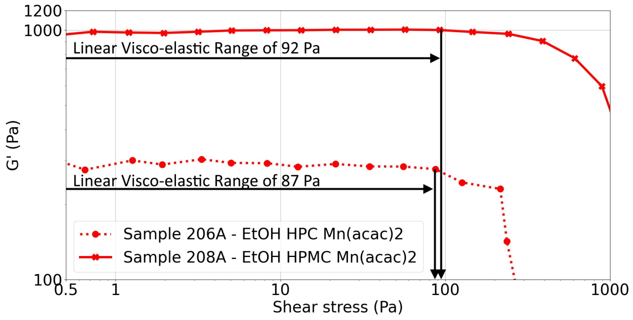

Figure 6.11: Amplitude stress sweep study of ethanol fuel with 2.5 wt% catalyst

6.5. CONCLUSION

An analysis of the performance of an ethanol fuel gelled with HPMC or HPC containing the catalyst manganese(II) acetylacetonate is performed. As an oxidizer, highly concentrated hydrogen peroxide is used (>96.0%). The analysis of the propellant consisted of three parts (1) the Ignition Delay Time, (2) the regression rate, and (3) the energy content of the fuel. The main focus is placed upon two different compositions of the fuel; An ethanol fuel gelled with 3.5 wt% HPC and 2.5 wt% catalyst (Sample 206) and an ethanol fuel gelled with 5.0 wt% HPMC, 15 wt% DI water, and 2.5 wt% catalyst (sample 208).

The Ignition Delay Time (IDT) of the fuel is experimentally determined with a multi-drop test with three droplets under atmospheric conditions. First, it was found that the ignition process of the fuels is quite constant. Regarding the fuels gelled with HPC, the observations are as follows. After the first droplet, the hydrogen peroxide starts fizzing. Then sparkling starts and smoke begin to form. Typically, a clear white dot of light is observed after which the fuel ignites. For fuels gelled with HPMC, this ignition process is different. After the first droplet, the hydrogen peroxide starts fizzing, small little sparkles are visible and foam is formed. After a second droplet more foam is formed, sometimes completely covering the fuel, after which ignition occurs. This foam can be seen as a 3D network and is an undesirable characteristic for a propellant. The reason that the foam forms has to do with either the presence of water in the system or by the fact that a methyl group is present.

The multi-drop test under atmospheric conditions is executed multiple times to obtain a reliable result. The average IDT ethanol fuel gelled with HPC and 2.5 wt% Mn(acac)2 is 539 *ms* and an average IDT of ethanol fuel gelled with HPMC and 2.5 wt% Mn(acac)2 is 1320 *ms*. The deviation from this average is roughly the same for both samples. Although these Ignition Delay Times are longer than the desirable <100 *ms*, the results are still promising. First of all, the longer Ignition Delay Times are a direct consequence of the testing environment, which was at atmospheric conditions. In a pressurized propulsion system, the Ignition Delay Time will decrease as pressure plays a vital role in the Ignition Delay Time. Additionally, considerable amounts of heat are lost to the environment. During the experiments a clear dot of light is visible, indicating the fuel's potential to ignite. However, due to this heat loss, it takes longer before the auto-ignition temperature of the fuel is reached and ignition is achieved. Hence, it can be expected that an Ignition Delay Time of < 100 *ms* can be achieved when the fuel is in an actual pressurized propulsion system with less heat loss. Moreover, even under these suboptimal conditions, sample 206 did have one experiment that has an IDT below 100 *ms*.

The difference in Ignition Delay Time between the two different fuels is caused by the fact it was required to add DI water to solidify ethanol with HPMC. This water acts as a heat sink, absorbing heat during the ignition process resulting in a longer IDT. Additionally, the critical concentration of HPMC to transform ethanol in a solid system is higher compared to the critical concentration of HPC. Lastly, as HPMC consist of two methyl groups, the length of the molecules is longer than that of HPC. This longer chain might have increased the Ignition Delay Time as well.

Additional experiments were performed with a higher (3.0 wt%) and lower (2.0 wt%) concentration of catalyst. The ethanol fuel gelled with HPC and 2.0 wt% catalyst had an average Ignition Delay Time of 1003 ms, which is almost twice as long as the IDT of the ethanol fuel gelled with HPC and 2.5 wt% catalyst. Furthermore, the ethanol fuel gelled with HPC and 3.0 wt% catalyst had an average Ignition Delay Time of 342 ms. This shows the strong dependency between the IDT and the concentration of catalyst. For the experiments with ethanol fuel gelled with HPMC and 2.0 wt% and 3.0 wt% catalyst, also such a trend was visible, but the change in IDT was less.

The regression rate experiments were executed with a small grain. It was found that the burn time of the ethanol fuel gelled with HPC and 2.5 wt% catalyst is relatively constant and on average equals 0.10 mm/s. This shows that the ethanol fuel gelled with HPC has predictable performance. This is not the case for ethanol fuel gelled with HPMC. There, ignition was not always achieved and the regression rates were varying (on average 0.11 mm/s). Furthermore, additional experiments with a higher concentration of catalyst or with a higher volume of oxidizer added to the system showed results that are in line with the prediction when testing ethanol fuels gelled with HPC. Again, showing its constant performance. On the other hand, the results of these additional experiments for ethanol fuels gelled with HPMC do not show this steady behaviour.

The energy content of the fuel is based on the temperature profile of the fuel as a calorimeter was unavailable. The temperature profile revealed that both fuels are capable of achieving high temperatures of around or above 1260 ^oC. Furthermore, this temperature profile revealed that the foam that is formed during the ignition process of ethanol fuels gelled with HPMC has a temperature of around 70 ^oC. This indicates that the foam also acts as a heat sink, providing a third reason for the longer Ignition Delay Time of fuels gelled with HPMC compared to fuels gelled with HPC. Additionally, the temperature profiles also showed that around 20% to 30% of the temperature is lost over an area of only 1 cm. This further confirms that the IDT of the fuels will decrease when tested in a propulsion system.

Hence, it can be concluded that the performance of ethanol fuel gelled with HPC (sample 206) shows more promising results than ethanol fuels gelled with HPMC (sample 208). First of all, the critical amount of gelling agent to achieve a solid system is lower. Only 3.5 wt% of HPC was required to obtain a solidified system against 5.0 wt% of HPMC. Moreover, the gelling process of HPMC is more complex as additional water has to be added to the system. The addition of water or the molecule structure of the gelling agent itself has as a consequence that during the ignition process of ethanol fuels gelled with HPMC, a lot of foam is formed. This is an undesirable characteristic of a propellant. Regarding the performance, the temperature profiles show that the energy content of ethanol fuels is high. Temperatures of >1260 ^oC are reached. On other performance parameters, the ethanol fuels gelled with HPC show more promising results compared to fuels gelled with HPMC. The IDT of the ethanol fuel gelled with HPC and 2.5% catalyst is 538 ms on average, while the IDT of ethanol fuel gelled with HPMC is 1320 ms on average. Additionally, the regression rate experiments showed that consistency in the performance of the ethanol fuels gelled with HPMC is missing. On the other hand, ethanol fuels gelled with HPC do show predictable results. Hence, based on the low critical gelling concentration, a simple formulation of the fuel, lower Ignition Delay Time and consistent performance ethanol fuels gelled with HPC are the favourable fuel for the propellant.

7

CONCLUSION AND RECOMMENDATIONS

The purpose of this thesis is to investigate and develop a novel green hybrid hypergolic bi-propellant system with a viscoelastic nature of the fuel. The two main research questions are: (1) how to develop a viscoelastic fuel for a hybrid bi-propellant system, and (2) how to achieve a hybrid bi-propellant hypergolic system. These questions were answered by performing experimental research.

7.1. CONCLUSION

The first main research question was divided into three sub-questions, which can all be answered. The first two sub-questions are: (1a) what kind of fuel can be used that is green in nature and can be used in hybrid systems, and (1b) how can the liquid fuel be transformed into a solid phase through viscoelasticity. The answer to these questions is as follows: the basis of this green fuel will be alcohol, as alcohols are green, non-toxic, and economically beneficial. Ethanol (EtOH) is the alcohol that has the lowest carbon chain alcohol that exists and is therefore selected as the base for the fuel. Butanol (BuOH) was also studied in order to investigate the influence of the carbon chain length on the fuel's viscoelastic behaviour. The viscoelastic nature of the fuel is achieved by making use of gelling technology. With gelling technology, the viscosity of a substance is altered through a weak cohesive internal structure. As a gelling agent, an organic gelling agent was chosen as it adds positive heat of formation to the fuel, improving its performance. The literature revealed that propyl cellulose showed promising results and suggests that the presence of an -OH group has a synergistic effect with the catalyst. Therefore, hydroxypropyl cellulose (HPC) and hydroxypropyl methylcellulose (HPMC) were selected as gelling agents. Many samples were formulated and investigated in order to find the critical concentrations based on visual appearance and behaviour. It resulted in the formulation of four fuels with critical gelling concentrations. The gellant's critical concentration of the ethanol fuel is found to be between 3.0 wt% HPC and 3.5 wt% HPC. These samples showed solidified behaviour. As for the butanol fuel, the critical concentration to achieve solidification was found to be around 3.0 wt% HPC. Regarding the gelling agent HPMC, the solidification does not occur with ethanol nor butanol as the methyl groups prevent the connection between the OH-group of the alcohol to the methyl-group of the gelling agent. Water had to be added to act as a bridge to obtain a solidified fuel. The ethanol fuel showed solidified behaviour at compositions of 15 wt% water and between 4.5 wt% and 5.0 wt% of HPMC. The butanol fuel showed solidification at a lower concentration of the gelling agent, namely at compositions of 15 wt% water and between 4.0 wt% and 4.5 wt% of HPMC. This difference can be explained based on the length of the carbon chain. Butanol has a carbon chain that is twice as long as the carbon chain of ethanol. This longer chain results in the packing of molecules that is more viscous.

The third sub-question is: (1c) what are the characteristics of the solid fuel. To answer this question a rheology study was performed to analyse and characterize the solidified fuel's viscoelastic nature. The main characteristics to evaluate the fuel's viscoelastic nature are the linear viscoelastic range, the yield point, and the loss factor which expresses the ratio between the elastic modulus (G') over the viscous modulus (G"). The Linear Viscoelastic Range (LVR) indicates the range at which the internal structure remains intact, and this range can be investigated via an amplitude stress sweep study. When G' > G", the fuel shows a gel-like or solid structure and can be termed a viscoelastic solid material. It is found that the butanol fuels gelled with HPMC have a longer Linear Viscoelastic Range than ethanol fuel gelled with HPMC. The yield point indicates the transition from a gel-like (elastic dominant) to a liquid-like state (viscous dominant) induced by shearing. A stress ramp study revealed that fuels gelled with HPMC have a higher yield point than fuels gelled with HPC, independent of alcohol basis. The loss factor and time-dependent behaviour can be found via a frequency sweep study. It revealed that fuels gelled with HPC show less dependency on frequency than fuels gelled with HPMC. Additionally, fuels gelled with HPC show behaviour that is more closely resembling that of an ideal elastic material than fuels gelled with HPMC. A stability study was performed for one month to observe the change in viscoelastic behaviour of the fuel during storage. It was found that most fuels showed a large increase in LVR (>50%), and some change slightly or remained constant. Additionally, the yield point decreased over time for all fuels except for the butanol fuel gelled with 5.0 wt% HPC. A temperature study ranging from 0 ^oC to 45 ^oC was attempted, but due to dysfunctioning of the rheometer, many issues were encountered. The temperature study showed that the apparent viscosity of the fuel has a strong dependency on the higher temperatures, especially.

Hence, the first main research question can be answered. Low carbon chain alcohols such as ethanol or butanol can be used as a green fuel. The liquid can be transformed into a solid phase by using gelling technology. Suitable gelling agents are HPC and HPMC, although the latter does require the addition of DI water to achieve solidification. The critical concentrations for ethanol gelled fuel are 3.5 wt% HPC or 5.0% HPMC with 15wt % DI water. The fuels' behaviour in terms of viscoelastic nature is promising, the viscoelastic range, yield point, and loss factor confirms this.

The second main research question consists of four sub-questions. The first sub-question was: (2a) what kind of oxidizer can be used to achieve a green hypergolic bi-propellant system? As current green bi-propellants do not have the combination to achieve hypergolicity naturally, a catalyst has to be suspended to the fuel to achieve hypergolicity with a suitable oxidizer. A suitable oxidizer is a highly concentrated hydrogen peroxide (>90% H2O2) as it decomposes into environmentally friendly products. However, when ordering hydrogen peroxide, stabilizers are added to prevent the decomposition of hydrogen peroxide. These additional elements may influence the performance of the propellant when the catalyst particles are suspended in the fuel. So, a pure as possible H2O2 solution is desired. Based on an ion chromatography and inductively coupled plasma mass spectrometry analysis, it was found that highly concentrated hydrogen peroxide made from a 30% production bottle of 1 L is purest.

To create a catalytically induced hypergolic system, a suitable catalyst had to be found. To determine which catalyst is most suitable, four different catalysts were tested: iron(II, III)oxide, manganese(III)oxide, copper(II)oxide, and manganese(II) acetylacetonate with ethanol gelled fuel. The concentration of these catalysts was equal to 2.5 wt%. The amount of catalyst should be high enough to sufficiently lower the activation energy of the fuel to achieve hypergolic ignition with a high concentration of hydrogen peroxide without compromising propellant performance. The hypergolicity was evaluated by means of a multi-drop test consisting of three or four drops with 98.2 % H2O2. The results were clear; no ignition could be achieved with 2.5 wt% of iron(II, III)oxide, manganese(III)oxide, or copper(II)oxide. Hence, these are deemed unfit in rocket propellant applications. Ignition was achieved with 2.5wt% of manganese(II)acetylacetonate (Mn(acac)2)in both the ethanol fuel gelled with 3.5 wt% HPC and the ethanol fuel gelled with 5.0 wt% of HPMC. Hence, answering sub-question (2b) which was: how can the green propellant be made hypergolic.

The third sub-question that can be answered is: what are the characteristics of hypergolic system in terms of performance. A detailed analysis of the performance of the propellant consists of experiments evaluating the Ignition Delay Time (IDT), regression rate, and energy content. First, the ignition process is found to be constant but differs between the ethanol fuel gelled with HPC or HPMC. The ignition process of the ethanol fuel gelled with HPC can be described as follows: after the first droplet of hydrogen peroxide starts fizzing. Then sparkling starts, and smoke begins to form. Typically, a clear white dot of light is observed after which the fuel ignites. The ignition process of the ethanol fuel gelled with HPMC also shows fizzing of the hydrogen peroxide after the first droplet. Additionally, small sparkles are visible, and foam is formed. After the second (and third) droplet more foam is formed, sometimes even covering the entire fuel, after which ignition occurs. This foam can be seen as a 3D network and is an undesirable characteristic for a propellant. The reason that the foam forms has to do with either the presence of water in the system or the presence of the methyl group.

The average IDT of the ethanol fuel with 3.5 wt% HPC and 2.5 wt%Mn(acac)2 equals 539 ms, and the average IDT of the ethanol fuel with 5.0 wt% HPMC, 15 wt% DI water, and 2.5 wt% Mn(acac)2 equals 1320 ms. Also, the amount of droplets of H2O2 required to achieve ignition is higher for the ethanol fuels gelled with HPMC than that of the ethanol fuels gelled with HPC. These IDTs are determined experimentally with a multi drop-test under atmospheric conditions (atmospheric temperature and atmospheric pressure). Due to these conditions and the fact that a lot of heat is lost into the environment, the IDT is above the desired <100 ms. But these IDT will decrease in an actual pressurized propulsion system. Hence, the IDT is still promising. The difference in IDT (539 ms vs 1320 ms) can also be explained based on the solidification process. To solidify the ethanol with HPMC, DI water was required. This water acts as a heat sink, absorbing the heat released during the ignition process and thereby delaying the ignition. Additionally, the critical concentration of HPMC is higher than that of HPC (5.0 wt% vs 3.5 wt%) that might also prolonged IDT. Furthermore, experiments are executed with 2.0 wt% catalyst(acac)2 and 3.0 wt% catalyst Mn(acac)2. These results showed consistent performance of ethanol fuels gelled with HPC. However, this consistency was lacking in the ethanol fuels gelled with HPMC. It shows that the behaviour and performance of fuels gelled with HPMC are less predictable.

The regression rate of ethanol fuel with 3.5 wt% HPC and 2.5 wt% Mn(acac)2 is relatively constant and on average equals 0.10 mm/s. The regression rate of the ethanol fuel with 5.0 wt% HPMC, 15 wt% DI water, and 2.5 wt%Mn(acac)2 was less constant and on average equals 0.11mm/s.

The energy content of the fuel is based on the temperature profile of the fuel as a calorimeter was unavailable. The temperature profile revealed that both fuels are capable of achieving high temperatures of around or above 1260 ^oC. Furthermore, the temperature profile revealed that the foam that is formed during the ignition process of ethanol fuels gelled with HPMC has a temperature of around 70 ^oC. It indicates that the foam also acts as a heat sink, providing a third reason for the longer ignition delay time of fuels gelled with HPMC compared to fuels gelled with HPC. The temperature profile also showed that around 20% to 30% of the temperature is lost over an area of only 1 cm. This further confirms that the IDT of the fuels will decrease when tested in a propulsion system.

In conclusion, a hybrid hypergolic bi-propellant system was formulated and developed. The suspending of the catalyst Mn(acac)2 to the alcohol-based fuel results in hydrogen peroxide decomposition directly followed by auto-ignition of alcohol fuel without an external source of ignition. Therefore, sub-question 2d can be answered which was: which type of fuel is most promising to further develop a novel green hybrid propellant system? The performance of ethanol fuel gelled with HPC shows more promising results than with ethanol fuel gelled with HPMC. First, the critical amount of gelling agents to achieve a solid system is lower. Only 3.5 wt% of HPC was required to obtain a solidified system against 5.0 wt% of HPMC. Also, the gelling process of HPMC is more complex as additional water is introduced to the system. The addition of water or the molecule structure of the gelling agent itself has as a consequence that during the ignition process of ethanol fuel gelled with HPMC, a lot of foam formed. This is an undesirable characteristic of a hypergolic propellant. Regarding the performance, the temperature profile shows that the energy content of ethanol fuel is high. The alcohol-based hypergolic system with high concentrated H2O2 achieved temperatures of >1260 ^oC. On other performance parameters, the ethanol fuels gelled with HPC show more promising results compared with HPMC. The IDT of the ethanol fuel gelled with HPC and 2.5% catalyst is on average 538 ms, while the IDT of ethanol fuel gelled with HPMC is on average 1320 ms. Additionally, the regression rate experiments showed that consistency in the performance of the ethanol fuels gelled with HPMC is missing. On the other hand, ethanol fuels gelled with HPC do show predictable results. Hence, based on the low critical gelling concentration, a simple formulation of the fuel, lower ignition delay time, and consistent performance, ethanol fuels gelled with HPC are the favourable candidates.

7.2. RECOMMENDATIONS

This thesis has shown the feasibility of achieving a hypergolic system by suspending the catalyst Mn(acac)2 to the ethanol fuel gelled with HPC or HPMC. Also, critical concentrations well below those found in the literature are realized, which will improve the performance of the propellant. However, further research is required to advance this alternative hypergolic propellant and to provide an alternative for the existing hydrazine-based propellants in the future. Recommendations are:

- The stabilizers and other elements present in the hydrogen peroxide (oxidizer) are currently analysed based on IC analysis and IC-PMS analysis. However, these only measure certain elements. It is believed that there is 2,6-pyridine dicarboxylic acid present in the hydrogen peroxide. However, this can not be detected using IC or IC-MPS analysis. To investigate this further, blue sorption or potentiometric titration should be conducted [25]. The civil engineering Lab has the facilities to execute these experiments, but a safety test is required before performing the experiments.
- The activation energy of the fuel can be determined more accurately which would give more insight into the required energy to achieve ignition. The activation energy can be found by performing a temperature experiment. However, a different rheometer is required as the MARS III was unable to perform the test to determine the activation energy in a reliable manner.
- The exact energy content of the fuel can only be determined with a calorimeter. Therefore, investing in such a calorimeter is worth looking into as it would give valuable insight into the precise energy content of the propellant. When the amount of heat released during ignition is further investigated based on a temperature profile, other thermocouples are advised. Because temperatures above 1260 ^oC are reached during the ignition of the novel green propellant, the k-type thermocouples break. To avoid breaking, R-type or B-type thermocouples are advised. R-type and B-type thermocouples can be used for temperature applications up to 1480 ^oC and 1700 ^oC respectively.
- Improvements of the test-setup used for the multi-drop test to examine the hypergolicity can be made. For example, the accuracy to control the flow rate of the oxidizer can improve. There is a strong relation between Ignition Delay Time and flow rate of oxidizer, therefore, it would increase the repeatability of the experiments when this flow rate is controlled more accurately. Also, the alignment between the fuel and oxidizer droplet can be optimized, such that misalignment does not occur. This will improve the repeatability of the experiment. Additionally, the surrounding conditions can be improved by executing the experiments in a location absent of wind. Lastly, a colour camera could be used instead of a black and white camera. Also, a second camera can be used to image the ignition process in 3D.
- The Ignition Delay Time should be experimentally determined under conditions that more closely resemble that of the propulsion system. It will likely decrease the IDT but also the critical concentration of catalyst. Currently, the critical concentration is around 2.5 wt%, but this value can decrease under the conditions experienced in a propulsion system.
- The production process to make the fuel can be optimized to create a homogeneous mixture, which will further improve the performance. Currently, the samples are mixed by hand, resulting in a slightly non-homogeneous mixture of the samples, which was most clearly visible during the amplitude sweep study. A homogeneous mixture of the gelling agent and alcohol will make the viscoelastic nature of the fuel more invariable. Additionally, a uniform suspension of the catalyst will result in a more constant and stable performance of the propellant.

- To further investigated reducing the critical concentration of the gelling agent HPC. Although a critical concentration of 3.5 wt% is already a huge reduction compared with the concentrations found in literature, more research is required to continue decreasing this critical concentration.
- During this research, only two gelling agents are investigated, namely HPC and HPMC. More research into different gelling agents is required to further investigate potential fuels that are suited for the development of green propulsion for space applications. This research can still focus on already patented gelling agents, but could also be extended to new (not yet known) gelling agents.
- Further research into different types of catalysts could reveal whether the ignition delay time can be decreased and performance can be improved with respect to the ethanol fuel gelled with HPC. One catalyst that should be researched is copper(II)chloride. This catalyst has proven capabilities of lowering the activation energy of a gelled fuel and achieving ignition in combination with highly concentrated hydrogen peroxide. In addition, other patented catalysts or non-patented catalysts could be researched.

BIBLIOGRAPHY

[1] F. B. Ibrahim Sadek Khattab, *Density, viscosity, and surface tension of water+ethanol mixtures from 293 to 323 K,* Korean Journal of Chemical Engineering (2012), 10.1007/s11814-011-0239-6.

[2] B. T. C. Zandbergen, *Thermal Rocket Propulsion (version 2.08)* (2020).

[3] I. A. Molenberg, *Literature Study - A novel green hybrid hypergolic bipropellant with viscoelastic nature,* (2020).

[4] E. T. Cora van Nieuwenhuizen, Jozo Radoš, *Impact of REACH legislation on European space industry,* `https://www.europarl.europa.eu/doceo/document/E-8-2016-003827_EN.html` (2016).

[5] L. R. R. L. Sackheim, *Green propulsion advancement: Challenging the maturity of monopropellant hydrazine,* Journal of Propulsion and Power (2014).

[6] ESA, *Green Propellant for Space Propulsion,* `https://www.esa.int/Applications/Observing_the_Earth/Green_Propellant_for_Space_Propulsion` (2001).

[7] M. J. Baier, P. V. Ramachandran, and S. F. Son, *Characterization of the Hypergolic Ignition Delay of Ammonia Borane,* Journal of Propulsion and Power (2018), 10.2514/1.B37075.

[8] G. P. Sutton and O. Biblarz, *Rocket Propulsion Elements (9th edition)* (John Wiley & Sons, 2017).

[9] M. M. M. Kurilov, *A method for screening and identification of green hypergolic bipropellants,* International Journal of Energetic Materials and Chemical Propulsion (2018), 10.1615/IntJEnergeticMaterialsChemProp.2018028057.

[10] S. L. Guseinov, S. G. Fedorov, V. A. Kosykh, and P. A. Storozhenko, *Hypergolic propellants based on hydrogen peroxide and organic compounds: historical aspect and current state,* Russian Chemical Bulletin, International Edition (2018).

[11] A. Musker, C. Roberts, G., P., J. Grayson, and J. Holdsworth, *Optimisation Study of a Homogeneously-Catalysed HTP Rocket Engine,* Proceedings of the 2nd International Conference on Green Propellants for Space Propulsion (2004), 2004ESASP.557E...9M.

[12] F. Grafwallner, *Hydrogen Peroxide (HP) Potential for Space Applications,* Proceedings of the 2nd International Conference on Green Propellants for Space Propulsion (2004).

[13] V. K. Bhosale, J. Jeong, and S. Kwon, *Ignition of boron-based green hypergolic fuels with hydrogen peroxide,* Fuel (2019), 10.1016.

[14] M. N. Shoaib, B. V. S. Jyoti, S. W. Weak, H. J. Lee, and S. J. Cho, *Hypergolic Studies of Ethanol Based Gelled Bi-Propellant System for Propulsion Application,* Propellants, Explosives, Pyrotechnics (2017), 10.1002/prep.201700046.

[15] B. V. S. Jyoti and S. W. Beak, *Rheological Characterization of Ethanolamine Gel Propellants,* Journal of Energetic Materials (2016), :10.1080/07370652.2015.1061617.

[16] B. V. S. Jyoti, M. S. Naseem, S. W. Beak, H. J. Lee, and S. J. Cho, *Hypergolicity and ignition delay study of gelled ethanolamine fuel,* Combustion and Flame (2017), http://dx.doi.org/10.1016/j.combustflame.2017.05.007.

[17] B. V. S. Jyoti, M. S. Naseem, and S. W. Beak, *Hypergolicity and ignition delay study of pure and energized ethanol gel fuel with hydrogen peroxide,* Combustion and Flame (2016), http://dx.doi.org/10.1016/j.combustflame.2016.11.018.

[18] T. Department, *Hydrogen Peroxide Toxicological Overview,* Public Health England (2009).

[19] J. Reichert, *Stabilizing hydrogen peroxide solution with pyrophosphoric acid,* United states patent office (1936).

[20] K. J. S. D. Cavazos-Elizondo, *Functional Comparison of Bioactive Cellulose Materials Incorporating Engineered Binding Proteins,* Vol. 8 (American Chemical Society, 2021).

[21] J. M. M. V. L. N. Hernández, *Effect of ascorbic acid on hydrogen peroxide decomposition into an environmentally friendly mixture for pickling of 316L stainless steel,* Protection of Metals and Physical Chemistry of Surfaces (2014), https://doi.org/10.1134/S2070205114030058.

[22] J. Johna, P. Nandagopalana, S. W. Baeka, and S. J. Cho, *Hypergolic ignition delay studies of solidified ethanol fuel with hydrogen peroxide for hybrid rockets,* Combustion and Flame (2019).

[23] M. N. Shoaib, B. V. S. Jyoti, S. W. Weak, and J. Huh, *Effect of Alcohol Carbon Chain on Enthalpy of Combustion and Ignition Delay Time for Gelled Hypergolic Propellant System,* Propellants, Explosives, Pyrotechnics (2018), 10.1002/prep.201700268.

[24] J. Quesada Mañas, *Propellant grade hydrogen peroxide production and thermo pseudo hypergolicity investigation for dual mode green propulsion system,* Student theses (2020).

[25] N. D. T. K. Shoulaifar, *Measuring the concentration of carboxylic acid groups in torrefied spruce wood,* Bioresource Technology (2012), https://doi.org/10.1016/j.biortech.2012.07.069.

A

Composition and Specifics of the Samples

Samples of "Formulation of the Fuel"

Table A.1: Detailed composition and specifics of the samples containing HPC (samples 1, 2, 21, 3 and 4)

Sample number	Mass empty bottle	Mass fraction	Ideal mass	Measured mass	Date and time
1	13.6767 g	3.0 wt% HPC	0.15 g HPC	0.1515 g HPC	11-01-2021 at 16.21 h
		97.0 wt% ethanol	4.85 g ethanol	4.8638 g ethanol	
2	13.6382 g	3.5 wt% HPC	0.175 g HPC	0.1734 g HPC	18-01-2021 at 14:15 h
		96.5 wt% ethanol	4.825 g ethanol	4.8266 g ethanol	
21	13.2990 g	4.0 wt% HPC	0.200 g HPC	0.2005 g HPC	02-02-2021 at 16:50 h
		96.0 wt% ethanol	4.800 g ethanol	4.8024 g ethanol	
3	13.4430 g	3.0 wt% HPC	0.15 g HPC	0.1509 g HPC	19-01-2021 at 11:00 h
		97.0 wt% butanol	4.85 g butanol	4.8530 g butanol	
4	13.4651 g	3.5 wt% HPC	0.175 g HPC	0.1751 g HPC	19-01-2021 at 11:30 h
		96.5 wt% butanol	4.825 g butanol	4.824 g butanol	

Table A.2: Detailed composition and specifics of the samples containing HPMC (samples 5, 6, 7 and 8)

Sample number	Mass empty bottle	Mass fraction	Ideal mass	Measured mass	Date and time
5	13.4119 *g*	3.0 wt% HPMC	0.15 *g* HPMC	0.1504 *g* HPMC	27-01-2021 at 14:25 h
		97.0 wt% ethanol	4.85 *g* ethanol	4.8528 *g* ethanol	
6	13.6404 *g*	3.5 wt% HPMC	0.175 *g* HPMC	0.1754 *g* HPMC	27-01-2021 at 15:00 h
		96.5 wt% ethanol	4.825 *g* ethanol	4.8278 *g* ethanol	
7	13.6703 *g*	3.0 wt% HPMC	0.15 *g* HPMC	0.1506 *g* HPMC	27-01-2021 at 15:30 h
		97.0 wt% butanol	4.85 *g* butanol	4.8522 *g* butanol	
8	13.5662 *g*	3.5 wt% HPMC	0.175 *g* HPMC	0.1728 *g* HPMC	27-01-2021 at 16:30 h
		96.5 wt% butanol	4.825 *g* butanol	4.7475 *g* butanol	

Table A.3: Detailed composition and specifics of the sample 9

Sample number	Mass empty bottle	Mass fraction	Ideal mass	Measured mass	Date and time
9	13.5285 *g*	3.0 wt% HPMC	0.09 *g* HPMC	0.0902 *g* HPMC	29-01-2021 at 8:30 h
		97.0 wt% ethanol	2.91 *g* ethanol	2.9117 *g* ethanol	
		0 - 10 wt% water	- - -	0 - 0.3239 *g* water	see note 1

Table A.4: Detailed composition and specifics of the samples containing ethanol, HPMC and water (samples 10, 13 and 14)

Sample number	Mass empty bottle	Mass fraction	Ideal mass	Measured mass	Date and time
10	13.5665 *g*	3.5 wt% HPMC	0.105g HPMC	0.1053 *g* HPMC	29-01-2021 at 9:30 h
		96.5 wt% ethanol	2.895 *g* ethanol	2.8958 *g* ethanol	
		10 wt% water	- - -	0.333 *g* water	see note 2
13	13.4778 *g*	3.0 wt% HPMC	0.09 *g* HPMC	0.0906 *g* HPMC	29-01-2021 at 10:00 h
		97 wt% ethanol	2.91 *g* ethanol	2.9131 *g* ethanol	
		13 wt% water	- - -	0.4496 *g* water	see note 2
14	13.5192 *g*	3.5 wt% HPMC	0.105g HPMC	0.1053 *g* HPMC	29-01-2021 at 10:30 h
		96.5 wt% ethanol	2.895 *g* ethanol	2.8966 *g* ethanol	
		15 wt% HPC	- - -	0.5301 *g* water	see note 2

Note 1:
Preparing this sample took around 60 minutes. The starting point was a concentration of 1 wt% water and this was increased by steps until a concentration of 10 wt% water. Due to the slow process, ethanol evaporated and the reliability of this sample is low.

Note 2:
These samples were constructed based on an X wt% fuel and an Y wt% of water (10, 13 and 15). This consequently result in a lower concentration of gelling agent.

Table A.5: Detailed composition and specifics of the samples containing ethanol, HPMC and water (samples 15, 16, 17, 19 and 22)

Sample number	Mass empty bottle	Mass fraction	Ideal mass	Measured mass	Date and time
15	13.3729 *g*	3.0 wt% HPMC	0.12 *g* HPMC	0.1208 *g* HPMC	01-02-2021 at 11:45 h
		82 wt% ethanol	3.28 *g* ethanol	3.2800 *g* ethanol	
		15 wt% water	0.60 *g* water	0.6086 *g* water	
16	13.3729 *g*	3.5 wt% HPMC	0.14 *g* HPMC	0.1409 *g* HPMC	01-02-2021 at 11:30h
		81.5 wt% ethanol	3.26 *g* ethanol	3.2610 *g* ethanol	
		15 wt% water	0.60 *g* water	0.6144 *g* water	
17	13.4169 *g*	4.0 wt% HPMC	0.16 *g* HPMC	0.1599 *g* HPMC	01-02-2021 at 12:00h
		81 wt% ethanol	3.24 *g* ethanol	3.2472 *g* ethanol	
		15 wt% water	0.60 *g* water	0.6072 *g* water	
19	13.4039 *g*	4.5 wt% HPMC	0.18 *g* HPMC	0.1809 *g* HPMC	02-02-2021 at 11:30h
		80.5 wt% ethanol	3.22 *g* ethanol	3.2208 *g* ethanol	
		15 wt% water	0.60 *g* water	0.6231 *g* water	
22	13.3671 *g*	5.0 wt% HPMC	0.20 *g* HPMC	0.2009 *g* HPMC	02-02-2021 at 16:15h
		80 wt% ethanol	3.20 *g* ethanol	3.2002 *g* ethanol	
		15 wt% water	0.60 *g* water	0.6280 *g* water	

Table A.6: Detailed composition and specifics of the samples containing butanol, HPMC and water (samples 11, 12, 18, 20 and 23)

Sample number	Mass empty bottle	Mass fraction	Ideal mass	Measured mass	Date and time
11	13.543 g	3.0 wt% HPMC	0.12 g HPMC	0.1202 g HPMC	01-02-2021 at 15:30h
		82 wt% butanol	3.28 g butanol	3.2854 g butanol	
		15 wt% water	0.60 g water	0.6141 g water	
12	13.5179 g	3.5 wt% HPMC	0.14 g HPMC	0.1400 g HPMC	01-02-2021 at 15:45h
		81.5 wt% butanol	3.26 g butanol	3.2644 g butanol	
		15 wt% water	0.60 g water	0.6066 g water	
18	13.3102 g	4.0 wt% HPMC	0.16 g HPMC	0.1599 g HPMC	01-02-2021 at 16:00h
		81 wt% butanol	3.24 g butanol	3.2446 g butanol	
		15 wt% water	0.60 g water	0.6194 g water	
20	13.5273 g	4.5 wt% HPMC	0.18 g HPMC	0.1808 g HPMC	02-02-2021 at 11:15 h
		80.5 wt% butanol	3.22 g butanol	3.2222 g ethanol	
		15 wt% water	0.60 g water	0.5999 g water	
23	13.4037 g	5.0 wt% HPMC	0.20 g HPMC	0.2001 g HPMC	02-02-2021 at 16:30h
		80 wt% butanol	3.20 g butanol	3.2020 g butanol	
		15 wt% water	0.60 g water	0.6001 g water	

Samples of "Analysis of the Fuel"

Table A.7: Detailed composition and specifics of the samples used for the rheology study (samples 101, 102, 103, 104, 119, 120, 122 and 123)

Sample number	Mass empty bottle	Mass fraction	Ideal mass	Measured mass	Date and time
101	13.2916 *g*	3.0 wt% HPC	0.36 *g* HPC	0.3602 *g* HPC	04-02-2021 at 14:10h
		97.0 wt% ethanol	11.64 *g* ethanol	11.6426 *g* ethanol	
102	13.3867 *g*	3.5 wt% HPC	0.42 *g* HPC	0.4210 *g* HPC	04-02-2021 at 14:30h
		96.5 wt% ethanol	11.58 *g* ethanol	11.5838 *g* ethanol	
103	13.3939 *g*	3.0 wt% HPC	0.36 *g* HPC	0.3600 *g* HPC	04-02-2021 at 14:50h
		97.0 wt% butanol	11.64 *g* butanol	11.6417 *g* butanol	
104	13.3511g	3.5 wt% HPC	0.42 *g* HPC	0.4209 *g* HPC	04-02-2021 at 15:15h
		96.5 wt% butanol	11.58 *g* butanol	11.5836 *g* butanol	
119	13.3458 *g*	4.5 wt% HPMC	0.54 *g* HPMC	0.5408 *g* HPMC	04-02-2021 at 15:35h
		80.5 wt% ethanol	9.66 *g* ethanol	9.6632 *g* ethanol	
		15 wt% water	1.80 *g* water	1.8171 *g* water	
122	13.3869 *g*	5.0 wt% HPMC	0.60 *g* HPMC	0.6004 *g* HPMC	04-02-2021 at 15:50h
		80 wt% ethanol	9.60 *g* ethanol	9.6020 *g* ethanol	
		15 wt% water	1.80 *g* water	1.8028 *g* water	
120	13.4568 *g*	4.5 wt% HPMC	0.45 *g* HPMC	0.4502 *g* HPMC	04-02-2021 at 16:05h
		80.5 wt% butanol	8.05 *g* butanol	8.0553 *g* butanol	
		15 wt% water	1.50 *g* water	1.5031 *g* water	
123	13.3253 *g*	5.0 wt% HPMC	0.50 *g* HPMC	0.5006 *g* HPMC	04-02-2021 at 16:05h
		80 wt% butanol	8.00 *g* butanol	8.0013 *g* butanol	
		15 wt% water	1.50 *g* water	1.5083 *g* water	

Samples of "Achieving Hypergolicity"

Table A.8: Detailed composition and specifics of the samples with different catalyst (samples 206, 208, 209, 210, 211, 212, 213 and 214)

Sample number	Mass Empty bottle	Mass fraction	Ideal mass	Measured mass	Date and time
206	13.4953	3.5 wt% HPC	0.105 *g* HPC	0.1054 *g* HPC	13-04-2021 at 15:30
		94.0 wt% ethanol	2.820 *g* ethanol	2.8392 *g* ethanol	
		2.5 wt% Mn(acac)2	0.075 *g* Mn(acac)2	0.0752 *g* Mn(acac)2	
207		Production error			
208	13.5801 *g*	5.0 wt% HPMC	0.150 *g* HPMC	0.1507 *g* HPMC	13-04-2021 at 16:00
		77.5 wt% ethanol	2.325 *g* ethanol	2.3240 *g* ethanol	
		15.0 wt% water	0.450 *g* water	0.450 *g* water	
		2.5 wt% Mn(acac)2	0.075 *g* Mn(acac)2	0.0749 *g* Mn(acac)2	
209	13.5544 *g*	3.5 wt% HPC	0.105 *g* HPC	0.1051 *g* HPC	15-04-2021 at 14:45h
		94.0 wt% ethanol	2.820 *g* ethanol	2.8215 *g* ethanol	
		2.5 wt% Fe3O4	0.075 *g* Fe3O4	0.0762 *g* Fe3O4	
210	13.5209 *g*	5.0 wt% HPMC	0.150 *g* HPMC	0.1516 *g* HPMC	15-04-2021 at 15:55h
		77.5 wt% ethanol	2.325 *g* ethanol	2.3269 *g* ethanol	
		15.0 wt% water	0.450 *g* water	0.4521 *g* water	
		2.5 wt% Fe3O4	0.075 *g* Fe3O4	0.0758 *g* Fe3O4	
211	13.5347 *g*	3.5 wt% HPC	0.105 *g* HPC	0.1050 *g* HPC	15-04-2021 at 15:05h
		94.0 wt% ethanol	2.820 *g* ethanol	2.8195 *g* ethanol	
		2.5 wt% Mn2O3	0.075 *g* Mn2O3	0.0763 *g* Mn2O3	
212	13.3843 *g*	5.0 wt% HPMC	0.150 *g* HPMC	0.1501 *g* HPMC	15-04-2021 at 15:40h
		77.5 wt% ethanol	2.325 *g* ethanol	2.3301 *g* ethanol	
		15.0 wt% water	0.450 *g* water	0.4477 *g* water	
		2.5 wt% Mn2O3	0.075 *g* Mn2O3	0.0754 *g* Mn2O3	
213	13.5480 *g*	3.5 wt% HPC	0.105 *g* HPC	0.1050 *g* HPC	15-04-2021 at 15:20h
		94.0 wt% ethanol	2.820 *g* ethanol	2.8212 *g* ethanol	
		2.5 wt% CuO	0.075 *g* CuO	0.0752 *g* CuO	
214	13.4792 *g*	5.0 wt% HPMC	0.150 *g* HPMC	0.1509 *g* HPMC	15-04-2021 at 15:50h
		77.5 wt% ethanol	2.325 *g* ethanol	2.3239 *g* ethanol	
		15.0 wt% water	0.450 *g* water	0.4605 *g* water	
		2.5 wt% CuO	0.075 *g* CuO	0.0748 *g* CuO	

Samples of "Analysis of the Performance of the Propellant"

Table A.9: Detailed composition and specifics of the samples with different concentration of the catalyst Mn(acac)2

Sample number	Mass Empty bottle	Mass fraction	Ideal mass	Measured mass	Date and time
201	13.4577 *g*	3.5 wt% HPC	0.175 *g* HPC	0.1759 *g* HPC	06-04-2021 at 13:25h
		94.5 wt% ethanol	4.725 *g* ethanol	4.7258 *g* ethanol	
		2.0 wt% Mn(acac)2	0.100 *g* Mn(acac)2	0.1018 *g* Mn(acac)2	
217	13.6483	5.0 wt% HPMC	0.150 *g* HPMC	0.1505 *g* HPMC	20-04-2021 at 15:10h
		78.0 wt% ethanol	2.340 *g* ethanol	2.3454 *g* ethanol	
		15.0 wt% water	0.450 *g* water	0.4678 *g* water	
		2.0 wt% Mn(acac)2	0.060 *g* Mn(acac)2	0.0604 *g* Mn(acac)2	
206A	13.476	3.5 wt% HPC	0.210 *g* HPC	0.2105 *g* HPC	20-04-2021 at 15:25h
		94.0 wt% ethanol	5.6426 *g* ethanol	5.6426 *g* ethanol	
		2.5 wt% Mn(acac)2	0.150 *g* Mn(acac)2	0.1505 *g* Mn(acac)2	
208A	13.2843	5.0 wt% HPMC	0.300 *g* HPMC	0.3001 *g* HPMC	20-04-2021 at 15:35h
		77.5 wt% ethanol	4.650 *g* ethanol	4.6512 *g* ethanol	
		15.0 wt% water	0.900 *g* water	0.9015 *g* water	
		2.5 wt% Mn(acac)2	0.150 *g* Mn(acac)2	0.1506 *g* Mn(acac)2	
215	13.5553	3.5 wt% HPC	0.105 *g* HPC	0.1055 *g* HPC	20-04-2021 at 14:45h
		94.0 wt% ethanol	2.805 *g* ethanol	2.8044 *g* ethanol	
		3.0 wt% Mn(acac)2	0.090 *g* Mn(acac)2	0.0904 *g* Mn(acac)2	
216	13.6483	5.0 wt% HPMC	0.150 *g* HPMC	0.1504 *g* HPMC	20-04-2021 at 15:00h
		77.0 wt% ethanol	2.310 *g* ethanol	2.3046 *g* ethanol	
		15.0 wt% water	0.450 *g* water	0.4580 *g* water	
		3.0 wt% Mn(acac)2	0.090 *g* Mn(acac)2	0.0904 *g* Mn(acac)2	

Pictures

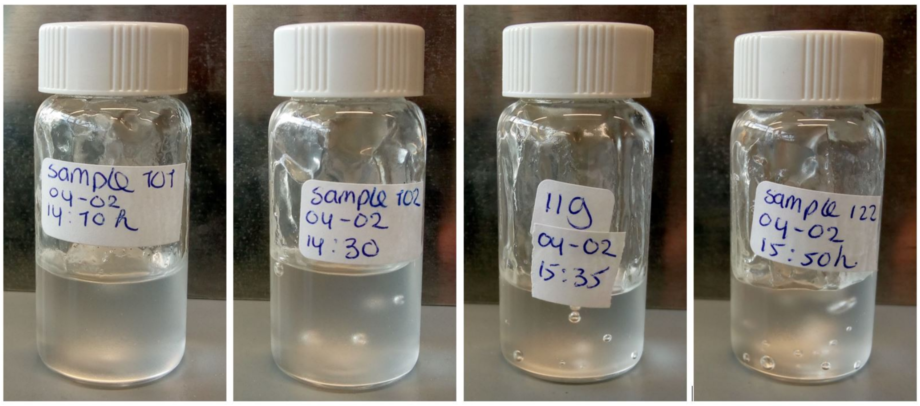

Figure A.1: Visual appearance of gelled butanol fuels at t=35 days

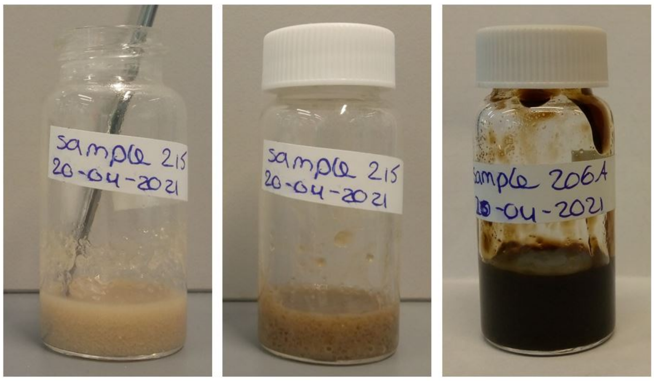

Figure A.2: Visual appearance of gelled ethanol fuels containing Mn(acac)2 as catalyst (samples 206 and 208)

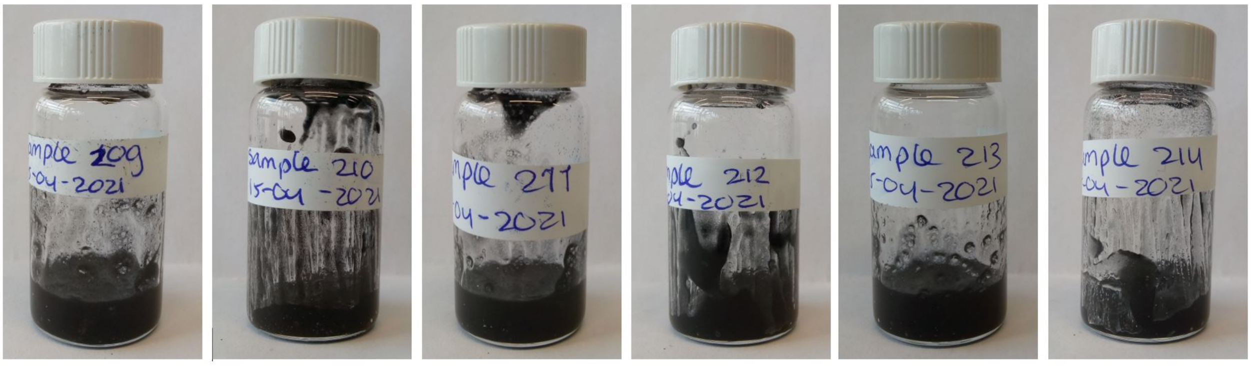

Figure A.3: Visual appearance of samples 209, 210, 211, 212, 213, and 214

B

ADDITIONAL DATA OF THE EXPERIMENTS

IC DATA

Table B.1: Verification of the IC results

Sample number		Standard100	Standard50	Standard10	Standard1	blank2
Element		concentration (ppm)	concentration (ppm)	concentration (ppm)	concentration (ppm)	concentration (ppm)
Anion	F	99.99	50.04	**9.60**	**1.25**	0.00
	NO2	100.01	**49.89**	**9.87**	1.01	0.00
	NO3	99.99	50.00	10.00	1.00	0.00
	PO4	100.00	50.00	10.00	1.00	0.00
	SO4	99.99	50.00	10.00	1.00	0.00
Cation	Na	100.01	50.00	10.00	1.00	0.00
	NH4	99.96	**50.21**	9.96	1.00	0.00
	Mg	100.00	50.00	10.00	1.00	0.00
	Ca	100.02	50.00	10.00	1.00	0.00
	Cl	99.97	50.00	10.00	1.00	0.00
	K	100.01	50.00	10.00	1.00	0.00

INITIAL RHEOLOGY STUDY

The data of the amplitude sweep study test C of sample 101 was considered faulty. The data is shown in Figure B.1 and Figure B.2. It can clearly be seen that one data point is faulty as the G" shows a strange dip.

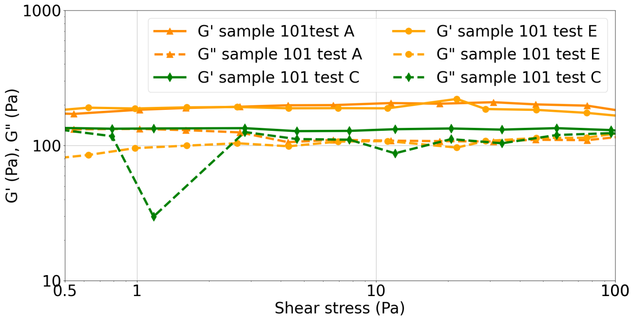

Figure B.1: Amplitude stress sweep study of ethanol and varying concentrations of HPC

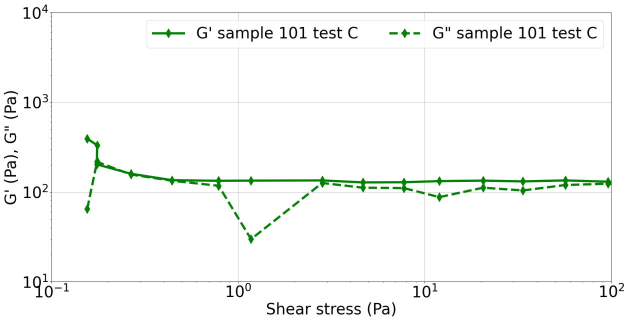

Figure B.2: Amplitude stress sweep study of ethanol and 3.0 wt% HPC (only test C - raw data)

The data of the amplitude sweep study test C sample 103 was not used. This data was not in line with the values of G’ of test B and test E. Additionally, it can be seen that the data of the shear stress moves backward at values above 100 Pa. This did not occur for test A and E. See Figure B.3 and Figure B.4

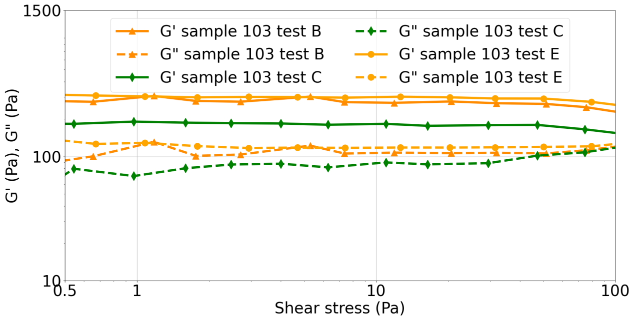

Figure B.3: Amplitude stress sweep study of butanol and varying concentrations of HPC

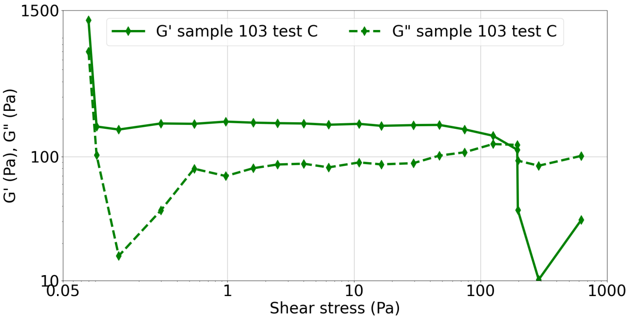

Figure B.4: Amplitude stress sweep study of butanol and 3.0 wt% HPC (only test C - raw data)

Regarding the frequency sweep study of sample 119 test B, the settings were incorrect. The frequency was set incorrectly from 0.01, which results in a very long experiment duration. The G’ is therefore also in the order of 10^4 instead of 10^3 like all other results showed. See Figure B.5.

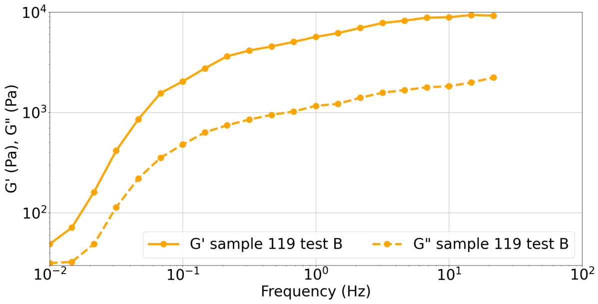

Figure B.5: Frequency sweep study of ethanol, water and 4.5 wt% HPMC (only test B - raw data)

Regarding the shear stress ramp study, also some settings were incorrect for test 119D. Almost no data points were obtained and the result is also deviating from test C and test E. See Figure B.6. For sample 123, a strange discontinuous slope was measured, this could be caused by the rotating disk, which might slip on the sample for high shear stress. See Figure B.7.

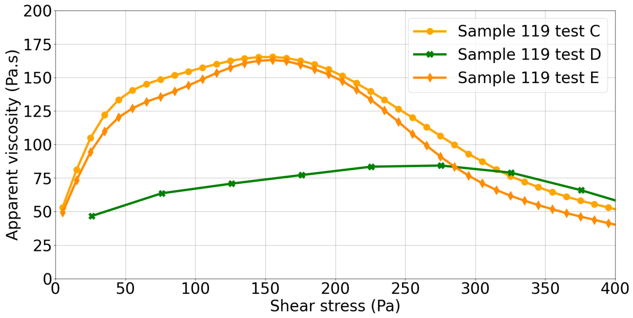

Figure B.6: Shear stress ramp study of ethanol, water and 4.5 wt% HPMC

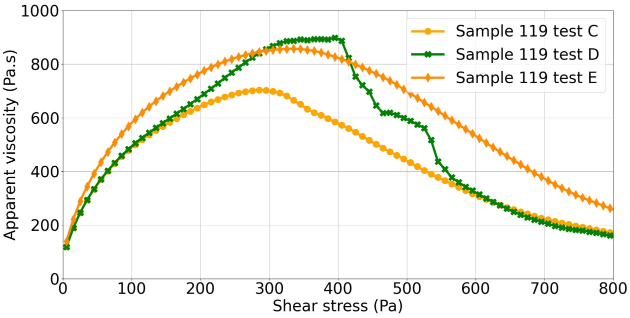

Figure B.7: Shear stress ramp study of butanol, water and 5.0 wt% HPMC

Table B.2: Average temperature during initial rheology study

Amplitude sweep study			
Sample	Average temperature in ^{o}C first test (test A or B)	Average temperature in ^{o}C second test (test C or E)	Notes
101	20.3	20.8	Temperature increase
102	20.0	19.8	
103	20.8	22.1	Temperature increase
104	20.9	20.4	
119	20.5	19.6	
122	19.7	19.2	
120	20.2	19.4	
123	20.2	19.5	
Frequency sweep study			
Sample	Average temperature in ^{o}C first test (test A or B)	Average temperature in ^{o}C second test (test C or E)	Notes
101	20.9	20.1	
102	20.6	19.4	
103	21.7	20.2	
104	21.4	20.2	
119	19.5	20.5	Temperature increase
122	20.5	19.4	
120	21.1	20.4	
123	21.0	20.3	
Ramp study			
Sample	Average temperature in ^{o}C first test (test C)	Average temperature in ^{o}C second test (test D or E)	Notes
101	19.4	20.2	All have a temperature increase
102	18.6	19.1	
103	19.1	19.8	
104	19.7	20.2	
119	19.3	20.2	
122	19.0	19.6	
120	19.2	20.0	
123	19.3	20.2	

RHEOLOGY STUDY INTO STABILITY OF THE FUEL

AMPLITUDE STRESS SWEEP STUDY

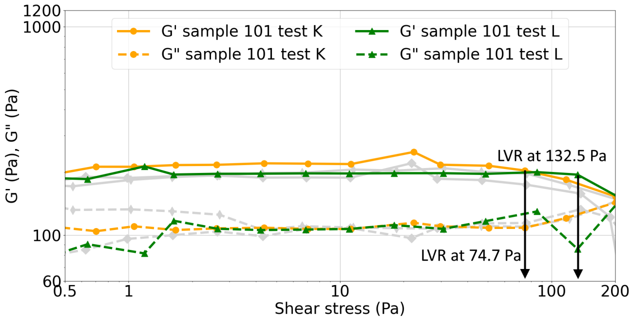

Figure B.8: Amplitude stress sweep study of ethanol and 3.0 wt% HPC at t=35 days

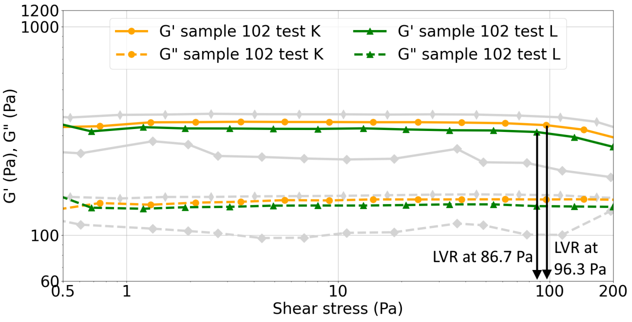

Figure B.9: Amplitude stress sweep study of ethanol and 3.5 wt% HPC at t=35 days

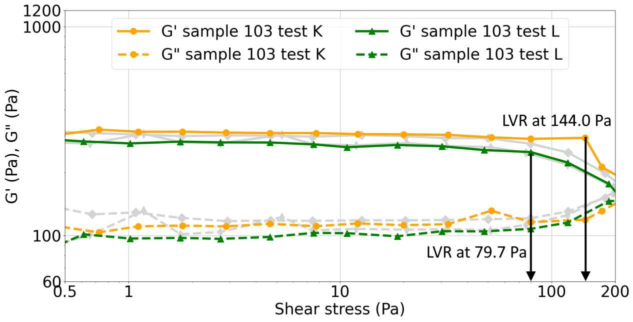

Figure B.10: Amplitude stress sweep study of butanol and 3.0 wt% HPC at t=35 days

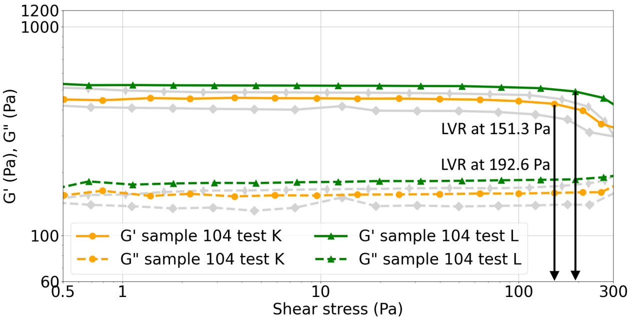

Figure B.11: Amplitude stress sweep study of butanol and 3.5 wt% HPC at t=35 days

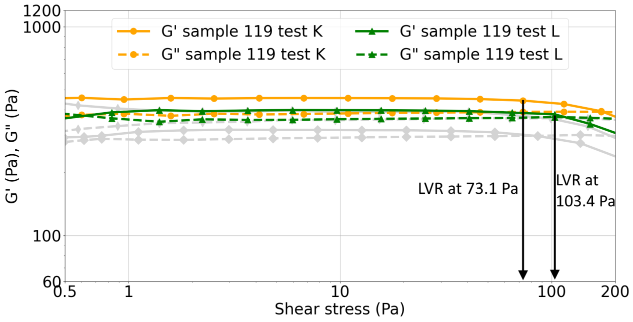

Figure B.12: Amplitude stress sweep study of ethanol, water and 4.5 wt% HPMC
at t=35 days

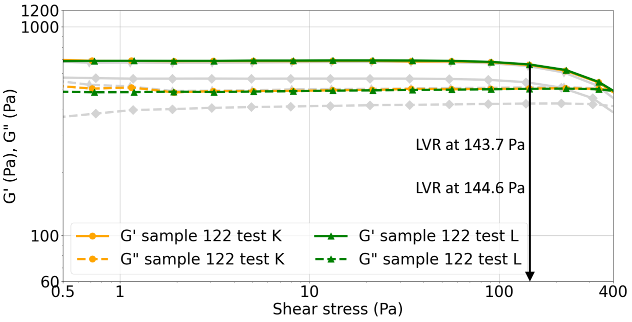

Figure B.13: Amplitude stress sweep study of ethanol, water and 5.0 wt% HPMC
at t=35 days

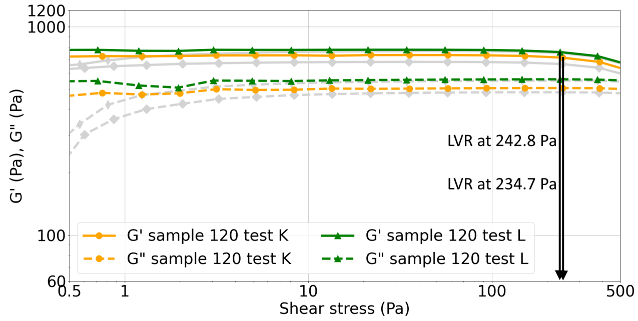

Figure B.14: Amplitude stress sweep study of butanol, water and 4.5 wt% HPMC
at t=35 days

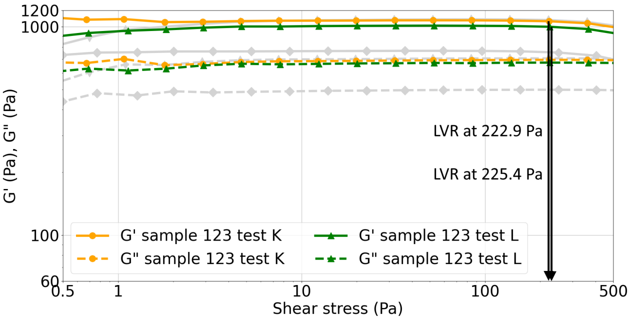

Figure B.15: Amplitude stress sweep study of butanol, water and 5.0 wt% HPMC
at t=35 days

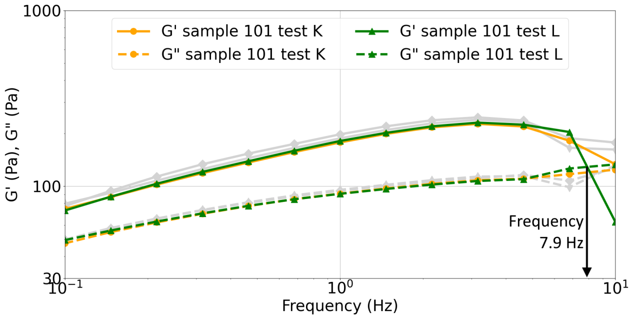

Figure B.16: Frequency sweep study of ethanol and 3.0 wt% HPC at t=35 days

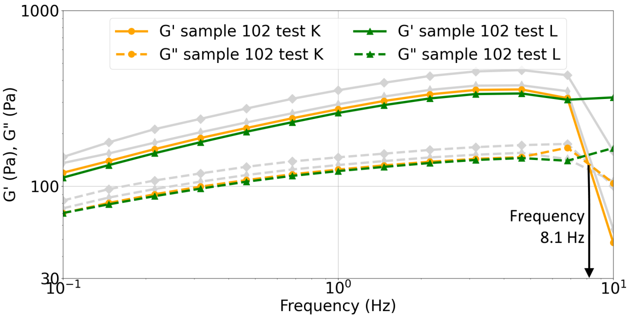

Figure B.17: Frequency sweep study of ethanol and 3.5 wt% HPC at t=35 days

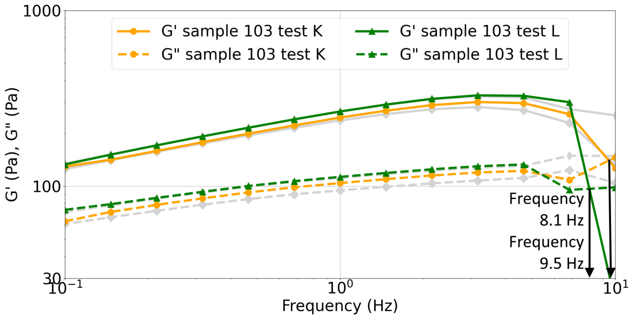

Figure B.18: Frequency sweep study of butanol and 3.0 wt% HPC at t=35 days

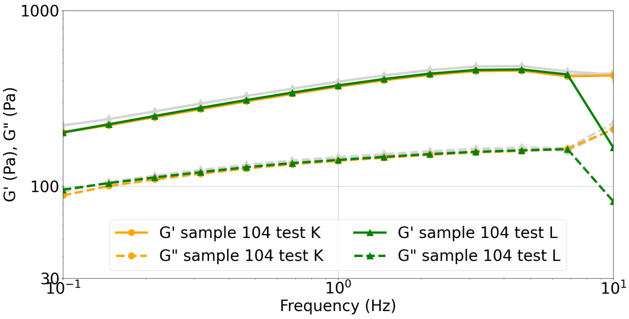

Figure B.19: Frequency sweep study of butanol and 3.5 wt% HPC at t=35 days

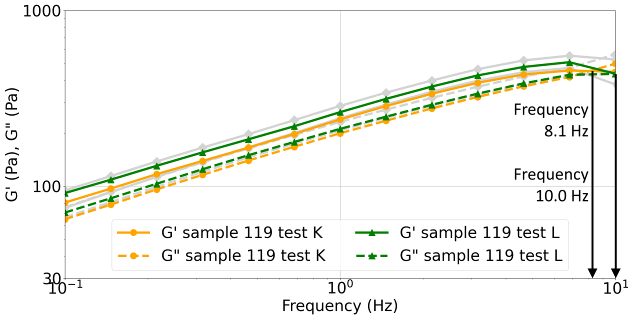

Figure B.20: Frequency sweep study of ethanol, water and 4.5 wt% HPMC at t=35 days

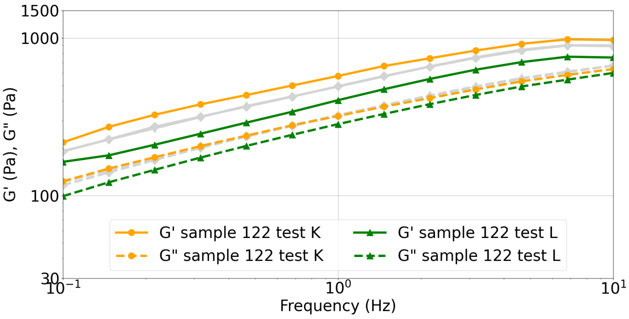

Figure B.21: Frequency sweep study of ethanol, water and 5.0 wt% HPMC at t=35 days

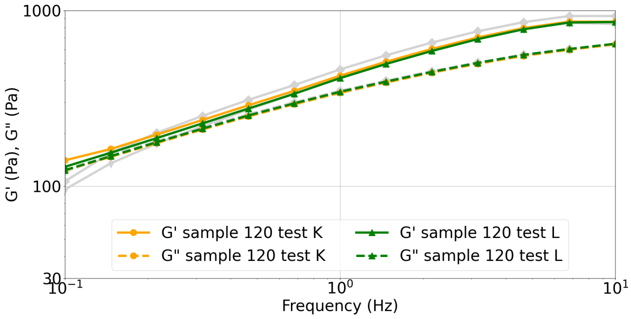

Figure B.22: Frequency sweep study of butanol, water and 4.5 wt% HPMC at t=35 days

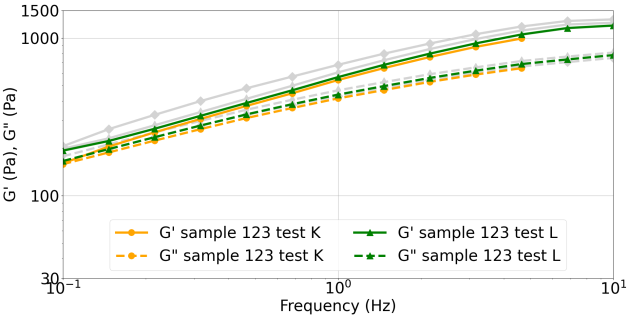

Figure B.23: Frequency sweep study of butanol, water and 5.0 wt% HPMC at t=35 days

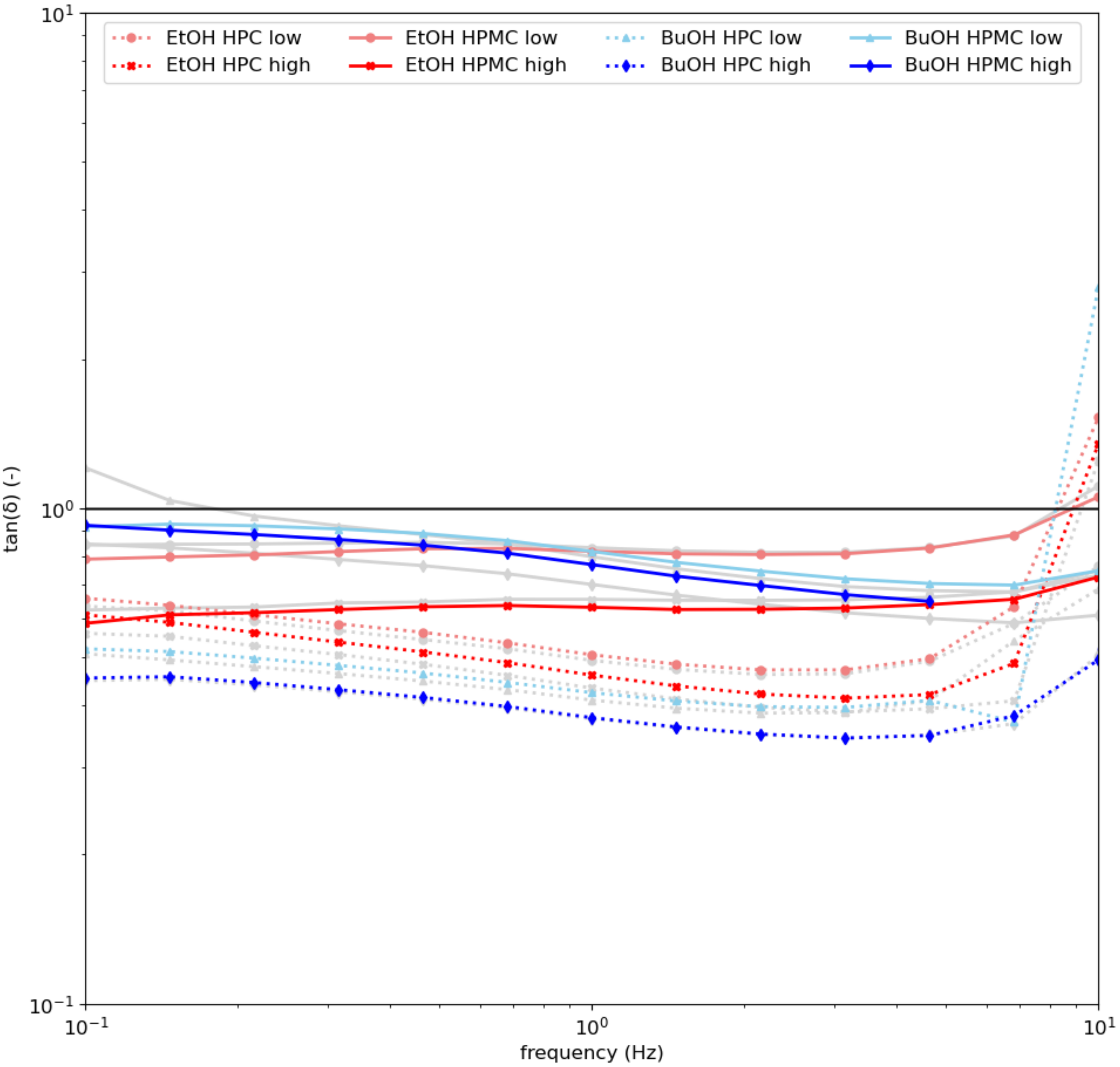

Figure B.24: Loss factor stability study

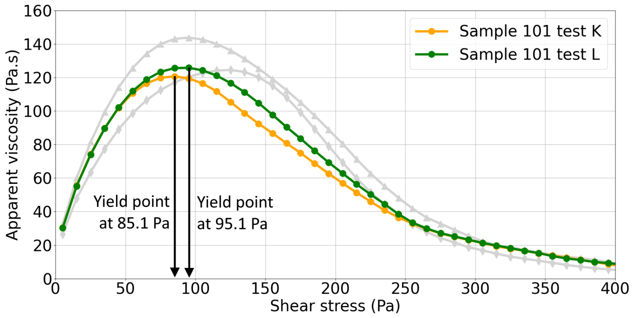

Figure B.25: Shear stress ramp study of ethanol and 3.0 wt% HPC at t=35 days

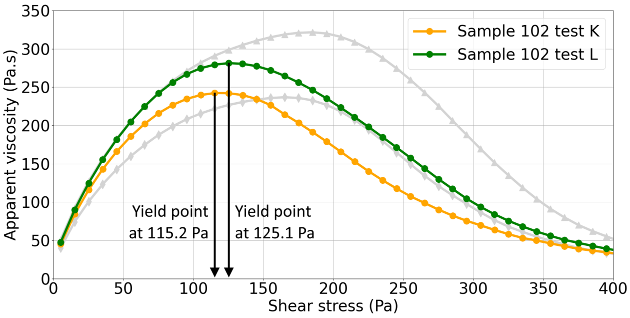

Figure B.26: Shear stress ramp study of ethanol and 3.5 wt% HPC at t=35 days

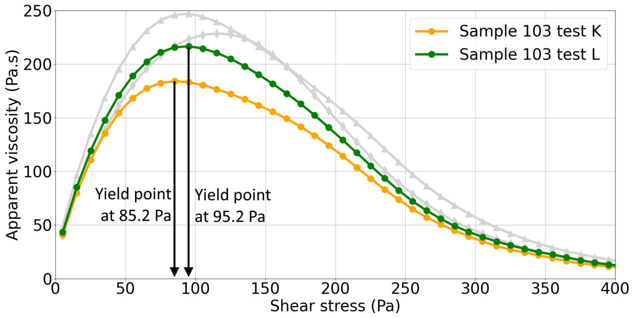

Figure B.27: Shear stress ramp study of butanol and 3.0 wt% HPC at t=35 days

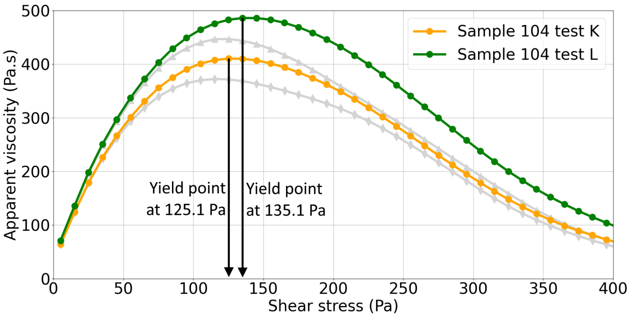

Figure B.28: Shear stress ramp study of butanol and 3.5 wt% HPC at t=35 days

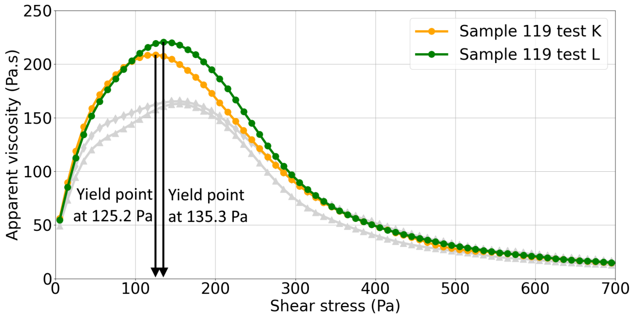

Figure B.29: Shear stress ramp study of ethanol, water and 4.5 wt% HPMC at t=35 days

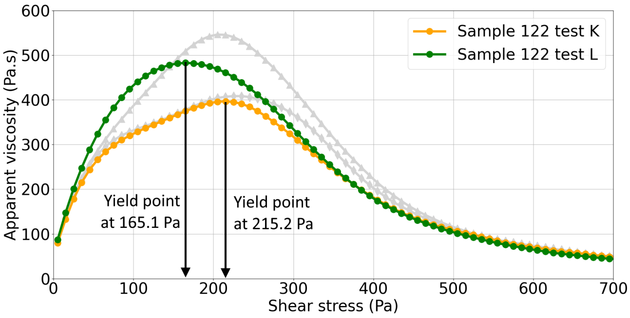

Figure B.30: Shear stress ramp study of ethanol, water and 5.0 wt% HPMC at t=35 days

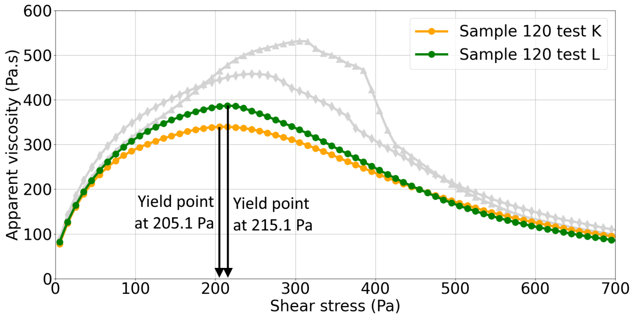

Figure B.31: Shear stress ramp study of butanol, water and 4.5 wt% HPMC at t=35 days

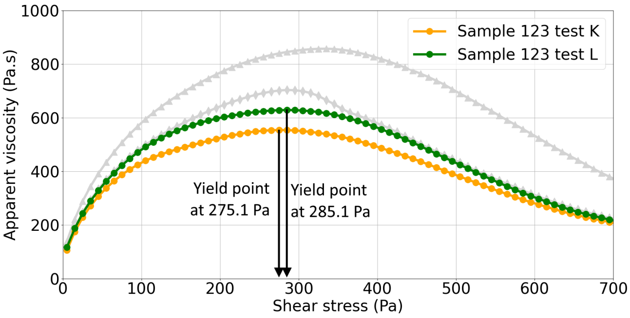

Figure B.32: Shear stress ramp study of butanol, water and 5.0 wt% HPMC at t=35 days

TEMPERATURE STUDY

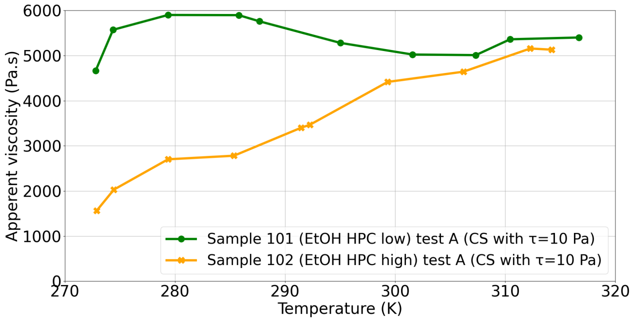

Figure B.33: Temperature study of ethanol and 3.0 wt% or 3.5 wt% HPC

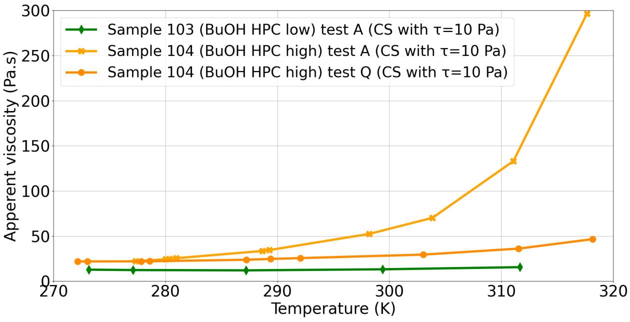

Figure B.34: Temperature study of butanol and 3.0 wt% or 3.5 wt% HPC

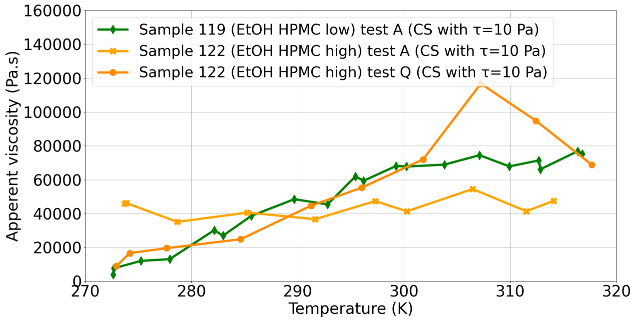

Figure B.35: Temperature study of ethanol and 4.5 wt% or 5.0 wt% HPMC

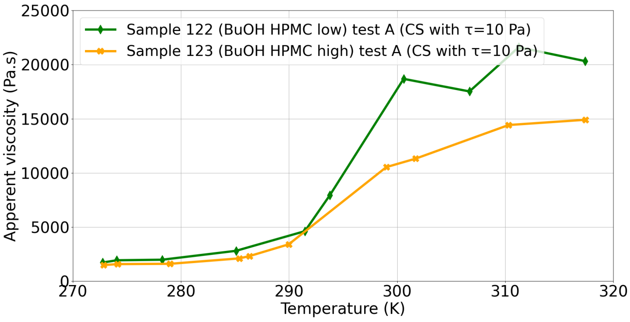

Figure B.36: Temperature study of butanol and 4.5 wt% or 5.0 wt% HPMC

Figure 4.42 and Figure 4.43 can be changed to Figure B.37 and Figure B.38 by taken the natural log of the apparent viscosity on the y-axis and the inverse of the temperature on the x-axis. For sample 122 test Z, the last two point are not included. The graphs in the form $y = m\,x + b$ is shown in the legend. Note that the m value has to be multiplied by a 1000 due to the change in axis.

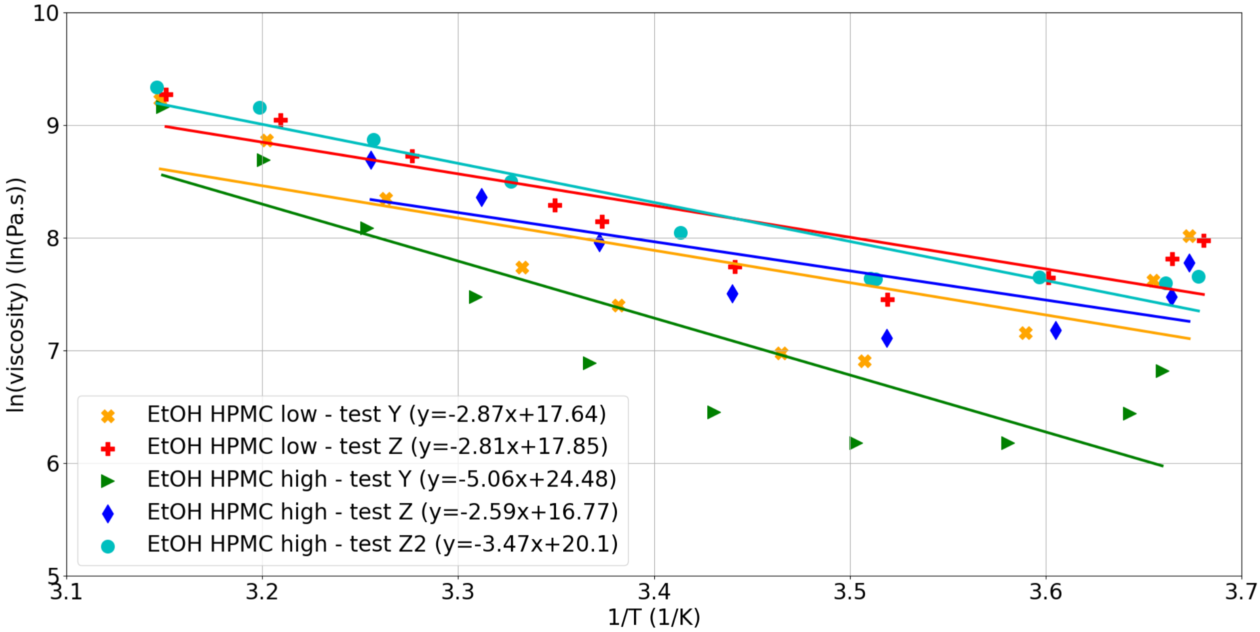

Figure B.37: Arrhenius plot of ethanol and 4.5 wt% or 5.0 wt% HPMC

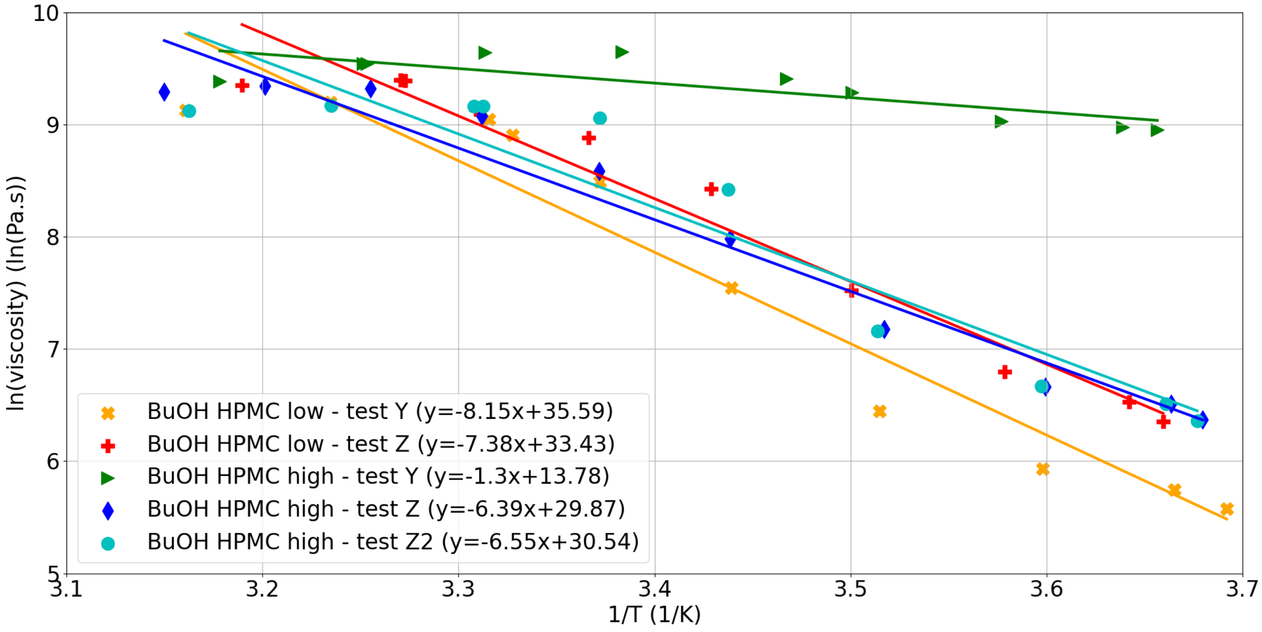

Figure B.38: Arrhenius plot of butanol and 4.5 wt% or 5.0 wt% HPMC

Table B.3: Overview of the starting time, normal force and gab size during the temperature study

Description	Test	Starting time of phase two (min)	Average normal force (N)	Average gab (mm)
EtOH HPC low (101)	test Y	12	0.096	0.89
	test Z	10	0.095	0.95
EtOH HPC high (102)	test Y	13	0.099	0.96
	test Z	12	0.099	0.94
BuOH HPC low (103)	test Y	7	**0.056**	1.11
	test X	14	**0.016**	1.08
	test Z	10	**0.012**	0.99
BuOH HPC high (104)	test Y	20	**0.050**	0.89
	test Z	9	**0.028**	1.18
EtOH HPMC low (119)	test Y	12	0.099	1.06
	test Z	10	0.100	1.06
EtOH HPMC high (122)	test Z	16	0.100	1.06
	test Z	12	0.098	1.10
	test Z2	9	0.099	1.10
BuOH HPMC low (120)	test Y	7	0.099	1.15
	test Z	13	0.101	1.16
BuOH HPMC high (123)	test Y	**21**	0.100	**1.11**
	test Z	**10**	0.100	**1.14**
	testZ2	**10**	0.100	**1.14**

TESTING ORDER

Table B.4: Chronological order of testing whereby [S] means success and [F] means failure

Testday	Type of test	Sample number							
		101	102	103	104	119	122	120	123
4 days	Amplitude sweep test A	S	S	F	F	F	F	F	F
	Amplitude sweep test B			S	S	S	S	S	S
	Frequency sweep test A	S	S		S		S	S	S
	Frequency sweep test B			S		F			
	Temperature study							F F	
5 days	Amplitude sweep test C	F	S	F	S	S	S	S	S
	Ramp study test C	S	S	S	S	S	S	S	S
	Frequency sweep test C	S	S	S	S	S	S	S	S
	Ramp study Test D	S	S	S	S	F	S	S	F
	Amplitude sweep test E	S		S					
	Frequency sweep test E					S			
	Ramps study test E					S			S
25 days	Temperature study A	F	F	F	F	F	F	F	F
35 days	Amplitude sweep test K	S	S	S	S	S	S	S	S
	Frequency sweep test K	S	S	S	S	S	S	S	S
	Ramp study test K	S	S	S	S	S	S	S	S
	Amplitude sweep test L	S	S	S	S	S	S	S	S
	Frequency sweep test L	S	S	S	S	S	S	S	S
	Ramp study test L	S	S	S	S	S	S	S	S
43 days	Temperature study Q		F		F		F		
	Temperature test random	F	F F		F		F		
44 days	Temperature study Y	S	S	F	F	S	S	S	S
	Temperature study X			F					
48 days	temperature study Z	S	S	F	F	S	S	S	S
	temperature study Z2						S		S

C

MISCELLANEOUS INFORMATION

DATA FROM THE RHEOMETER

Measuring device: MARS III (HAAKE MARS III)
Driver version: 121
Firmware version 1: 50.23.000
Firmware version 2: 50.18.000
Firmware version 3: 50.25.000
Modification: MSCMode=CR
Modification: MSCNumFreq=12
Modification: MinTorque=0.0
Modification: TrimPos=1
Modification: Damping=30
TCP/IP (192.168.2.140)
Inertia: 9,7451e-06 kgm²
Options: HS,HT,NF
Serial number: 112002150001
Serial number head: 1201201952001
Last service: 15-1-2021
Last calibration: 15-1-2021
Camera: No camera
Check G’: [—]
Oscillation raw data: [X]
Inertia correction OSC: [X]
Active compliance correction CD-OSC: [X]
Active inertia correction CS-OSC: [X]
Use MicroTorqueCorrection: [X]
Use MicroStressControl: [X]
Inertia correction Ramp ROT: [—]
Use Halfwave: [—]
Accept data against set direction ROT: [X]
Communication log: [—]

Measuring geometry: PP20
Driver version: 58
A-factor: 6,366e+05 Pa/Nm
M-factor: 10,05 (1/s)/(rad/s)
Inertia: 4,300e-07 kg m²
Damping: 30,00
Thermal expansion coefficient: 1,100 µm/°C
Compliance: 0,003157 rad/Nm
Torque offset: off
Gap: 0,100 mm

Temperature device: CTC <—> MARS III (CTC)
Driver version: 38
Firmware version 1: OTC :01.01.000
Remote (MARS III)
Cooling media: LN2, liquid nitrogene

Test Setup Multi-Drop Test

Figure C.1: Overview of the test setup for the multi-drop test

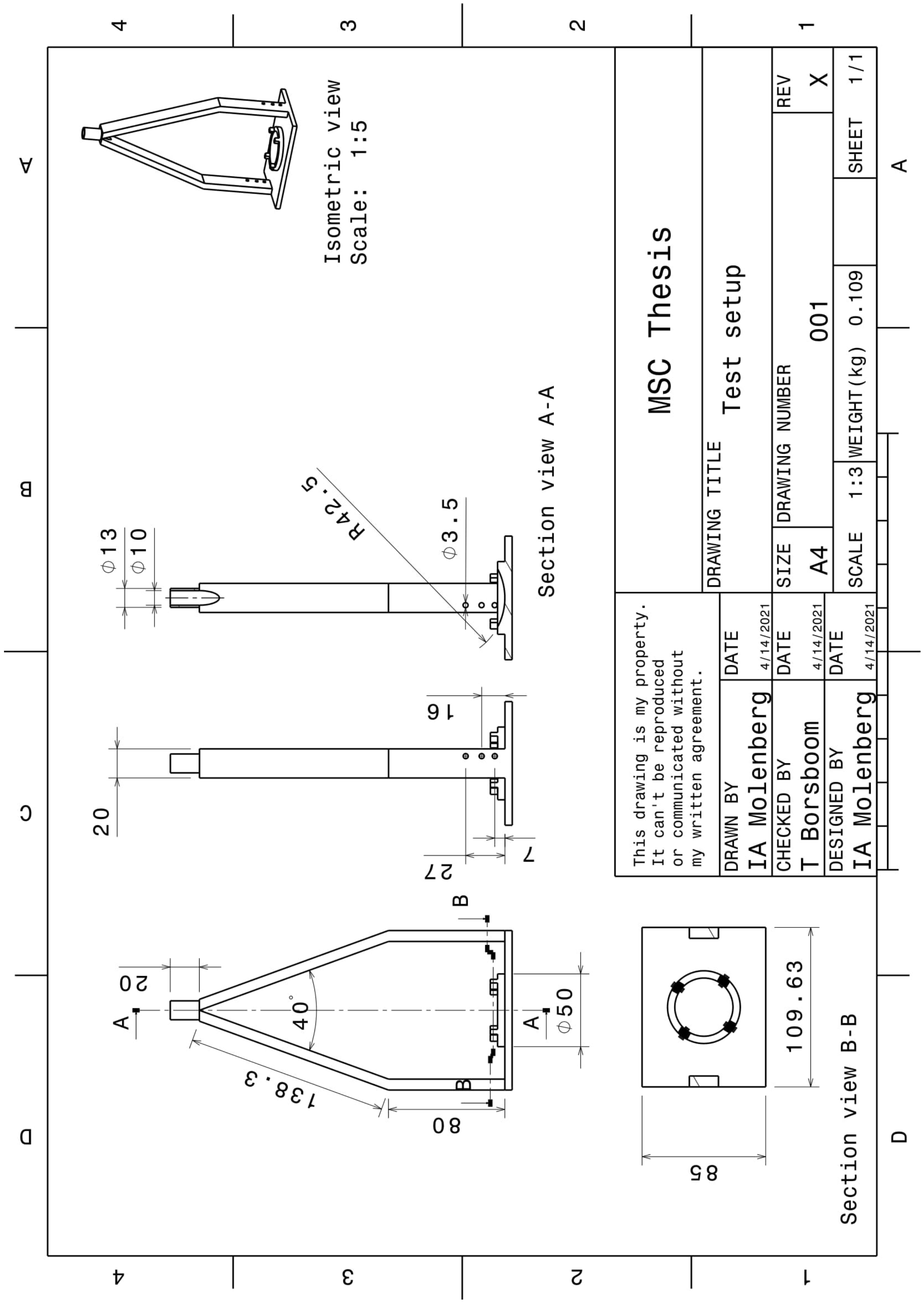

Figure C.2: Technical drawing of the test setup used for the multi-drop test

TEST PROCEDURE FOR MULTI-DROP TEST

Test setup preparations

1. The highspeed camera is placed in position inside the fume hood
2. The external light source is placed in position inside the fume hood
3. The tripod with a base plate that holds the glass tube that contains the H2O2 is placed in the fume hood
4. The structure to hold the watch glass and direct the droplet is placed in position
5. The settings of the highspeed camera, external light source and structure are optimised [1]
6. The table is covered with aluminium foil

Before the experiment

1. A big bottle of at least 500 mL of DI water is present for emergencies
2. The concentration of the hydrogen peroxide is measured
3. A smaller bottle is filled with hydrogen peroxide, the larger bottle (that SolvGE produces) is put in a safe location
4. The desk area is clear and clean
5. Only the used chemicals are located at the desk to avoid confusion
    - The fuel sample that is tested
    - The small bottle of H2O2

Preparation of experiment

1. The glass tube is filled with H2O2 (inside fume hood)
2. The fuel is shaped into the form of a grain (at the desk)
3. The fuel is placed at the watch glass (at the desk)
4. The watch glass (with fuel) is positioned in the test setup (in the fume hood)
5. The camera is activated

Conduction of experiment

6. Camera is started
7. Two droplets are dropped upon the fuel
8. (hopefully) ignition of the fuel

After the experiment

9. The video is added and the movie is saved.
10. During step 9 the watch glass has time (around 20 minutes) to cool down
11. DI water is added to the glass to dilute the remains
12. The glass is removed from the test set up and rinsed above the waste bottle
13. The glass is dried with paper
14. The desk is diluted with water and wiped dry with paper

Emergency procedures – leakage of H2O2 from the glass tube

- In case no fuel is yet present the chemical spillage is diluted using DI water and the test setup is dried before a new test is done
- In case fuel is present the test is aborted, continue at item 10.

Emergency procedure – fire

- In case of a smoldering fire or a small fire, it can be extinguished using the 500 ml water bottle
- In case of a larger fire, the nearest fire extinguisher should be used

---

[1] This is already done using water and the correct position is marked on the floor and table